CHARACTERIZATION OF ALSIN AND ITS ROLE IN

IGF-1-MEDIATED NEURONAL SURVIVAL

APPROVED BY SUPERVISORY COMMITTEE

Bruce Horazdovsky   _____

Helmut Kramer   _____

Michael Rosen   _____

Xiaodong Wang   _____

This dissertation is dedicated to my mother, who always put my education first and instilled in me the desire to do great things, and to do them well.

CHARACTERIZATION OF ALSIN AND ITS ROLE IN

IGF-1-MEDIATED NEURONAL SURVIVAL

by

JUSTIN DAVID TOPP

DISSERTATION

Presented to the Faculty of the Graduate School of Biomedical Sciences

The University of Texas Southwestern Medical Center at Dallas

In Partial Fulfillment of the Requirements

For the Degree of

DOCTOR OF PHILOSOPHY

The University of Texas Southwestern Medical Center at Dallas

Dallas, TX

April, 2005

CHARACTERIZATION OF ALSIN AND ITS ROLE IN IGF-1-MEDIATED

NEURONAL SURVIVAL

JUSTIN DAVID TOPP, PH.D.

The University of Texas Southwestern Medical Center at Dallas, 2005

Supervising Professor: BRUCE F. HORAZDOVSKY, PH.D.

The transport of proteins between organelles is a highly regulated and complex process that is crucial for many of the functions required for cellular homeostasis. Many distinct proteins are involved in each trafficking step with roles in vesicle formation, budding, movement, and fusion. One class of proteins, the Rab GTPases, is required for docking and fusion of transport vesicles with their target membrane. These proteins are regulated by their state of nucleotide binding, with GTP-bound Rabs thought to provide specificity to transport steps via their interactions with specific effector proteins.

While much work has been focused on proteins downstream of Rab GTPases, little is known as to how the activation of these proteins is controlled. This is particularly true of Rab5, the Rab protein required for vesicle fusion at the endosome. Endocytosis of plasma membrane proteins requires Rab5•GTP, and humans possess at least seven proteins (Vps9 family) that are expected to activate Rab5. An intriguing aspect of the Vps9 family of proteins is that they appear to link signal transduction to receptor trafficking via the specific coupling of particular receptors to Rab5-mediated endocytosis.

Cell biological, biochemical, and immunohistochemical techniques were employed to characterize one of the Vps9 family proteins named Alsin. Alsin is required for motor neuron maintenance and/or survival, as loss-of-Alsin function results in multiple juvenile-onset neurodegenerative disorders (ALS2, JPLS, IAHSP). It was found here that Alsin is an endosomal protein that activates both Rac1 and Rab5. This protein is present in all of the tissues associated with the aforementioned diseases and intriguingly is upregulated in the cerebellum, an unknown site of pathology for this class of disorders. Alsin was found to couple Rab5 activation specifically to the IGF-1 signal transduction pathway via its regulation of IGF-1 receptor endocytosis. This function of Alsin was shown to be essential for IGF-1-mediated cell survival. These results provide the first characterization of Alsin and identify a novel cause for neurodegeneration.

Table of Contents

CHAPTER 5. *Discussion*

Publications

Present work:

Topp, J.D., Gray N.W., Gerard, B., and B.F. Horazdovsky (2004). Alsin is a Rab5 and Rac1 exchange factor. J. Biol. Chem. 279, 24612.

Devon, R.S., Schwab, C., **Topp, J.D.**, Orban, P.C , Yang, Y., Pape, T.D., Helm, J.R., Davidson, T., Rogers, D.A., Gros-Luis, F., Rouleau, G., Horazdovsky. B.F., Leavitt, B.R., and M. Hayden (2005). Cross-species characterization of the Als2 gene and analysis of its pattern of expression in development and adulthood. Neurobiol. Dis. 18, 243 (cover).

Topp, J.D., Severson, S.R., Orban, P.C., Hayden, M.R., and B.F. Horazdovsky. Alsin Rab5 GEF activity is required for IGF-1 receptor trafficking and signal transduction (submitted).

Topp, J.D., and B.F. Horazdovsky. Molecular pathogenesis of ALS. (invited review, in preparation for Archives of Neurology).

Topp, J.D., Sikkink, R.A., and B.F. Horazdovsky. Biochemical characterization of Alsin (invited manuscript, in preparation for Methods of Enzymology).

Devon, R.S., Orban, P.C., **Topp, J.D.**, Gerrow, K., Barbieri, M.A., Schwab, C., Witmer, J., McCaffery, J.M., Davidson, T., Leavitt, B., El-Husseini, A., Horazdovsky, B.F., and M. Hayden. Alsin deletion disrupts neuronal receptor trafficking (in preparation).

Other work (not in thesis):

Davies, B.A., **Topp, J.D.**, Sfeir, A.J., Katzmann, D.J., Carney, D.S., Tall, G.G., Friedberg, A.S., Deng, L., Chen, Z., and B.F. Horazdovsky (2003). Vps9p CUE domain ubiquitin binding is required for efficient endocytic protein traffic. J. Biol. Chem. 278, 19826.

Previous work:

Ahluwalia, J.P., **Topp, J.D.**, Weirather, K., Zimmerman, M., and M. Stamnes. (2001) A role for calcium in stabilizing transport vesicle coats. J. Biol. Chem. 276, 34148.

List of Abbreviations

[^{3}H]	radio-active hydrogen
[^{125}I]	radio-active iodine
ηg	nanogram
ηM	nanomolar
μg	microgram
μl	microliter
μM	micromolar
ΔVps9d	Alsin lacking an intact Vps9 domain (truncated at residue 1602)
AAV	adeno-associated virus
Ag	*Anopheles gambiae*
ALS	amyotrophic lateral sclerosis
ALS2CL	ALS2 COOH-terminal like
AMPA	α-amino-3-hydroxy-5-methyl-4-isoxazole propionic acid
APPL	adaptor protein containing PH domain, PTB domain, and leucine zipper motif
ARF	ADP-ribosylation factor
ATP	adenosine triphosphate
BDNF	brain-derived neurotrophic factor
bp	basepair of DNA
BSA	bovine serum albumin
cDNA	complementary DNA
CHAPS	3[(3-Cholamidopropyl)dimethylammonio]propanesulfonic acid
CNBr	cyanogen bromide
CNS	central nervous system
CNTF	ciliary neurotrophic factor
cpm	counts per minute
CPY	carboxypeptidase Y
CUE	coupling of ubiquitin to ER degradation domain
DAG	diacylglycerol
Dbl	diffuse B-cell lymphoma
DH	Dbl homology domain
Dm	*Drosophila melanogaster*
DMEM	Dulbecco's modified eagle medium
DME/F12	1:1 ratio of DMEM + Ham's F12 medium
DN	dominant-negative
DNA	deoxyribonucleic acid
DOC	deoxycholate
DPBS	Dulbecco's modified PBS
Dr	*Danio rerio*
DsRed	red fluorescent fusion protein
DTT	dithiothreitol
E3	ubiquitin protein ligase domain
EAAT2	excitatory amino acid transporter 2
EDTA	ethylenediamine-tetraacetic acid

EEA1	early-endosomal antigen 1
EGF	epidermal growth factor
EGFR	epidermal growth factor receptor
EGTA	ethyleneglycol-*bis*(β-aminoethyl)-N,N,N',N'-tetraacetic acid
ELISA	enzyme-linked immunosorbent assay
ER	endoplasmic reticulum
ERK	extracellular signal-related kinase
EST	expressed sequence tag
FALS	familial amyotrophic lateral sclerosis
FBS	fetal bovine serum
FDA	Unites States Food and Drug Administration
FKH	forkhead (family of transcription factors)
Fr	*Fugu rubripes*
FREAC	forkhead-related activator
FYVE	domain that interacts specifically with PI(3)P, named for the first four protein shown to have this domain (Fab1, YOTB/ZK632.12, Vac1, EEA1)
g	gram
GAP	GTPase-activating protein
GAPDH	glyceraldehyde-3-phosphate dehydrogenase
GDI	GDP-dissociation inhibitor
GDF	GDI-dissociation factor
GDP	guanosine diphosphate
GDNF	glial-derived neurotrophic factor
GEF	guanine nucleotide exchange factor
GFAP	glial fibrillary acidic protein
GFP	green fluorescent protein
GGA	Golgi-localized, γ-ear containing, ARF-binding
GPCR	G protein-coupled receptor
GST	glutathione S-transferase
GTP	guanosine triphosphate
H_2O_2	hydrogen peroxide
HBSS	Hank's balanced salt solution
HDL2	Huntington disease-like 2
His_6	tag with 6 histidine residues, used in affinity purification
HLF	hepatic leukemia factor
HFH-3	hepatocyte nuclear factor-3 /forkhead homolog family
HRP	horseradish peroxidase
hrs	hours
Hs	*Homo sapiens*
IAHSP	infantile-onset ascending hereditary spastic paraplegia
IGF	insulin-like growth factor (refers to both IGF-1 and IGF-2)
IGF-1	insulin-like growth factor 1
IGF-2	insulin-like growth factor 2
IGF-1R	IGF-1 receptor
IGFBP	IGF-binding protein

IP3	inositolpolyphosphate 3
IPTG	isopropyl-β-D-thiogalactopyranoside
IRS-1	insulin receptor substrate 1
JPLS	juvenile primary lateral sclerosis
kb	kilobase of DNA
kDa	kilodalton (atomic mass)
lacZ	encodes the enzyme β-galactosidase
LB	Luria-Bertani medium
LP1	pellet from 25,000 xg spin (P2 as input)
LP2	pellet from 165,000 xg spin (LS1 as input)
LS1	supernatant from 25,000 xg spin (P2 as input)
LS2	supernatant from 165,000 xg spin (LS1 as input)
M6P	mannose-6-phosphate
M6PR	mannose-6-phosphate receptor
MAP2B	microtubule-associated protein 2B
MAPK	mitogen-activated protein kinase
MBP	maltose-binding protein, used as tag for affinity purification
MEF	mouse embryonic fibroblast
mg	milligram
mGlu	metabotropic glutamate
min	minutes
ml	milliliter
mM	millimolar
Mm	*Mus musculus*
MMT	manual muscle testing
MORN	membrane occupation and recognition nexus
MR46	cation-dependent mannose-6-phosphate receptor
MR300	cation-independent mannose-6-phosphate receptor
mRNA	messenger RNA
NADPH	nicotinamide adenine dinucleotide phosphate, reduced form
NaK-ATPase	sodium potassium ATPase
NGF	nerve growth factor
NeuN	neuron specific nuclear protein
NF-κB	nuclear factor kappa B
nm	nanometer
NMDA	*N*-methyl-D-aspartate
NP-40	Nonidet P-40
NSF	*N*-ethylmaleimide-sensitive factor
NTA	nitrilotriacetic acid
OD_{600}	optical density at 600nm
P1	pellet from 500 xg spin
P2	pellet from 10,500 xg spin
P3	pellet from 165,000 xg spin
P13	pellet from 13,000 xg spin
P100	pellet from 100,000 xg spin
PAK	p21-activated kinase

PBD	protein-binding domain (Rac•GTP-binding domain of PAK)
PBS	phosphate-buffered saline
PBS-T	phosphate-buffered saline plus 0.3% Triton X-100
PCR	polymerase chain reaction
PFAM	Protein Family (database)
PH	Pleckstrin homology
PI(3)P	phosphatidylinositol-3-phosphate
PI(4,5)P$_2$	phosphatidylinositol-4,5-bisphosphate
PI(3,4,5)P$_3$	phosphatidylinositol-3,4,5-triphosphate
PI(3)K	phosphatidylinositol-3-phosphate kinase
pM	picomolar
pmol	picomoles
PMSF	phenylmethyl sulfonyl fluoride
PLS	primary lateral sclerosis
PROSITE	database of protein families and domains
Pt	*Pan troglodytes*
PTB	phospho-tyrosine binding domain
PVDF	poly(vinylidene difluoride)
QPCR	quantitative polymerase chain reaction
RA	Ras association
RCC1	regulator of chromatin condensation 1
RFP	red fluorescent protein
RIN	Ras inhibitor
RING	E3 ubiquitin ligase domain
RLD	RCC1-like domain
Rn	*Rattus norvegicus*
RNA	ribonucleic acid
ROS	reactive oxygen species
rpm	revolutions per minute
rps	reverse position specific
RTK	receptor tyrosine kinase
RT-PCR	reverse transcription polymerase chain reaction
S1	supernatant from 500 xg spin
S2	supernatant from 10,500 xg spin
S3	supernatant from 165,000 xg spin
S13	supernatant from 13,000 xg spin
S100	supernatant from 100,000 xg spin
SALS	sporadic amyotrophic lateral sclerosis
SCA	spino-cerebellar ataxia
SDS	sodium dodecyl sulfate
SDS-PAGE	sodium dodecyl sulfate-polyacrylamide gel electrophoresis
sec	seconds
Sec	secretory
SH2	Src homology domain 2
SNARE	soluble NSF-attachment protein receptor
SOD1	superoxide dismutase 1

synp	synaptophysin
TAP	tandem affinity purification
TBS	tris-buffered saline
TFBS	transcription factor-binding sites
TGN	trans-Golgi network
TLCK	N^a-*p*-tosyl-L-lysine-chloromethyl ketone
TPCK	*N*-tosyl-L-phenylalanine-chloromethyl ketone
t-SNARE	target SNARE
Triton X-100	t-octylphenoxypoly-ethoxyethanol
Tween-20	polyoxyethylene-sorbitan monolaurate
UTR	untranslated region
vEGF	vascular epidermal growth factor
Vps	vacuolar protein sorting
v-SNARE	vesicle SNARE
WC	whole-cell (homogenate)
WGS	whole genome shotgun
WT	wild-type
X-Gal	5-bromo-4-chloro-3-indolyl-β-d-galactoside
Ypt	yeast protein transport (Rab protein)

List of Figures and Table

Figures

Table

Chapter 1. Introduction

Overview

Eukaryotic cells contain numerous organelles that function independently
or in tandem to promote cell survival, growth, and differentiation. In many
instances, cellular processes require the sequential activities of proteins that reside
in different organelles. In other circumstances, cellular homeostasis necessitates
chemical reactions that are in direct competition with each other. Sequestering
these reactions in different organelles ensures that each can occur unabated. In
both of these cases, specific compartmentalization within cells is crucial to normal
cellular function. To this end, cells must go to great lengths to ensure that each
organelle has its own identity and that this identity is maintained. The premier
paradigm that illustrates this is the complex regulation that is observed in the
secretory pathway (Palade, 1975). Proteins destined for secretion are synthesized
and transported in a precise order to a number of specific locations throughout the
cell prior to their delivery to the cell surface. This pathway is not only involved
in protein secretion, but it is also responsible for the transport of proteins to
organelles of the endocytic system.

Mammalian lysosomal sorting system

Protein transport to the lysosome is one of the major trafficking diversions found in the secretory pathway. The lysosome is involved in macromolecular turnover, due to its acidic nature and high content of hydrolases (Glauman and Ballard, 1987). Both proteins destined for degradation and the lysosomal proteases that degrade these proteins must be transported to the lysosome. An intriguing aspect of the hydrolase trafficking is that they must be kept catalytically inactive prior to lysosomal delivery; otherwise proteins with which they come into contact may be degraded prematurely.

Like secretory proteins, many lysosomal hydrolases contain signal sequences that direct these proteins to the endoplasmic reticulum (ER) where they enter the secretory pathway. Upon translocation into the lumen of the ER, the signal peptide is cleaved and core oligo-saccharides are added to the protein (Kornfeld and Mellman, 1989). The hydrolases are then transported to the Golgi complex, where they are further modified resulting in the acquisition of a specific modification of mannose-6-phosphate (M6P) (Kornfeld and Mellman, 1989). At the trans-Golgi network (TGN), lysosomal proteins containing M6P are sorted away from proteins destined for secretion by specific M6P receptors (M6PRs) (Ghosh *et al.*, 2003). Two M6PRs have been identified (MPR46, MPR300) that can be distinguished by their size and affinity for divalent cations (Kornfeld, 1992). Both of these receptors are required for appropriate lysosomal protease

trafficking as cell lines that lack either secrete lysosomal proteins to varying

degrees (Gabel *et al.*, 1983); (Koster *et al.*, 1993). Receptor-bound M6P-

containing proteins are incorporated into clathrin-coated vesicles at the TGN

(reviewed in (Ghosh *et al.*, 2003)) by means of two signals in the cytoplasmic

tails of the M6PR (Johnson and Kornfeld, 1992). Interaction with AP1 (Honing

et al., 1997) and Golgi-localized, γ-ear-containing, ADP-ribosylation factor-

binding (GGA) (Puertollano *et al.*, 2001); (Zhu *et al.*, 2001); (Doray *et al.*, 2002)

adaptor proteins is required for the M6PR:M6P complex to leave the TGN (Ghosh

et al., 2003). After fission of the clathrin-coated vesicle, the coat is removed and

the vesicles are transported to endosomes, where the decrease in lumenal pH

drives the dissociation of M6P-containing molecules from their receptors (Ghosh

et al., 2003). The hydrolases are then delivered to the lysosome, while the

receptors are recycled back to the TGN in an unknown process that is thought to

involve the mammalian retromer complex (Arighi *et al.*, 2004), Rab9, and TIP47

(Ghosh *et al.*, 2003).

     The importance of lysosomal protease trafficking is appreciated when

considering the number of diseases that are associated with mutations in this

pathway. These diseases affect different stages of the pathway and can be severe

(Kornfeld, 1986). In addition, carcinoma cell lines have been characterized that

secrete lysosomal proteases, and it has been argued that this may increase

metastatic potential by enabling these cells to degrade the extracellular matrix of

target tissues (Poole *et al.*, 1978); (Dobrossy *et al.*, 1980). These findings show the importance of appropriate lysosomal trafficking and thus provide a rationale for thorough investigation of this protein transport pathway.

Yeast vacuolar sorting system

While much information was gained from studies in mammalian cell systems, the utility of yeast genetics and the apparent conservation of the secretory pathway (Overdier *et al.*, 1997); (Pryer *et al.*, 1992); (Rothman and Orci, 1992) led researchers to perform genetic selections in yeast with hopes of identifying the trans-acting machinery that was responsible for lysosomal protein trafficking. Three independent genetic selections and/or screens were conducted to uncover mutant yeast strains that were unable to transport protein to the yeast vacuole, which is the equivalent of the mammalian lysosome (Jones, 1977); (Rothman and Stevens, 1986); (Bankaitis *et al.*, 1986); (Robinson *et al.*, 1988); (Rothman *et al.*, 1989); (Wada *et al.*, 1992). The vacuolar protein sorting (*vps*) mutants identified were placed into 36 complementation groups, presumably representing 36 different gene products whose function is required for vacuolar protein transport. Additional *vps* complementation groups were also identified in a number of studies leading to the identification of more than 50 gene products involved in this protein trafficking pathway ((Raymond *et al.*, 1992); reviewed in (Stack *et al.*, 1995); (Conibear and Stevens, 1998)). Research over the last 15

years has been focused on determining the functions of the specific gene products identified by these genetic approaches, which has greatly furthered our understanding of not only the vacuolar protein sorting pathway, but also the general processes involved in protein trafficking events.

Biochemical and genetic characterization of the yeast vacuolar protein transport pathway has revealed that, similar to the mammalian system, transport is receptor-mediated. In contrast with mammalian cells, however, yeast do not have a carbohydrate recognition system for vacuolar proteases. Instead, soluble hydrolases are transported by receptors that recognize specific NH_2-terminal amino acid sequences found in these vacuolar proteins (Stevens *et al.*, 1982); (Klionsky *et al.*, 1988); (Schwaiger *et al.*, 1982); (Winther *et al.*, 1991). One of these receptors, Vps10p, was identified as the receptor responsible for vacuolar delivery of carboxypeptidase Y (CPY) (Marcusson *et al.*, 1994). Vps10p binds CPY in the trans-Golgi and transports it to the endosome, a prevacuolar carrier. Upon arrival and fusion with the endosomal intermediate, the receptor dissociates from CPY and is delivered back to the Golgi for another round of sorting. CPY moves on to the vacuole where it is activated. The vesicle-mediated transport of the receptor:ligand complex from the TGN to the prevacuolar endosome involves many trans-acting cellular components and these are briefly described in Figure 1.
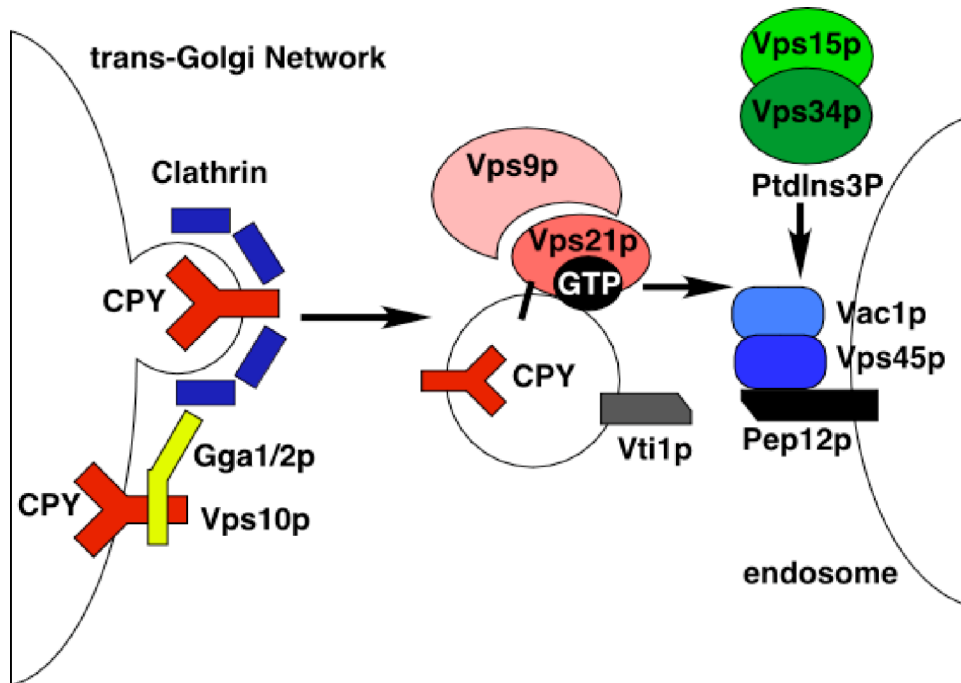
Figure 1. Vesicular transport of CPY to the endosome. CPY binds to its receptor, Vps10p, in the late Golgi where it is packaged into clathrin-coated vesicles via interactions between Vps10p and AP1 (not shown) and the GGA proteins (Hirst *et al.*, 2000); (Deloche *et al.*, 2001); (Deloche *et al.*, 2001). Transport of the vesicle requires activation of the Rab GTPase, Vps21p, by Vps9p (Tall *et al.*, 2001), a process which is necessary for endosomal fusion (Horazdovsky *et al.*, 1994). Activated GTP-bound Vps21p interacts directly with Vac1p to dock the transport vesicle with the early endosome (Peterson *et al.*, 1999); (Tall *et al.*, 1999). Vac1p binds to Vps45p (Sec1 homologue) (Peterson *et al.*, 1999); (Tall *et al.*, 1999), which then interacts with Pep12p (Burd *et al.*, 1997) to drive fusion mediated by the SNARE proteins on both the vesicle (v-SNARE: Vti1p) and target (t-SNARE: Pep12p) membranes. Recruitment of Vac1p to the early endosome also requires the local production of PI(3)P (Peterson *et al.*, 1999); (Tall *et al.*, 1999), generated by the sequential action of the protein and lipid kinases, Vps15p, and Vps34p, respectively (Stack *et al.*, 1995). In humans, the Vps34 homologue (hVps34) binds directly to GTP-bound Rab5 (Vps21p homologue), suggesting that PI(3)P production may also be regulated by Rab activation (Christoforidis *et al.*, 1999b).

Regulation of the Vps21p/Rab5 nucleotide-binding cycle

The yeast protein Vps21p and its mammalian homologue, Rab5, are Rab

GTPases and members of the Ras superfamily of GTPases. Based on the large

number of Rab GTPases in yeast (11) and humans (>60) (Pfeffer, 2001); (Zerial

and McBride, 2001) and their distinct patterns of localization (reviewed in (Zerial

and McBride, 2001), Rab GTPases are thought to provide specificity to

membrane transport events. Like other GTPases, Rabs are regulated by their state

of nucleotide binding. Activated or GTP-bound Rab proteins are capable of

binding to a host of effector proteins which are responsible for vesicle docking

and fusion with target membranes (Zerial and McBride, 2001). Thus, Rab

GTPases can be considered as molecular switches which are "turned on" by GTP

loading and "turned off" by GTP hydrolysis. Not only does this ensure

directionality in trafficking events, it also provides a mechanism of recycling Rab

proteins to donor membrane (GDP-bound) for repeated use.

Activation of Rabs, like other GTPases, occurs by the action of specific

proteins called guanine nucleotide exchange factors (GEFs) (see Figure 2 for

Rab5 cycle). Structural studies of Ras have shown that GTP-binding causes the

GTPase to undergo a conformational change in two regions of the protein,

designated switch 1 and switch 2 (Sprang, 1997), creating a new surface for

interaction with specific effector proteins. Recent studies have shown this to be a

common method used by many small GTPases of the Ras superfamily (e.g.

Vps21p/Rab5: (Esters *et al.*, 2000); (Merithew *et al.*, 2001); (Zhu *et al.*, 2003)).

Rab effector proteins have a diverse array of functions and are thought to create

unique microdomains which ensures the specificity of each trafficking event

(Zerial and McBride, 2001). Although Rab GTPases have an intrinsic rate of GTP hydrolysis, GTPase-activating proteins (GAPs) are capable of catalyzing this event (e.g. Rab5: (Xiao *et al.*, 1997); (Lanzetti *et al.*, 2000)). In the GDP-bound state, Rabs can be sequestered by Rab•GDP-dissociation inhibitor (GDI) proteins and returned to the donor membrane, where they can participate in another round of trafficking (Pfeffer, 1994). Recently, Pfeffer and colleagues showed that Yip3 functions as a RabGDI-dissociation factor (GDF) and catalyzes the release of GDI from the endosomal Rab, Rab9 (Sivars *et al.*, 2003). In this form, GEFs are capable of interacting with the Rab, stimulating GTP-loading and activating the Rab (e.g. Rab5: (Horiuchi *et al.*, 1997); (Hama *et al.*, 1999); (Tall *et al.*, 2001); (Saito *et al.*, 2002)).
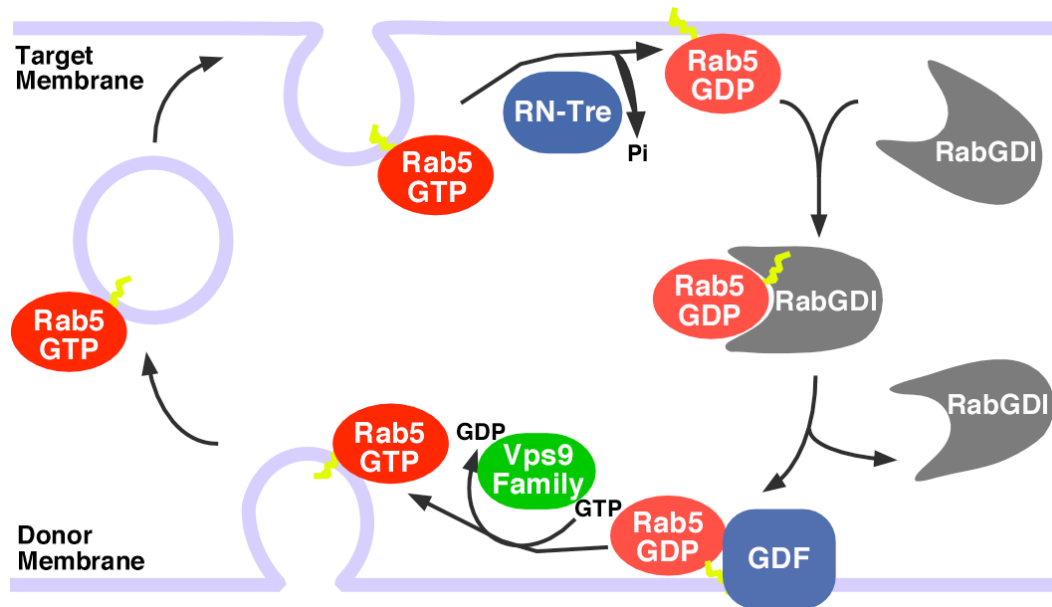
Figure 2. Rab5 nucleotide-binding cycle. GEFs of the Vps9 family catalyze GDP release on Rab5 on the donor membrane. Subsequently, GTP is loaded and Rab5 is competent to interact with its specific effector proteins and drive fusion at the target membrane. GTP hydrolysis is catalyzed by Rab5 GAP proteins RN-Tre and tuberin (not shown) and GDP-bound Rab5 is recycled back to the donor membrane by RabGDI. RabGDI is then displaced by a GDF activity, which is thought to belong to the Yip family of proteins. Free GDP-bound Rab5 is then capable of interacting with Rab5 GEFs and the cycle can proceed again.

Though small G-proteins can be regulated at many points in the nucleotide-binding and hydrolysis cycle, in the case of Rab proteins, the main aspect of specificity and regulation appears to be controlled at the level of exchange factor. It is well appreciated that Rab GEFs show extreme substrate specificity, even among related Rab proteins (reviewed in (Seabra and Wasmeier, 2004); for Vps21p/Rab5 GEFs: (Hama *et al*., 1999); (Tall *et al*., 2001). Furthermore, mutant forms of Rabs that are locked in their GTP-bound or

activated state can often fully replace a wild-type Rab protein that undergoes the

standard GTP-GDP cycle. Thus activation of Rab proteins is necessary and

sufficient for their function.
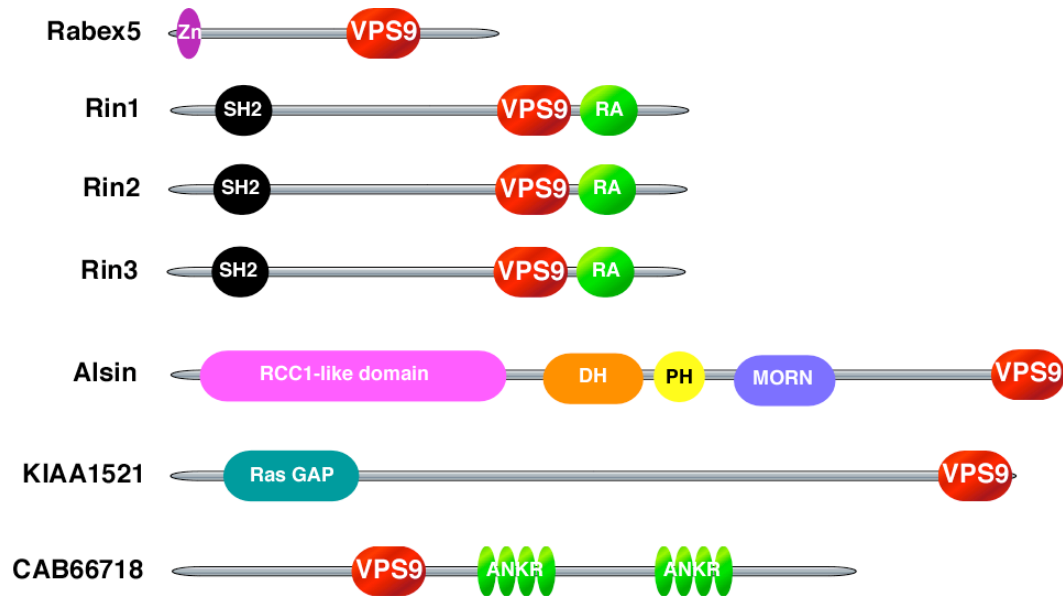
Figure 3. Mammalian proteins containing Vps9 domains. Shown are the seven proteins known to possess Vps9 domains. Note the presence of other domains commonly found in proteins involved in signal transduction cascades (SH2, RA), phospholipid binding (PH, MORN), and cytoskeletal interactions and/or rearrangements (AnkR, DH/PH). Abbreviations: Zn-Zinc^{2+} binding domain, SH2-Src homology 2, Rin-Ras inhibitor, RCC1-Regulator of chromatin condensation, RA-Ras association domain, DH-Dbl homology domain, PH-Pleckstrin homology domain, MORN-Membrane occupation and recognition nexus, Ras GAP-Ras GTPase-activating protein, AnkR-Ankyrin repeats.

Vps21p/Rab5 function

Vps21p and Rab5 are the Rab GTPases that regulate trafficking to

endosomal structures. In yeast, Vps21p is involved in transport of proteins from

both biosynthetic (TGN-derived) and endocytic routes (plasma membrane-derived) (Horazdovsky *et al.*, 1994); (Gerrard *et al.*, 2000). While one study has implicated Vps21p's mammalian homologue, Rab5, in the biosynthetic delivery of proteins from the TGN (Mattera *et al.*, 2003), the function of Rab5 in the endocytic pathway is far more appreciated. Studies by Zerial and colleagues showed that Rab5 regulates membrane trafficking to early endosomes during endocytosis (Gorvel *et al.*, 1991); (Bucci *et al.*, 1992), and that GTP hydrolysis by Rab5 was a timer that regulated the rate of endosomal fusion (Rybin *et al.*, 1996). How does Vps21p/Rab5 coordinate endosomal fusion events? In the case of Vps21p, GTP-bound Vps21p interacts with Vac1p, which interacts with Vps45p (Sec1 homologue), to couple the transport vesicle to Pep12p, the t-SNARE (Tall *et al.*, 1999); (Peterson *et al.*, 1999). In the case of Rab5, the situation is much more complex. Activated Rab5 binds to a host of effector proteins that have distinct functions in endosomal fusion and/or vesicle motility (Zerial and McBride, 2001). Early-endosomal antigen 1 (EEA1), which was shown to be recruited to endosomes in a Rab5•GTP and phosphotidylinositol-3-phosphate kinase (PI(3)K)-dependent manner (Simonsen *et al.*, 1998), is the critical component required for endosomal fusion (Christoforidis *et al.*, 1999a). EEA1 contains two phosphatidylinositol-3-phosphate (PI(3)P) and two Rab5•GTP interaction domains and functions to pull together or "tether" transport vesicles and early endosomes (heterotypic fusion), or two populations of early endosomes

(homotypic fusion) (Zerial and McBride, 2001). This fits well with previous data that showed Rab5 must be present on both target and donor membranes for fusion to occur (Barbieri *et al.*, 1998); (Rubino *et al.*, 2000). The mechanism for endosomal fusion is not well understood but seems to involve transient recruitment of syntaxin-13 (t-SNARE) via the formation of oligomeric structures of EEA1 containing NSF (McBride *et al.*, 1999).

In addition to EEA1, other effector proteins bind to Rab5 in a GTP-dependent manner. For instance, rabenosyn-5 was recently shown to play a role in endosomal fusion by interacting with hVps45, in a mechanism similar to that described above for Vac1p in the yeast system (Nielsen *et al.*, 2000). In addition, rabaptin proteins are known to stimulate endosomal fusion events, apparently through a positive feedback loop mediated by their interaction with and activation of the Rab5 exchange factor, Rabex-5 (Horiuchi *et al.*, 1997); (Gournier *et al.*, 1998); (Lippe *et al.*, 2001). Activated Rab5 has also been shown to bind two PI(3) kinases (Christoforidis *et al.*, 1999b), one of which, hVps34/p150, is thought to generate PI(3)P on the endosomal membranes (Zerial and McBride, 2001). This local production of PI(3)P is expected to recruit PI(3)P-binding proteins such as EEA1 to endosomes. Human Vps34/p150-also regulates vesicle loading and transport along microtubules in a Rab5•GTP-dependent manner (Nielsen *et al.*, 1999). It is clear that Rab5 activation results in its interaction with

a multitude of effector proteins, which function in endosomal delivery, targeting, and subsequent fusion of transport vesicles.

Rab5-mediated endocytosis and signal transduction

The requirement for Rab5 activation in endocytosis was originally identified by the work of Zerial and colleagues, who showed that mutant Rab5 that was incapable of binding GTP inhibited both fluid-phase and receptor-mediated endocytosis (Bucci *et al.*, 1992). Rab5 modulates endocytosis by regulating fusion of plasma membrane-derived vesicles with endosomes and homotypic endosome-endosome fusion (Gorvel *et al.*, 1991); (Bucci *et al.*, 1992). It has been shown that Rab5 is rate-limiting for endosomal fusion (Bucci *et al.*, 1992) and that Rab5 activation serves as a timing mechanism for this reaction (Rybin *et al.*, 1996). GTP-bound Rab5 interacts with several effector proteins which promote membrane tethering, docking, and fusion (Zerial and McBride, 2001). In addition, roles for Rab5 in modulating the half-life of clathrin-coated pits and/or vesicle budding have been proposed (Bucci *et al.*, 1992); (McLauchlan *et al.*, 1998).

The initial work describing Rab5 function in endocytosis focused simply on constitutive endocytosis (Bucci *et al.*, 1992). Since then, numerous studies have shown that Rab5 activation is required for receptor-mediated endocytosis of many different extracellular ligands. Rab5 regulates endocytic trafficking of both

receptor-tyrosine kinases (RTKs) and G-protein coupled receptors (GPCRs),

indicating that it is a general modulator of endocytosis (Somsel Rodman and

Wandinger-Ness, 2000); (Sorkin and Von Zastrow, 2002); (Seachrist and

Ferguson, 2003). Rab5 activation in response to ligand stimulation requires the

GEF activity of proteins of the Vps9 family (Figure 3). In addition to published

reports, database mining suggests the presence of at least seven different human

proteins that contain Vps9 domains. Rabex-5, the first mammalian Rab5 GEF to

be discovered, appears to function in complex with the Rab5 effector protein,

Rabaptin (Horiuchi *et al.*, 1997). The mechanism for regulation of Rabex-5 is

unknown but we have shown that Rabex-5 is monoubiquitinated and that

membrane association requires the NH_2-terminus (Topp, J.D., Davies, B.A., and

B.F. Horazdovsky, unpublished results). Vps9p, the founding member of the

Vps9 family and homologue of Rabex-5, interacts with ubiquitin and is also

monoubiquitinated. Mutation of a key residue that blocks ubiquitin binding and

monoubiquitination impairs Ste3p endocytosis presumably by impairing Vps9

GEF activity towards Vps21p (Davies *et al.*, 2003). Studies are underway to

determine if Rab5 activation by Rabex-5 is similarly regulated.

In addition to Rabex-5, mammals possess several other Vps9 domain-

containing proteins, all of which have other domains implying roles for these

proteins in signal transduction, cytoskeletal rearrangement, and membrane

trafficking events. For instance, the Rin proteins all contain SH2 domains, which

are known to interact with phosphorylated tyrosine residues. Our lab has shown

that the Rab5 GEF activity of Rin1 specifically modulates EGFR endocytosis

through its interactions with phosphorylated receptor (Barbieri *et al.*, 2003) and

activated Ras (Tall *et al.*, 2001) (Figure 4). Since the SH2 domains of the

different Rin proteins are quite distinct, it is intriguing to speculate that the Rin

proteins interact with and regulate the endocytosis of distinct RTKs.
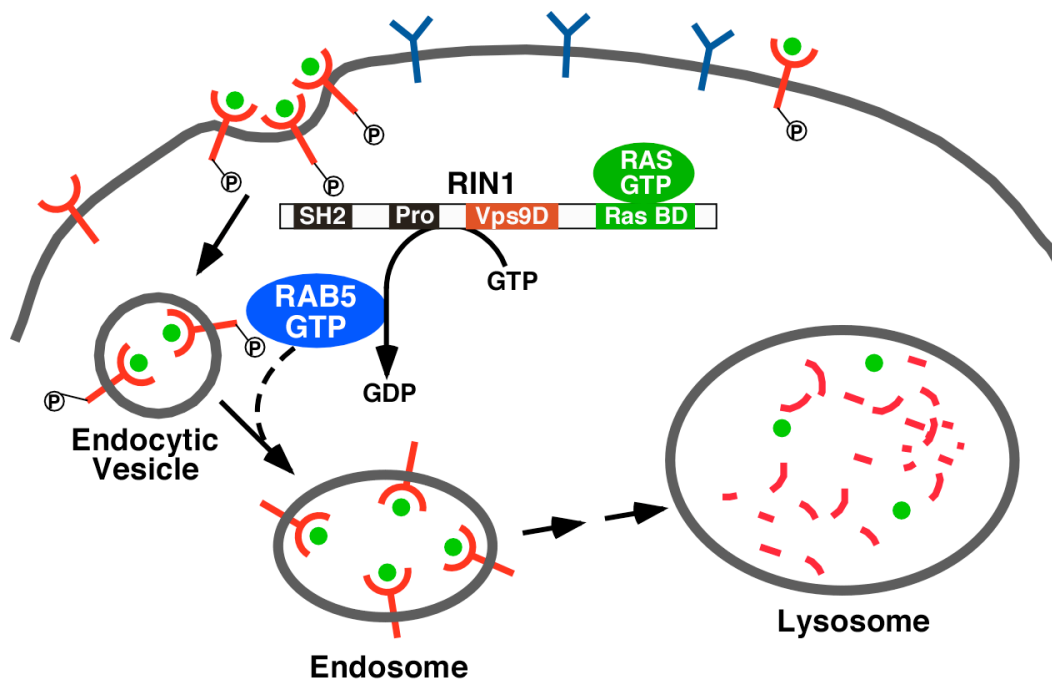
Figure 4. Rin1 regulation of EGFR endocytosis. EGF interacts with its receptor, EGFR, stimulating EGFR dimerization, autophosphorylation, and activation of signaling pathways including Ras. Phosphorylated EGFR recruits Rin1 and GTP-bound Ras potentiates Rin1 Rab5 GEF activity, serving to modulate EGFR endocytosis by activated Rab5.

Endocytosis has long been considered simply a mechanism of downregulation of extracellular ligands following their activation of signal transduction pathways at the cell surface. Indeed, receptor downregulation is crucial to normal cellular function, as cells containing high levels of hyperactivated EGF-receptor become transformed (reviewed in (Yarden and Sliwkowski, 2001)). However, work over the last ten years has shown that endocytosis is not simply a means of attenuating signaling. Much work has been focused on the interplay between signal transduction and endocytosis, as evidenced by the number of excellent reviews devoted to this topic in the last few years alone (Ceresa and Schmid, 2000); (Cavalli *et al.*, 2001); (Di Fiore and De Camilli, 2001); (McPherson *et al.*, 2001); (Clague and Urbe, 2001); (Wiley and Burke, 2001); (Sorkin and Von Zastrow, 2002); (Grimes and Miettinen, 2003); (Teis and Huber, 2003); (Miaczynska *et al.*, 2004b). The idea that endocytosis and signaling may be more intimately connected was put forth initially by Bergeron, Posner, and colleagues. They showed that upon EGF or insulin stimulation endosomes contain the majority of phosphorylated receptor and that insulin receptor tyrosine kinase activity was highest in endosomes (reviewed in (Baass *et al.*, 1995); (Bevan *et al.*, 1996)). In addition, it was observed that several intermediate proteins in both signaling cascades were localized to endosomes upon ligand stimulation (Baass *et al.*, 1995); (Bevan *et al.*, 1996). While these data indicate that signaling may occur on endosomes, they do not

demonstrate that endocytosis is required for signaling. To address this, Vieira et

al. inhibited receptor internalization and analyzed the effects on the EGF signal

transduction pathway. They found that endocytosis was required for some aspects

of EGF signaling, but not all (Vieira *et al.*, 1996). Others have disputed this and

shown that impairment on internalization has no effects on the EGF signaling

pathway (reviewed in (Leof, 2000)). While this discrepancy may be frustrating, it

is probably due to differences in receptor expression and cellular context. Many

of these studies use model systems in which the receptor is overexpressed 100-

1000-fold. Therefore, it will be of great importance in the future to study the

effects of receptor endocytosis on EGF signal transduction in cells expressing

physiologically relevant levels of receptor.

       Work on other receptors has suggested that indeed internalization is

required for signal transduction by some extracellular ligands. For instance, IGF-

1 signaling has been shown to require endocytosis (Chow *et al.*, 1998) mediated

by dynamin and beta-arrestin (Lin *et al.*, 1998). Expression of mutant versions of

both of these proteins blocked endocytosis of the IGF-1 receptor and impaired the

activation of the signaling intermediates ERK1/2 and Akt and also inhibited IGF-

1 stimulated gene activation (Lin *et al.*, 1998); (Povsic *et al.*, 2003). An

overwhelming amount of evidence suggests that signal transduction by the

neurotrophic growth factors also requires endocytosis (reviewed in (Howe and

Mobley, 2005)). This is of particular interest in neurons where the retrograde

transport of activated receptors from the axon tip to the cell body is required for a robust signaling response (Riccio *et al.*, 1997); (Watson *et al.*, 1999); (Watson *et al.*, 2001); (Ye *et al.*, 2003).

How could Rab5 activation regulate signal transduction? If a receptor signals primarily from the cell surface, endocytosis would be expected to attenuate signaling by decreasing the half-life of the interaction between activated receptors and signaling intermediates. Studies with the Rab5 GEF Rin1 showed that overexpression of wild-type protein stimulated endocytosis and caused a decrease in ERK1/2 activation (Tall *et al.*, 2001) (Figure 4). Furthermore, a naturally occurring splice variant of Rin1 which lacks an intact Vps9 domain increased ERK1/2 phosphorylation while inhibiting EGFR endocytosis (Tall *et al.*, 2001).

In neurons, however, Rab5-mediated endocytosis may serve to positively modulate signal transduction pathways. It is known that retrograde transport of nerve growth factor (NGF) and its receptor, TrkA, is required for NGF-mediated signal transduction in sympathetic neurons (Riccio *et al.*, 1997). Similar results were obtained with the related neurotrophin, BDNF (brain-derived neurotrophic factor) and its receptor, TrkB (Watson *et al.*, 1999). In PC12 cells, NGF stimulation results in the formation of signaling endosomes (Beattie *et al.*, 1996) which seem to function as a platform for signal transduction since they contain many activated signaling intermediates as well as Rab5 (Howe *et al.*, 2001).

Thus, in neurons, Rab5 activation would be expected not to inhibit, but possibly promote signal transduction.

Scenarios can be drawn in which Rab5 can positively or negatively regulate signaling, albeit indirectly, by modulating receptor localization upon ligand stimulation. Recent work has also shown that Rab5 can regulate signaling directly. Miaczynska et al. reported that two effectors of Rab5, APPL1/2 (adaptor protein containing PH domain, PTB domain, and leucine zipper motif; PTB: phospho-tyrosine binding domain), translocate to the nucleus and modify gene expression upon EGF stimulation (Miaczynska *et al.*, 2004a). This signaling pathway required internalization of the EGFR and GTP-bound Rab5 (Miaczynska *et al.*, 2004a). A direct role for Rab5 in signal transduction was also shown in another study in which activation of Rab5 was shown to be required for the formation of actin-enriched circular ruffles (Lanzetti *et al.*, 2004). These direct effects on signal transduction, coupled with the indirect effects described above, show that the outcome of Rab5 activation may be much greater and more diversified than originally anticipated. Clearly, further work is required to characterize the function of Rab5 and its activators.

The ALS2 gene product, Alsin, and ALS

In 2001, two groups independently discovered that mutations in a putative Rab5 GEF, termed Alsin, lead to juvenile forms of amyotrophic lateral sclerosis (ALS) and primary lateral sclerosis (PLS) (Hadano *et al.*, 2001); (Yang *et al.*, 2001). Since the initial discovery, several other mutations in Alsin have been described that result in ALS, JPLS, and infantile-onset ascending hereditary spastic paralysis (IAHSP) (Eymard-Pierre *et al.*, 2002); (Devon *et al.*, 2003); (Gros-Louis *et al.*, 2003). All of the mutations identified are predicted to result in the premature truncation of Alsin (Figure 5). Thus, it is expected that loss-of-Alsin function leads to the diseased state. Northern analysis revealed the presence of two forms of ALS2: the normal or "long" form and a shorter form (Hadano *et al.*, 2001) (see Figure 5). The short form of Alsin has never been detected at the protein level, and when referring to Alsin herein, only the long form is considered.

ALS is a heterogeneous neurodegenerative disorder characterized by the progressive degeneration of upper and motor neurons (Brown, 2001); (Rowland and Shneider, 2001). Neurons in the cerebral cortex, brainstem, and spinal cord are primarily effected, and death due to respiratory failure is common within 3-5 years of symptom onset (Brown, 1995). Although most cases of ALS are sporadic (sporadic ALS, SALS), approximately 5-10% of cases have known genetic links (Cleveland and Rothstein, 2001) and are referred to as familial ALS

(FALS). Eight chromosomal loci have been described and further mapping has revealed two genes that when mutated lead to ALS (Bruijn *et al.*, 2004). The first gene identified encodes SOD1 (superoxide dismutase 1), mutations in which are responsible for 15-20% of FALS and 1-2% of all of the cases of ALS (Cleveland and Rothstein, 2001). Mutations have been identified throughout the SOD1 protein, some of which have no effect on normal SOD1 free radical scavenger activity, indicating that SOD1-related disease is due to a toxic, but unknown gain-of-function (Bruijn *et al.*, 2004). This is in contrast with Alsin-related disease, in which mutations in Alsin are expected to lead to a loss-of-function (see above).

The utility of mouse genetics has provided researchers with much insight into the pathology of ALS. Many of the SOD1 point mutants identified in patients have been introduced into mice, and these mice have proven to be useful models for SOD1-related disease. In addition, these animals exhibit markedly similar pathology to patients with sporadic ALS (Bruijn *et al.*, 2004). Based on these and other studies, five hypotheses have been proposed for the neurodegeneration observed in ALS (Bruijn *et al.*, 2004). The first hypothesis postulates that toxicity is due to the aggregation of proteins. This hypothesis has been proposed for other neurodegenerative diseases, including Alzheimer's disease, spino-cerebellar ataxia (SCA), Huntington's disease, and Parkinson's disease (Ross and Poirier, 2004). While the formation of intracellular aggregates has been observed in neurons affected by disease, it is unknown whether this is

responsible for disease progression or is, in fact, a protective mechanism used by cells to sequester toxic proteins. An important characteristic of these aggregates is that they are intensely reactive to anti-ubiquitin antibodies (Bruijn *et al.*, 2004). These data would suggest that aggregation may lead to a disruption in proteasome-mediated degradation of other proteins. However, it is also likely that accumulation of protein aggregates within the cell would disrupt several normal cellular functions indirectly.

The second hypothesis for ALS disease manifestation is motor neuron death due to aberrant oxygen radical processing. Although this hypothesis is now considered less favorable than others, it was initially proposed due to the normal function of SOD1. However, studies have shown that several of the mutations identified in patients with ALS do not affect SOD1 activity (Cleveland and Rothstein, 2001), indicating that SOD1-related disease is not due to a defect in SOD1 function. Although a role for oxygen radicals in neurodegeneration may still exist, it is not likely the primary causative factor in motor neuron death.

Abnormal regulation of the neurofilament cytoskeleton has also been suggested to play a role in ALS disease. ALS is known to affect neurons which have high levels of neurofilaments (Bruijn *et al.*, 2004), and mutations in or accumulation of neurofilament subunits have been observed in patients with ALS (Shaw and Eggett, 2000). Remarkably, it has been shown that overexpression of the heavy neurofilament subunit (NF-H) is the most effective treatment for SOD1

mutant mice (Bruijn *et al.*, 2004), prolonging survival by up to six months

(Couillard-Despres *et al.*, 1998). How this protects the animal is unknown, but it

has been proposed that NF-H acts as a sink or buffer for some other harmful

process (Bruijn *et al.*, 2004). Perhaps overexpressed NF-H binds directly to

SOD1 and prevents the accumulation of the larger toxic aggregates. However, it

has also been shown that overexpression of human NF-H in normal mice itself

leads to a phenotype similar to ALS, due to a disruption in axonal trafficking

(Cote *et al.*, 1993); (Collard *et al.*, 1995). Clearly, motor neurons must precisely

regulate the level and location of neurofilament proteins, and further work is

required to explain the role of these proteins in neurodegeneration.

The fourth hypothesis for ALS disease manifestation is apoptotic neuronal

death due to glutamate excitotoxicity. Glutamate binding to receptors causes ion

channels to open allowing calcium to enter through NMDA receptors, AMPA

receptors lacking the GluR2 subunit (see below), or voltage-gated calcium

channels (Heath and Shaw, 2002). Normally, this influx is regulated by receptor

endocytosis of the glutamate receptors or by the removal of glutamate at the

synaptic cleft via the glutamate transporter proteins. However, increases in

glutamate could bypass both of these protective mechanisms leading to

hyperactivation of the channels and continuous membrane permeability to

calcium. Intracellular calcium activates a number of calcium-dependent pathways

that contribute to cytotoxicity including: proteases, endonucleases, protein kinases/phosphatases, and phospholipases (Heath and Shaw, 2002).

Elevated levels of glutamate in the cerebrospinal fluid have been reported in patients with ALS (Bruijn *et al.*, 2004). In addition, a mutation in the primary glutamate transporter, EAAT2 (excitatory amino acid transporter 2), has been observed in a patient with sporadic ALS, and decreased levels of EAAT2 protein diminish glutamate uptake, leading to neuronal death (Trotti *et al.*, 2001); (Rothstein *et al.*, 1995); (Rothstein *et al.*, 1996). It is possible that this excess glutamate then binds to cell surface glutamate receptors and triggers calcium influx. Indeed, the only drug approved by the FDA (United States Food and Drug Administration) for ALS, riluzole, appears to act in part by limiting glutamate release (Cleveland and Rothstein, 2001). Motor neurons appear to be the cell type most susceptible to ALS and they are also deficient in the calcium-binding proteins paravalbumin and calbindin D28K (Ludolph *et al.*, 2000). These observations suggest that motor neurons may lack an ability to sequester calcium. In addition, motor neurons are thought to express a much lower level of the calcium-impermeable glutamate receptor, GluR2 (Cluskey and Ramsden, 2001), implying that the glutamate receptor channels in these neurons may be more permeable to calcium. Elevated calcium triggers apoptosis in motor neurons as evidenced by the activation of caspases and mitochondrial release of cytochrome c (Kostic *et al.*, 1997); (Li *et al.*, 2000); (Vukosavic *et al.*, 2000); (Pasinelli *et al.*,

2000); (Guegan *et al*., 2001). Preventing apoptosis by the overexpression of Bcl-2 and inhibition of caspase activity and/or cytochrome c release prolongs survival in SOD1 mouse models of ALS (Kostic *et al*., 1997); (Li *et al*., 2000); (Zhu *et al*., 2002). It is currently unknown when exactly glutamate excitotoxicity appears in disease progression, however, as dead neurons are expected to release their glutamate into the extracellular fluid. Therefore, it may be that glutamate excitotoxicity is critical to the late stages of ALS, but other factors are more important to the initial onset of the disease.

The final and most recently proposed hypothesis for the neurodegeneration associated with ALS is toxicity due to abnormal retrograde axonal trafficking. Studies in mice showed that overexpression of dynamitin, a key negative regulator of the dynactin:dynein complex, resulted in the disruption of retrograde axonal transport (LaMonte *et al*., 2002). Intriguingly, these mice developed motor neuron and muscle defects that clearly resembled those observed in mouse models or patients with ALS (LaMonte *et al*., 2002). Soon after this study was published, it was reported that mutations in the dynein heavy-chain also result in progressive motor neuron degeneration (Hafezparast *et al*., 2003) and that mutations in dynactin may be a risk factor for ALS (Munch *et al*., 2004). Taken together, this work strongly suggests that retrograde transport mediated by the dynein:dynactin complex is required for normal motor neuron function. This makes sense since motor neurons are extremely large asymmetric cells in which

the cell body can be separated from the axon by up to one meter (Bruijn *et al.*, 2004). Thus, it is crucial that signals are appropriately transported from the axon to the cell body where gene activation occurs.

Although these five hypotheses for motor neuron degeneration have been presented independently, it is likely that several or all are responsible in part for ALS disease progression. For instance, axonal transport defects have been observed prior to disease onset in mouse models of ALS (Williamson and Cleveland, 1999), whereas aggregate formation better coincides temporally with neurodegeneration. As mentioned above, glutamate excitotoxicity may be involved later in disease progression, which might explain why riluzole has only a modest effect on survival (Bruijn *et al.*, 2004). While more work is required to characterize the involvement of retrograde transport defects in ALS, it is clear that this pathway is crucial for normal motor neuron function. Future studies that focus on the dissection of disease progression temporally are crucial to further our understanding of the mechanisms responsible for the neurodegeneration observed in ALS.

SHORT FORM

RCC1   DH   PH   MORN   VPS9

amino acid: 1   200   400   600   800   1000   1200   1400   1600

LONG FORM

nucleotide: 124   1000   2000   3000   4000   5000

261delA[1] 1130delTA   1990delCT 2660delAT[6] C3115T 3742delA[6] 4844delT[5]
138delA[2] 1130delAT[6] 1867delCT[2]

1594delGTTTCCCCCA
1471delGTTTCCCCCA[6]

1548delAG[1]

mutations affect both forms ← | → mutations affect long form only

Mutation	261 delA	1130 delTA	1548 delAG	1594 delGTTT CCCCCA	1990 delCT	2660 delAT	C3115T	3742 delA	4844 delT
Diagnosis	ALS2	IAHSP	JPLS	IAHSP	JPLS	IAHSP	IAHSP	IAHSP	IAHSP
Age of Onset	3–10 yr	18 mo	14 mo	18 mo	1–2 yr	16 mo	1 yr	1 yr	18 mo
First Symptom	SP or PS	MD	ST	MD	GD	SP	SP	ST	GD
Loss of Independent Walking (age)	12-50	4	NW-2	4	NW- 6	5	NW	NW	yes, age unknown
Dysarthria (age)	yes, age unknown	11	4	4	2–10	10	3	13	yes, age unknown
Current Age	7–60 (1990)	20	2–14 (1996)	18	10 & 15 (1995)	23	6 & 9	24–36	12
Age at Death	n/a	n/a	n/a	n/a	14	n/a	n/a	n/a	n/a

Figure 5. Mutations in Alsin leading to neurodegenerative disorders. Reproduced from Devon et al. (2003) with copyright permission. Shown are both the short and long forms of Alsin. Expression of the short form of Alsin has not been observed at the protein level. The table lists all of the published mutations with the corresponding clinical information for each patient (if known). Abbreviations for symptoms: ST = stiffness in legs; NW = no development of walking; GD = gait disturbance; SP = spasticity of legs; MD = motor disability in legs; PS = pseudobulbar syndrome; mo, months; yr, year/years; n/a, not applicable.

Research aims

The discovery that mutations in the Rab5 GEF Alsin lead to ALS (Hadano *et al.*, 2001); (Yang *et al.*, 2001) coincided precisely with the time that I began my doctoral work in the Horazdovsky lab. Our lab focuses primarily on the Vps9 family of proteins that catalyze guanine nucleotide exchange on Vps21p/Rab5. Therefore, my overall research goal was to determine how loss-of-Alsin function causes motor neuron degeneration. With this goal in mind there were several research aims that I was specifically interested in investigating: (1) Characterize the individual enzymatic activities of Alsin and determine the subcellular localization of Alsin and its domains; (2) Investigate the time of expression and tissue distribution of Alsin; (3) Determine the overall function of Alsin.

First, I wanted to perform an "initial characterization" of Alsin.   Since nothing was known about Alsin function, I was interested in determining the subcellular localization of Alsin and the individual activities of its subdomains. Computational methods suggested that Alsin would act as a GEF towards Rab5 and at least one member of the Rho family. To determine if Alsin indeed possesses these activities, I expressed and purified each of these domains (Vps9, DH/PH) and performed *in vitro* binding and guanine nucleotide exchange assays with the appropriate substrates. It was expected that the Vps9 domain of Alsin would interact specifically with and promote GEF activity on Rab5. Since computational methods cannot be used to determine which Rho GTPase Alsin

acts on, multiple Rho family members were expressed and tested for their interaction with Alsin. Once a candidate substrate was identified, nucleotide exchange assays were performed. It was necessary to perform these experiments *in vivo* since unlike Rab GEFs, many Rho GEFs require post-translational modification and/or phospholipids to promote activity.

Second, I used fractionation and indirect immunofluorescence methods to determine the subcellular localization of Alsin. An antibody to the Vps9 domain was generated for use in these studies. In addition, I overexpressed the individual domains of Alsin to determine if there are competing localization signals in Alsin.

Next, I was interested in exploring the pattern of expression of Alsin in mice. Preliminary evidence suggests that Alsin is expressed in most tissues, but with expression highest in the cerebellum (Hadano *et al.*, 2001). ALS pathology has never been reported in the cerebellum, and this suggests that Alsin-related disease may represent a completely novel form of neurodegeneration. To confirm the previous Northern results (Hadano *et al.*, 2001), the tissue distribution of Alsin protein was investigated. In addition to cerebellar expression, it was expected that Alsin is present in motor neurons of the cerebral cortex, brainstem, and spinal cord, as these areas are known to be key areas of pathology in ALS (Brown, 1995). Since mutations in Alsin lead to juvenile forms of disease, it was of interest to determine when and where Alsin is expressed throughout development. The cerebellum is composed of glia and two types of neuronal

cells, granule neurons and Purkinje fibers. It was thought to be of great interest to determine if Alsin is specifically expressed in one of these types of neurons, as this could aid in the development of hypotheses for Alsin function. These studies were conducted in collaboration with Michael Hayden's group at the Centre for Molecular Medicine, University of British Columbia, in Vancouver, B.C.

Finally, I wanted to determine the overall function of Alsin. Previous work in the Horazdovsky lab showed that the Vps9 domain-containing protein Rin1 specifically regulates the endocytosis of EGFR (Tall *et al.*, 2001); (see Figure 4). Due to the diversity of Vps9 family members, our lab postulates that different members of this family regulate the endocytosis of specific and distinct growth factors. To determine the receptor(s) that Alsin regulates, stable cell lines were generated that overexpressed full-length Alsin or Alsin lacking an intact Vps9 domain (ΔVps9d). Work on Rin1 showed that a naturally occurring splice variant which abolished Rab5 GEF activity affected EGF-mediated signaling by impairing EGFR endocytosis (Tall *et al.*, 2001). The Alsin stable cell lines were stimulated with various ligands, and signal transduction was monitored by the measurement of phosphorylation of intermediate molecules (ERK1/2, Akt) and the transcription of downstream target genes (*c-fos*). Once a signaling pathway was identified, the role of Alsin and ΔVps9d Alsin in the endocytic trafficking of the receptor was investigated.

Chapter 2. Alsin is a Rab5 and Rac1 guanine nucleotide exchange factor

Overview

   ALS2 is the gene mutated in a recessive juvenile form of amyotrophic lateral sclerosis (ALS2). *ALS2* encodes a large protein termed Alsin, which contains a number of predicted cell signaling and protein trafficking sequence motifs. To gain insight into the overall function of Alsin and to begin to evaluate its role in motor neuron maintenance, we examined the subcellular localization of Alsin and the biochemical activities associated with its individual subdomains. We found that the Vps9 domain of Alsin has Rab5 guanine nucleotide exchange activity. In addition, Alsin interacted specifically with and acted as a guanine nucleotide exchange factor for Rac1. Immunofluorescence and fractionation experiments in both fibroblasts and neurons revealed that Alsin is a cytosolic protein, with a significant portion associated with small, punctate membrane structures. Many of these membrane structures also contained Rab5 or Rac1. Upon overexpression of full length Alsin, the overexpressed material was largely cytosolic, indicating that the association with membrane structures could be saturated. We also found that Alsin was present in membrane ruffles and

lamellipodia. These data suggests that Alsin is involved in membrane transport events, potentially linking endocytic processes and actin cytoskeleton remodeling.

Introduction

Amyotrophic lateral sclerosis (ALS) is a heterogeneous neurological disorder characterized by progressive degeneration of motor neurons, usually causing death due to respiratory paralysis (Brown, 2001; Rowland and Shneider, 2001). Although mostly sporadic in nature, a genetic link has been established in 5-10% of ALS cases (Cleveland and Rothstein, 2001). Chromosomal mapping studies have identified six independent loci associated with the familial forms of ALS ((Siddique *et al.*, 1991; Rosen, 1993; Hentati *et al.*, 1994; Chance *et al.*, 1998; Hentati *et al.*, 1998; Hong *et al.*, 1998; Hosler *et al.*, 2000), and reviewed in (Cole and Siddique, 1999; Hand and Rouleau, 2002)). Molecular genetic analysis identified two genes, that when mutated, lead to ALS. The first discovered was the gene coding for Cu-Zn superoxide dismutase 1 (SOD1) (Rosen, 1993). Initially, mutations in SOD1 were thought to result in defective free radical scavenger activity. However, it is now generally accepted that the alterations in SOD1 that lead to ALS are due to an unknown, but toxic gain-of-function. The second gene identified is mutated in a juvenile form of ALS, *ALS2* (Hadano *et al.*, 2001; Yang *et al.*, 2001). Mutations in this gene lead to a rare recessive form of ALS that presents early in life and progresses much more

slowly than the classical form (Ben Hamida *et al.*, 1990; Hentati *et al.*, 1994).

Two small deletions in *ALS2* were originally associated with the disease (Hadano

et al., 2001; Yang *et al.*, 2001). Each is expected to severely truncate the

predicted protein product of *ALS2*. In addition, mutations in *ALS2* have recently

been associated with two other neurodegenerative disorders, juvenile-onset

primary lateral sclerosis (Yang *et al.*, 2001) and infantile-onset hereditary spastic

paraplegia (Eymard-Pierre *et al.*, 2002; Devon *et al.*, 2003; Gros-Louis *et al.*,

2003). Like the original mutations identified, these mutations are predicted to

generate prematurely truncated forms of the protein product.

The protein encoded by *ALS2*, Alsin, is predicted to contain numerous

domains implicating roles in cell signaling, membrane localization, and protein

transport events (Hadano *et al.*, 2001; Shaw, 2001; Yang *et al.*, 2001). The NH_2-

terminal region of Alsin consists of five repeats that show sequence homology

with RCC1 (Regulator of Chromatin Condensation 1; see Figure 6A). RCC1 has

been shown to function as a guanine nucleotide exchange factor (GEF) for the

Ran family of GTPases (Bischoff and Ponstingl, 1991). Although more than 90

proteins that contain one or more RCC1 repeats are present in databases (Bateman

et al., 2002), only RCC1 itself has Ran GEF activity. Alsin also contains

centrally located DH (Diffuse B-cell Lymphoma (Dbl) homology) and PH

(Pleckstrin homology) domains, a hallmark of guanine nucleotide exchange

factors for the Rho GTPase family (Zheng, 2001). Rho GTPases have been

shown to be involved in numerous signaling events, but their role in the regulation

of the actin cytoskeleton is the best characterized (Hall, 1998; Kaibuchi *et al.*,

1999; Sah *et al.*, 2000). C-terminal to the PH domain are eight copies of a

sequence motif called MORN (Membrane Occupation and Recognition Nexus)

(Takeshima *et al.*, 2000). This is a largely uncharacterized domain that is found

in a number of proteins, but its function is unknown. At its COOH-terminus,

Alsin also possesses a Vps9 domain. This domain specifically catalyzes guanine

nucleotide exchange on Rab5 and the yeast homologue Vps21p, thereby

activating the GTPases (Horiuchi *et al.*, 1997; Hama *et al.*, 1999; Tall *et al.*,

2001). Activation of Rab5 is essential for protein trafficking through the early

stages of the endocytic pathway.

To gain insight into the overall function of Alsin, we examined the

biochemical activities associated with its individual subdomains and explored the

subcellular localization of Alsin. We found that Alsin catalyzed guanine

nucleotide exchange on both Rab5 and Rac1. Endogenous Alsin localized to the

cytoplasm and punctate structures in neurons and fibroblasts. Overexpression of

full length Alsin indicated that association with these punctate structures could be

saturated. Moreover, endogenous Alsin partially colocalized with both Rab5 and

Rac. In addition, we found Alsin in actin-positive structures such as lamellipodia

and membrane ruffles. Taken together, our results suggest a potential role for

Alsin in membrane trafficking events through its regulation of the small GTPases
Rab5 and Rac1.

Material and methods

Strains and reagents

Bacterial strains used in this study were DH5α (Invitrogen), HMS174
(DE3) (Novagen), and BL21RIL (DE3) (Stratagene). Strains were grown in
Luria-Bertani (LB) medium supplemented with ampicillin and kanamycin as
needed (Miller, 1972). Vent DNA polymerase and restriction endonucleases were
purchased from New England Biolabs, Roche Molecular Biochemicals, and
Invitrogen. [^{3}H]-GDP was from PerkinElmers Life Sciences. Ni-NTA agarose
and penta-His antibody were from Qiagen Inc. Amylose resin was purchased
from New England Biolabs. Glutathione sepharose, CNBR-activated sepharose,
and Protein-A sepharose were from Amersham Biosciences. Monoclonal
antibody to GST was a generous gift of Drs. Michael Brown and Joseph Goldstein
(UT Southwestern Medical Center). Monoclonal Rab5, MAP2b, and EEA1
antibodies were from BD Biosciences. Monoclonal synaptophysin antibody was
from Sigma. Monoclonal Rac antibody was purchased from Upstate Cell
Signaling Solutions. Rhodamine-conjugated phalloidin and Alexa488/594-
conjugated rabbit and mouse secondary antibodies were from Molecular Probes.
Horseradish peroxidase-conjugated secondary antibodies were purchased from

Amersham Biosciences. SuperSignal West Femto Sensitivity substrate was from Pierce Biotechnology Inc. All other products were purchased from Sigma unless otherwise noted.

Plasmid and viral constructions

His$_6$-Rab5a, -5b, -5c, His$_6$-Rab4, and His$_6$-Rab11 E. coli expression constructs and Rab5A:S34N, 5B:S34N, and 5C:S34N-PVJL11 two-hybrid bait constructs were described previously (Tall *et al.*, 2001). RFP-Rab5a mammalian expression constructs were a generous gift of Dr. Richard Pagano (Mayo Clinic). The coding sequence for Ypt1 was inserted into pQE30 (Qiagen Inc.; Valencia, CA) for creation of His$_6$-Ypt1p. Wild-type Rac1, Rac3, cdc42, and RhoA GST-tagged E. coli expression constructs were kind gifts of Drs. Paul Sternweis and Mike Rosen (UT Southwestern Medical Center). The Vps9 domain of Alsin (Alsin $_{1360-1657}$) was PCR amplified from a KIAA1563 partial clone (Kazusa DNA Research Institute) and subcloned into pMBP-parallel 1 (Sheffield *et al.*, 1999), pET28b (Novagen, Inc.), pGADGH (Hannon *et al.*, 1993), and pEGFP-C3 (Clontech) for creation of the MBP-, His$_6$-, two-hybrid prey-, and GFP- fusion constructs. A fragment of Alsin containing the DH and PH domains (Alsin $_{685-1026}$) was PCR amplified from the KIAA1563 partial clone and subcloned into pFASTBacHTb (Invitrogen) and pEGFP-C3. To generate full-length Alsin, the 5' region of Alsin was obtained by RT-PCR on RNA derived from the SH-SY5Y

human neuroblastoma cell line (a kind gift of Dr. Martin Reick, UT Southwestern

Medical Center). The remainder of the gene was PCR amplified from the

KIAA1563 partial clone. These two fragments were digested and subcloned into

pFASTBacHTa (Invitrogen) by three-piece ligation to generate full-length Alsin.

This plasmid was used as template in subsequent PCR reactions to amplify the

NH_2-RCC1-like domain (RLD; Alsin $_{1-705}$), a fragment of Alsin consisting of the

NH_2-RCC1-like, DH, and PH domains (Alsin $_{1-1026}$), a fragment of Alsin lacking

the last 55 amino acids (ΔVps9, Alsin $_{1-1602}$), and full-length Alsin for subcloning

into pFASTBacHTb (Invitrogen), pACCMVpLpA (Gomez-Foix *et al.*, 1992),

and/or pEGFP-C3 (Clontech). Recombinant Alsin bacmids were generated in

DH10BAC E. coli using the BAC-TO-BAC Baculovirus Expression System

(Invitrogen) and transfected into S. frugiperda (Sf9) cells. Recombinant Alsin

adenovirus was constructed using methods described previously (Aoki *et al.*,

1999). Propagation and titration of the adenovirus were as described previously

(Gerard, 1995). Viral stocks were kept between 10^8-10^9 plaque-forming units

(PFUs) per ml and stored at −80°C for later use.

Protein purification

His$_6$-Rab5 (a, b, c), His$_6$-Rab4, and His$_6$-Ypt1 constructs were transformed

into HMS174 (DE3) E. coli. Cells were grown at 37°C to an OD$_{600}$ of 0.6 and

induced with 0.5mM isopropyl-β-D-thiogalactoside (IPTG) for 5 hrs at 37°C.

Cells were harvested and proteins purified using Ni-NTA agarose according to the manufacturer's instructions. GST-Rho GTPase fusions and MBP-Vps9 domain (Alsin $_{1360-1657}$) were transformed into HMS174 (DE3) E. coli. Cells were grown at 37°C to an OD_{600} of 0.5-0.6, shifted to 25°C, and induced with 0.3 mM IPTG for 10-15 hrs. Cells were harvested and proteins purified using glutathione sepharose or amylose resin according to the manufacturer's protocols. Recombinant His$_6$- Alsin $_{685-1026}$ (fragment consisting of DH and PH domains) was purified from 200 ml baculovirus-infected Sf9 cell lysates using Ni-NTA agarose as described. All proteins were buffer-switched or dialyzed into appropriate buffers, concentrated, and used immediately or stored at –80°C for later use. Protein concentrations were determined by Bradford assay (Biorad) and purity was estimated by Coomassie-blue staining of SDS-PAGEs.

Antibody production

His$_6$-Vps9 domain (Alsin $_{1360-1657}$) was transformed into BL21 RIL (DE3) E. coli. Cells were grown at 37°C to an OD_{600} of 0.5-0.6, switched to 30°C, and induced with 0.5 mM IPTG for 5-6 hrs. With these conditions, His$_6$-Alsin $_{1360-1657}$ was found exclusively in inclusion bodies. To isolate protein, cells were lysed, and the lysate was centrifuged at 13,000 xg. The resulting pellet containing the inclusion bodies was resuspended in SDS-sample buffer (20% glycerol, 10% β-mercaptoethanol, 6% sodium dodecyl sulfate (SDS), 125 mM Tris (6.8), 0.02%

bromphenol blue), separated by SDS-PAGE, and the band corresponding to the

His_6- Alsin $_{1360-1657}$ was excised. Protein was concentrated and used to immunize

a New Zealand White rabbit as described previously (Horazdovsky *et al.*, 1994).

CNBR-activated sepharose was coupled to purified MBP-Alsin $_{1360-1657}$ (described

above) and used to affinity-purify Alsin antibodies from antiserum according to

the manufacturer's instructions (Amersham).

Cell culture, transfections, and infections

Hippocampal neuron cultures from E18 Sprague-Dawley rats were

prepared and maintained as described previously (Gray *et al.*, 2003). NIH3T3

cells and SH-SY5Y cells were maintained in a 37°C, 5% CO_2 environment and

cultured in DMEM (Invitrogen) and DME/F-12 1:1 media (HyClone),

respectively, supplemented with fetal bovine serum (10%), penicillin (100

units/ml), and streptomycin (100 μg/ml). NIH3T3 cells were plated at various

densities on 12 mm glass coverslips a day prior to all experiments. Cells were

transfected with 0.2-0.5 μg GFP-Alsin constructs and 0.3-5 μg RFP-Rab5A

constructs using Fugene-6 (Roche) or Lipofectamine-2000 (Invitrogen) reagents

according to the manufacturers' instructions, and processed for

immunofluorescence approximately 24 hrs later. For SH-SY5Y infections, cells

were plated on 6 cm plates (Corning) and infected the next day with 10-25

plaque-forming units (PFUs) per cell recombinant Alsin or empty adenovirus in

minimal media (lacking serum). After 2 hrs, the media was aspirated and cells

were fed with media containing serum. Infections were continued for an

additional 18-24 hrs prior to experimentation.

Cerebellum fractionation

One fresh rat cerebellum from a female E18 Sprague-Dawley rat was

isolated and resuspended by douncing in 5ml lysis buffer [0.32 M sucrose, 5 mM

Tris (7.5), 0.5 mM $CaCl_2$, 1 mM $MgCl_2$, and 1x protease inhibitor cocktail (N-

tosyl-L-phenlalanine-chloromethyl ketone (TPCK), N^a-p-tosyl-L-lysine-

chloromethyl ketone (TLCK), phenylmethyl sulfonyl fluoride (PMSF), leupeptin,

trypsin inhibitor)]. DNA was sheared by passage through 18-gauge needle

repeatedly and the lysate was pelleted at 500 xg for 10 min to remove unlysed

cells and debris. The supernatant was separated into 4x 0.5 ml aliquots and used

in fractionations as described previously (Huttner *et al.*, 1983; Nishiki *et al.*,

2001). All four aliquots were centrifuged at 10,500 xg for 15 min. For one of the

aliquots, the supernatant (S2) and pellet (P2) were isolated. The supernatant from

a second aliquot was then pelleted at 165,000 xg for 2 hrs, generating S3

(supernatant) and P3 (pellet) fractions. For the other two aliquots, the pellets

from the 10,500 xg spin were resuspended in 50 μl lysis buffer, and hypotonically

lysed by the addition of 450 μl H_2O (with 1x protease inhibitor cocktail) and

passage through an 18-20 gauge needle 10 times. This mixture was then

centrifuged at 25,000 xg for 20 min, generating LS1 (supernatant) and LP1 (pellet) fractions. The supernatant from this spin was then pelleted at 165,000 xg for 2 hrs, generating LS2 (supernatant) and LP2 (pellet) fractions. Supernatants were added to 125 μl 5x SDS-sample buffer (0.312 M Tris (6.8), 10% SDS, 25% β-mercaptoethanol, 0.05% bromphenol blue) while pellets were resuspended in 625 μl SDS-sample buffer. Samples were then boiled at 95°C for 5 min and analyzed by SDS-PAGE and Western blotting.

Binding and guanine nucleotide exchange assays

Yeast two-hybrid assays were performed as described (Hama *et al.*, 1999; Tall *et al.*, 2001). Rab guanine nucleotide exchange assays were performed essentially as described previously (Hama *et al.*, 1999; Tall *et al.*, 2001). Recombinant proteins used in assays were all purified as described above. For time-course exchange assays, 200 pmol Rab5 (a, b, c) was incubated with either 600 pmol bovine serum albumin (BSA) or 600 pmol MBP-Vps9 domain of Alsin, and exchange was monitored at 0, 2, 5, 10, 20, and 30 min. In experiments aimed at determining Rab specificity, 100 pmol Rab was incubated with 300 pmol BSA or 300 pmol MBP-Vps9 domain and GDP release measured at 0 and 30 min.

In vitro binding assays were performed essentially as described (Hart *et al.*, 1994). Briefly, 5 μg GST-Rho or His$_6$-Rab GTPases were added to 50 μl glutathione sepharose or Ni-NTA agarose resins. The reaction was brought up to

400 μl in H_2O and incubated end-over-end at 25°C for 1 hr. The beads were

pelleted and resuspended in 500 μl buffer (20 mM Tris (7.5), 1 mM DTT, 10 mM

EDTA, 50 mM NaCl, 5% glycerol, 0.1% Triton X-100, 1x protease inhibitor

cocktail) and incubated end-over-end for 1 hr at 25°C to deplete the GTPases of

nucleotide. During this incubation, 1 μg His_6-Alsin $_{685-1026}$ (Rho binding assays)

or Alsin containing SH-SY5Y lysate (Rab binding assays) was incubated with

500 μl buffer at 4°C for 1 hr. The beads were pelleted, resuspended in 500 μl

buffer, and added to the 500 μl buffer-Alsin mixture. The reaction was incubated

at 25°C for 1 hr end-over-end. The beads were then pelleted, washed twice with 1

ml buffer, resuspended in 50 μl SDS-sample buffer and analyzed by SDS-PAGE

and Western blotting with GST and His antibodies.

In vivo Rac-GTP loading assay

A fusion construct (GST-PBD) consisting of GST and the Rac/cdc42

GTPase-binding domain of PAK (a generous gift of Dr. Paul Sternweis, UT

Southwestern Medical Center) was transformed into HMS174 (DE3) E. coli.

Cells (200ml) were grown at 37°C to an OD_{600} of 0.6 and induced with 0.3 mM

IPTG for 3 hrs at 37°C. Cells were harvested and resuspended in lysis buffer (20

mM HEPES (7.5), 120 mM NaCl, 10% glycerol, 2 mM EDTA, 1x protease

inhibitor cocktail), sonicated 2x 15 sec, and centrifuged for 30 min at 27,000 xg.

The supernatant was adjusted to 0.5% NP-40 and incubated with 300 μl glutathione sepharose beads end-over-end at 4°C for 1 hr. The GST-PBD glutathione sepharose conjugates were pelleted and washed 5x lysis buffer + 0.5% NP-40 and 3x lysis buffer without NP-40.

Sf9 cells (10-20 ml) were co-infected at with full-length Alsin baculovirus (described above) and Rac baculovirus (a generous gift of Dr. Paul Sternweis). After 48 hrs, cells were harvested and resuspended in 2 ml buffer A (50 mM Tris (7.5), 500 mM NaCl, 0.1% SDS, 0.5% deoxycholate, 1% Triton X-100, 0.5 mM $MgCl_2$, 1x protease inhibitor cocktail). Cells were lysed by douncing and passage through a 22-gauge needle and the resulting lysates were cleared at 16,000 xg for 10 min. Bradford assay was used to determine the protein concentration of the lysates and 2 mg total protein was incubated with 50 μg glutathione sepharose-conjugated GST-PBD in 1 ml total volume (buffer A) end-over-end at 4°C for 1 hr. Beads were pelleted, washed 4 times with buffer B (50 mM Tris (7.5), 150 mM NaCl, 1% Triton X-100, 0.5 mM $MgCl_2$, 1x protease inhibitor cocktail) and resuspended in 75 μl SDS-sample buffer. Proteins were eluted by boiling at 95°C for 5 min and sample was analyzed by SDS-PAGE and Western analysis with antibodies to Rac.

Immunoblotting

Samples were separated by SDS-PAGE (8-12%) and transferred to nitrocellulose. Blots were incubated with antibodies to Alsin (1:500-1:1000), GST (1:2000), Rac (1:2000), synaptophysin (1:2000) and His (1:2000) followed by the appropriate horseradish peroxidase- conjugated secondary antibodies (1:2000). Blots were developed by enhanced chemiluminescence using SuperSignal West Femto Sensitivity substrate (Pierce Biotechnology Inc.) and exposed to X-OMAT AR film (Kodak).

Immunofluorescence

Hippocampal neurons were processed for immunofluorescence as described previously (Gray *et al.*, 2003). Primary antibodies were incubated at dilutions of 1:50 (Alsin) and 1:250 (MAP2b) and secondary antibodies (Alexa488 anti-rabbit and Alexa568 anti-mouse) at 1:1000. Images were captured by laser scanning confocal microscopy (Zeiss LSM 510) using a 63x objective with an optical section of 1.5 microns. Images were prepared using Photoshop 7.0 (Adobe). For direct immunofluorescence of GFP- and RFP- fusion proteins, NIH3T3 cells were fixed in 4% formaldehyde (Tousimis) for 20 min and coverslips mounted using the Prolong antifade reagent (Molecular Probes). For indirect immunofluorescence, cells were fixed with 4% formaldehyde, permeabilized for 3 min with 0.1% Triton X-100, and blocked for at least 60 min

in PBS + 3% BSA. Primary antibodies were added for at least 60 min at dilutions

of 1:50 (Alsin) and 1:100 for Rac, Rab5, and EEA1. Secondary antibodies

(Alexa488 anti-rabbit and Alexa568 anti-mouse) and rhodamine-conjugated

phalloidin were added at 1:1000 for 60 min. Coverslips were mounted on slides

using the Prolong antifade reagent (Molecular Probes). NIH3T3 images were

captured by a Zeiss Axiovert S1002TV fluorescence microscope (FITC and

rhodamine filters) and Photometrix digital camera. Images were deconvoluted

with Delta Vision software (Applied Precision, Inc.) and prepared using

Photoshop 7.0 (Adobe).

Results

RCC1 repeats of Alsin

Alsin is predicted to be a relatively large protein of 1657 amino acids

(Hadano *et al.*, 2001; Yang *et al.*, 2001); (see Figure 6A). Comparison of Alsin

with other known proteins uncovered the presence of several sequence motifs

including RCC1, DH, PH, MORN, and Vps9 domains (Hadano *et al.*, 2001; Yang

et al., 2001); (see Figure 6A). The RCC1 motif derives its name from the RCC1

protein, a guanine nucleotide exchange factor for the Ran GTPase (Bischoff and

Ponstingl, 1991). RCC1 domains are comprised of approximately 50 amino acids

that adopt a β-sheet conformation (Bateman *et al.*, 2002). In the case of the

RCC1 protein, seven of these domains are tandemly arranged to comprise a

seven-bladed propeller (Renault *et al.*, 1998). It has been reported that Alsin

contains three (Hadano *et al.*, 2001) or six (Yang *et al.*, 2001) RCC1 repeats, and

it has been suggested that Alsin may also possess Ran guanine nucleotide

exchange activity (Hadano *et al.*, 2001). Close inspection of the NH_2-terminal

portion of Alsin identified five subdomains that fit the consensus RCC1 motif

(Bateman *et al.*, 2002). Although over 90 known proteins contain one or more

RCC1 repeats (Bateman *et al.*, 2002), only RCC1 itself has been shown to be a

Ran GEF (Bischoff and Ponstingl, 1991). Due to the diversity of proteins that

contain RCC1 repeats, it is likely that this motif does not serve an enzymatic role,

but instead functions as a protein-protein interaction motif. As expected,

secondary structure prediction using the JPred algorithm (Cuff *et al.*, 1998)

showed that the region of Alsin containing the RCC1 repeats consists primarily of

β-sheet with a central α-helix (Figure 6B). Despite the fact that it contains only

five RCC1 domains, there is ample β-sheet present to form a seven-bladed

propeller, making Alsin a likely member of the β-propeller family of proteins

(Murzin, 1992).
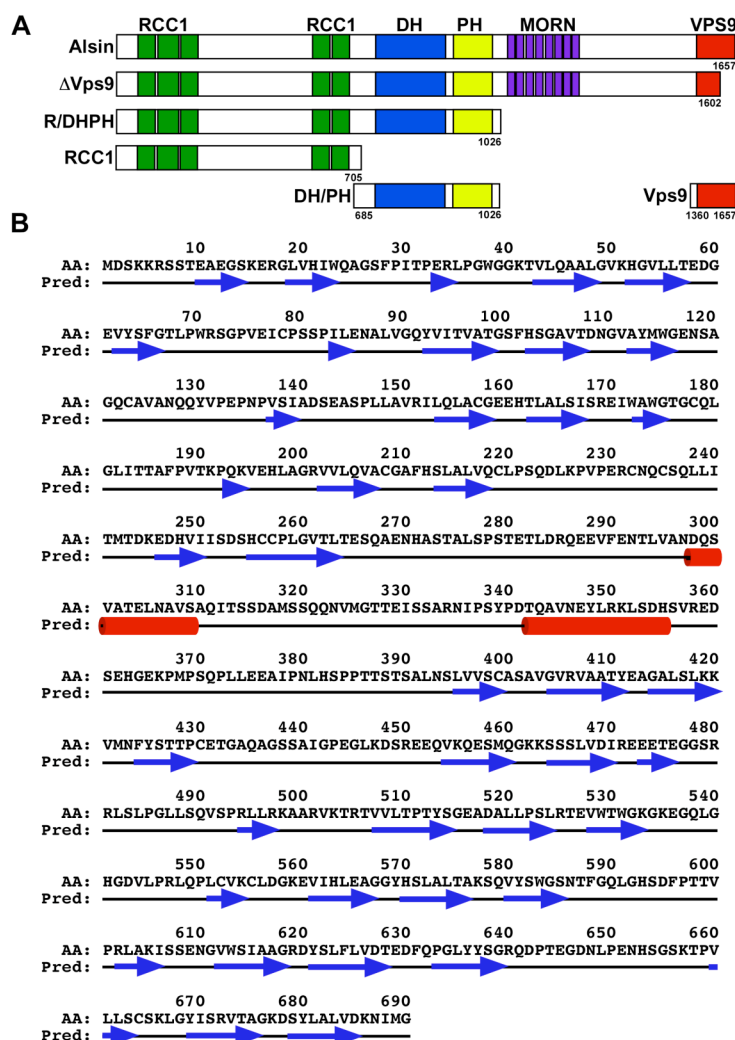
Figure 6. Secondary structure of Alsin and list of truncations referred to in studies. A) Alsin possesses NH$_2$-terminal RCC1 repeats (green), central DH (Dbl homology) (blue) and PH domains (Pleckstrin homology) (yellow), MORN (Membrane occupation and recognition nexus) repeats (purple), and a COOH-terminal Vps9 domain (red). Various fragments of the protein utilized are indicated with the corresponding amino acids noted. B) The amino terminal region of Alsin containing the RCC1 repeats was analyzed using the secondary structure prediction algorithm, JPred (Cuff *et al.*, 1998). The blue arrows indicate sequences predicted to adopt a beta sheet conformation and the red barrels indicate predicted alpha helixes.

Alsin stimulates guanine nucleotide exchange on Rab5

Alsin is predicted to have a number of domains implicated in protein trafficking and cell signaling events (Hadano *et al.*, 2001; Shaw, 2001; Yang *et al.*, 2001); (see Figure 6A). Three examples of these domains are the central DH

and PH domains and the COOH-terminal Vps9 domain. Since the disease-associated mutations in ALS2 are recessive and predicted to generate truncated proteins lacking some or all of the aforementioned domains (Hadano *et al.*, 2001; Yang *et al.*, 2001; Eymard-Pierre *et al.*, 2002; Devon *et al.*, 2003; Gros-Louis *et al.*, 2003), it is likely that these domains play an essential role in Alsin function. We examined the biochemical activities of these domains, starting with the Vps9 domain.

The four proteins examined to date that contain Vps9 domains all exhibit guanine nucleotide exchange activity toward the Vps21p/Rab5 family of small GTPases (Horiuchi *et al.*, 1997; Hama *et al.*, 1999; Tall *et al.*, 2001; Saito *et al.*, 2002). They function to activate these GTPases, which in turn regulate vesicle trafficking events through the endocytic pathway. To determine whether the Vps9 domain of Alsin possesses Rab5 nucleotide exchange activity, we first determined whether it interacted with Rab5. Both yeast two-hybrid and *in vitro* binding assays were used in these analyses. For the yeast two-hybrid experiments, the Vps9 domain of Alsin (Alsin $_{1360-1657}$; see Figure 6A) was fused to the Gal4 activation domain (prey) and co-expressed with various Rab5 LexA DNA-binding domain fusions (baits). Interaction between bait and prey drives HIS3 expression allowing the yeast transformants to grow in the absence of histidine. Both wild-type and a mutant form of Rab5 that is in the GDP-bound or nucleotide-free form (S34N) (Tall *et al.*, 2001) were tested for their ability to

interact with the Vps9 domain of Alsin (Figure 7A). All three isoforms of Rab5
(a, b, and c) were tested in this manner. Yeast expressing both the Alsin $_{1360\text{-}1657}$
prey and the S34N Rab5 baits were prototrophic for histidine, indicating that
Alsin interacted with the mutant Rab5 in its GDP-bound or nucleotide-free form
(Figure 7A). Yeast expressing wild-type Rab5 (WT) or empty LexA DNA
binding domain fusions (baits) were unable to grow in the absence of histidine
(panel 1), indicating that the Vps9 domain of Alsin did not interact or interacted
poorly with these baits. All of the strains were able to grow on media
supplemented with histidine (Figure 7A, panel 2). Full-length Alsin prey was also
observed to interact with the S34N Rab5 bait isoforms (data not shown).

To confirm the yeast two-hybrid result, in vitro binding experiments were
performed with recombinant proteins. SH-SY5Y cell lysates overexpressing full-
length Alsin were incubated in the presence of His-tagged nucleotide-free Rab5a
or Rab11 and the resulting complexes were precipitated with Ni-NTA agarose.
As shown in Figure 7B, Alsin bound His$_6$-Rab5a (lane 4) but not His$_6$-Rab11
(lane 3). Together, the *in vivo* two-hybrid and the *in vitro* binding assays
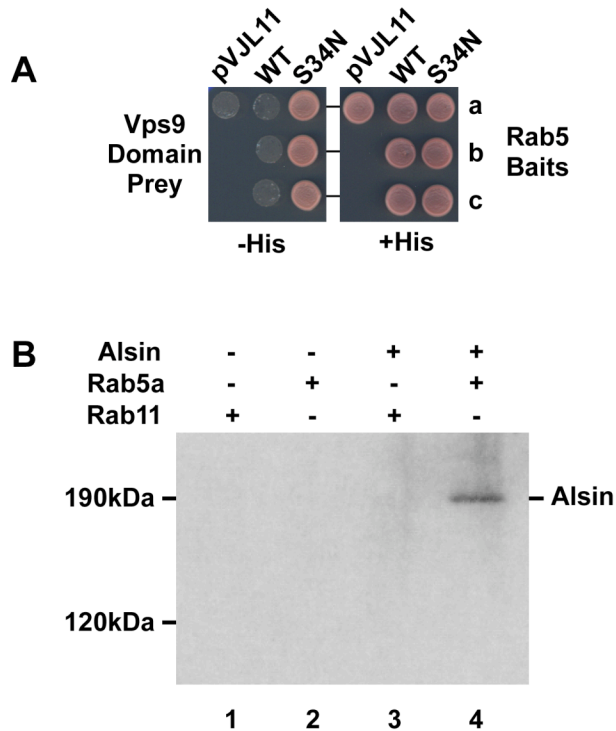indicated that Alsin and Rab5 specifically interact.

A

B

Alsin	-	-	+	+
Rab5a	-	+	-	+
Rab11	+	-	+	-

190kDa —   — Alsin

120kDa —

1   2   3   4

Figure 7. Alsin interacts with Rab5. A) The Vps9 domain of Alsin interacts with Rab5 by yeast two-hybrid. The Vps9 domain of Alsin (Alsin$_{1360\text{-}1657}$) fused to the Gal4 activation domain was co-expressed in L40 yeast with Rab5 isoforms (a, b and c) fused to the LexA DNA binding domain (WT and S34N) or the LexA DNA binding domain alone (pVJL11). Interaction was scored as strain growth in the absence of histidine (-His). B) Full-length Alsin interacts with Rab5. Lysates from SH-SY5Y cells infected with an adenovirus coding for Alsin or a control adenovirus were incubated in the presence of 5 µg His$_6$-Rab11 or 5 µg His$_6$-Rab5a as described in Experimental Procedures. The Rab GTPases were isolated by the addition of Ni-NTA agarose and the presence of Alsin was determined by SDS-PAGE and Western analysis with antibodies to Alsin.

To determine whether Alsin binding to Rab5 stimulated guanine nucleotide exchange activity, *in vitro* nucleotide exchange assays were performed. Purified recombinant Rab5a was preloaded with ^{3}[H]GDP and nucleotide release was monitored in the presence or absence of Alsin. For these experiments the Vps9 domain of Alsin (Alsin$_{1360\text{-}1657}$) was expressed and purified from E. coli as an MBP-fusion protein. As seen in Figure 8A, Alsin$_{1360\text{-}1657}$ greatly stimulated GDP release on Rab5a. More than 75% of Rab5a released its associated GDP in the presence of the Alsin Vps9p domain by 5 minutes. In comparison, when BSA

was added to the reaction instead of Alsin $_{1360\text{-}1657}$, only 10% of the Rab5a had

displaced GDP by 5 minutes, indicative of the low intrinsic activity exchange

associated with Rab5a (Horiuchi *et al.*, 1997; Tall *et al.*, 2001). Exchange factors

for the Rab GTPase family exhibit strict substrate specificity. To demonstrate

that this exchange activity was indeed specific to Rab5, nucleotide exchange

assays were performed with other Rab GTPases (Figure 8B). The Vps9 domain

of Alsin was unable to stimulate GDP release on the Rabs, Rab4, and Ypt1p.

Since the Vps9 domain of Alsin interacted with all three isoforms of Rab5 by

yeast two-hybrid (Figure 8A), we also tested whether it catalyzed nucleotide

release on Rab5b and c isoforms. Alsin was active on all three Rab5 isoforms in

vitro (Figure 8B), although highest activity was observed on Rab5a.

A
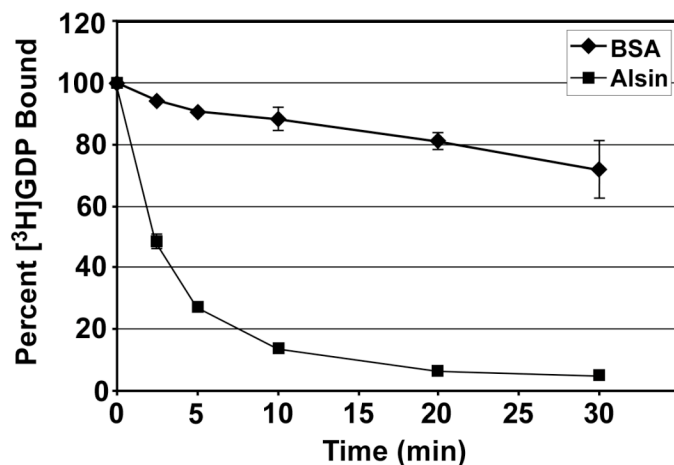
B
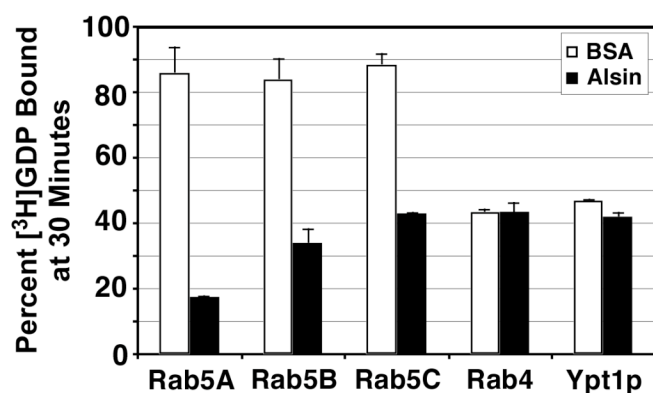
Figure 8. Alsin is a Rab5 guanine nucleotide exchange factor. A) Alsin stimulates GDP release on Rab5a. The Vps9 domain of Alsin (Alsin $_{1360\text{-}1657}$) was expressed and purified as an MBP-fusion protein from *E. coli*. 200 pmol His$_6$-Rab5a was preloaded with 0.7 μM [^{3}H]GDP for 30 minutes at 30°C. Samples were then incubated in the presence of 600 pmol BSA or 600 pmol MBP-Alsin $_{1360\text{-}1657}$ and excess unlabeled nucleotide and [^{3}H]GDP release was monitored over time by nitrocellulose filtration and scintillation counting. Samples were normalized to the [^{3}H] count at 0 minutes. Shown is the average of two independent experiments with error bars corresponding to one standard deviation. B) Alsin guanine nucleotide exchange activity is specific for Rab5. 100 pmol His$_6$-Rab GTPases were preloaded with [^{3}H]GDP as described above and release was monitored in the presence of 300 pmol BSA or 300 pmol MBP-Alsin $_{1360\text{-}1657}$. Results shown correspond to the amount of [^{3}H]GDP-bound His$_6$-Rab after 30 minutes incubation with Alsin (or BSA) normalized to the amount at 0 minutes and are the average of two independent experiments with error bars representing one standard deviation.

Alsin Is a Rac1 exchange factor

In addition to its Vps9 domain, Alsin possesses central DH and PH domains. This tandem repeat has been shown previously to catalyze guanine nucleotide exchange on members of the Rho family of GTPases (Zheng, 2001). Unlike Rab exchange factors, Rho GEFs are promiscuous and substrate specificity cannot be easily determined by computational analysis. Therefore, we first set out to identify Rho family members that interacted with Alsin. A His$_6$-tagged Alsin fragment containing the DH and PH domains (Alsin $_{685-1026}$, see Figure 6A) was expressed and partially purified from Sf9 cells. This fragment was then used in *in vitro* binding assays with various Rho GTPases expressed in *E. coli* as GST-fusions. The GST-Rho GTPases were complexed with glutathione sepharose, incubated with the DH/PH domains of Alsin, and the potential complexes were isolated. As shown in Figure 9A, Alsin $_{685-1026}$ interacted specifically with Rac1 (lane 2). No or very little interaction was observed with the related Rho family members Rac3, RhoA, or cdc42 (lanes 3, 4, 5) or with GST alone (lane 1). To address whether Rac1 interacts with Alsin in the context of the full-length protein, similar binding reactions were performed with Sf9 cell lysates overexpressing full-length Alsin. Full-length Alsin copurified with GST-Rac1 but not with GST or glutathione sepharose alone (data not shown).

The ability of Alsin to stimulate Rac1 nucleotide exchange was tested using an *in vivo* assay. This method utilizes the fact that proteins of the p21-

activated kinase family (PAKs) interact with Rac1 only when it is in the active

GTP-bound state. Using a GST-PAK fusion protein complexed with glutathione

sepharose beads, GTP-bound Rac1 can be specifically isolated from cell lysates

and quantified (Sander *et al.*, 1998; Benard *et al.*, 1999). To examine Rac1

activation by Alsin, Rac1 and Alsin were co-expressed in Sf9 cells, cell lysates

were generated, and GTP•Rac1 was complexed to GST-PAK. The

GTP•Rac1:GST-PAK complexes were then isolated, resolved by SDS-PAGE,

and the amount of Rac1•GTP bound was determined by densitometry. Shown in

Figure 9B is a representative example of this analysis. Coexpression of Alsin

with Rac1 resulted in a significant increase in the levels of activated Rac1 (lower

panel, lane 3) when compared to Rac1 alone (lower panel, lane 2).   The average

of six independent experiments showed that Alsin coexpression resulted in a ~4-

fold increase in relative Rac1•GTP levels (normalized to total Rac1). This value

was determined to be statistically significant using a one-sample t test ($P = 0.02$,

see Figure 9 legend). These results demonstrated that Alsin stimulated Rac1

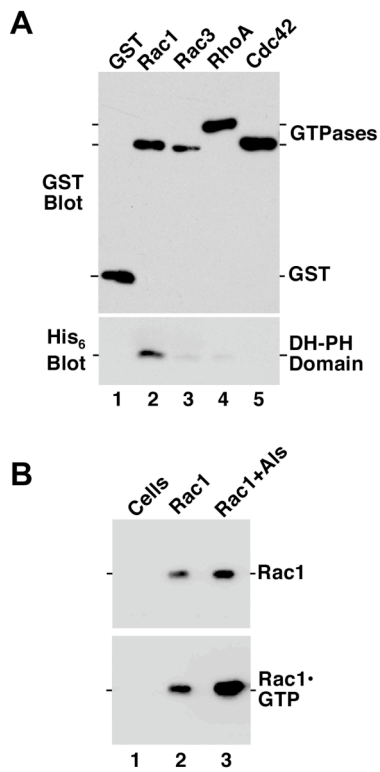guanine nucleotide exchange activity in vivo.

A

B

Figure 9. Alsin is a Rac1 guanine nucleotide exchange factor. A) Alsin interacts specifically with Rac1. A fragment of Alsin consisting of the DH and PH domains (Alsin $_{685-1026}$) was expressed and partially purified as a His$_6$-fusion from Sf9 cells. 5 µg of the indicated GST-Rho GTPases were conjugated to glutathione sepharose beads and incubated in the presence of Alsin $_{685-1026}$. Beads were isolated and the resulting complexes analyzed by SDS-PAGE and Western blotting with antibodies to His$_6$ (to identify Alsin) and GST (to identify the Rho family member). B) Alsin stimulates GTP loading on Rac1 *in vivo*. Sf9 cells expressing both Rac1 and full-length Alsin or Rac1 alone were lysed and supernatants incubated in the presence of GST-PBD as described in Experimental Procedures. GST-PBD binds specifically to activated Rac1 allowing isolation of the GTP-bound species. GST-PBD complexes were precipitated and analyzed by SDS-PAGE and Western blotting with antibodies directed against Rac1 (lower panel). Small fractions of whole cell lysates corresponding to 1-3% of the input used for the pull-down were analyzed to determine the relative levels of total Rac1 in each lysate (upper panel). The amount of Rac1•GTP precipitated was quantified by densitometry and normalized to the amount of Rac1 in each lysate. Shown is one example of the six experiments used to determine a mean 3.9 (+/- 2.2) fold increase (P = 0.02, using a one sample t test) in Rac1•GTP when Alsin was coexpressed with Rac1.

Alsin localizes to punctate membrane structures

To gain insight into Alsin's potential role in the maintenance of neuron function, we examined its subcellular localization. Rat embryonic hippocampal neurons were isolated and cultured *in vitro* and endogenous Alsin localization was determined by indirect immunofluorescence. The anti-Alsin antibodies used were directed against the COOH-terminal Vps9 domain of the protein. This polyclonal antiserum recognized a protein of the expected size for Alsin in an extract of rat

cerebellum (Figure 10A), which has been shown to be an enriched source of Alsin (Hadano *et al.*, 2001). Pre-immune serum did not cross-react with this protein species. The Alsin antiserum also specifically reacted with a unique 190kDa polypeptide in Sf9 and SH-SY5Y cells that were expressing full-length recombinant Alsin (data not shown). These data demonstrate that this antiserum specifically recognizes Alsin.

When affinity-purified Alsin antibodies were used to localize Alsin in rat embryonic hippocampal neurons, the protein was found primarily on small punctate structures (Figure 10B and insets). Additionally, some cytoplasmic staining was also observed. Specific decoration of dendrites with microtubule-associated protein 2B (MAP2b) antibody (upper panels) revealed that Alsin was present in dendrites, axon, and the cell body, with no apparent polarized localization. Localization was independent of time in culture as a similar pattern was seen at both seven and 14 days. To ensure that the pattern observed was indeed rat Alsin, we pre-incubated the Alsin antiserum with antigenic peptide (MBP-Alsin $_{1360\text{-}1657}$). Addition of the peptide effectively blocked the signal observed, indicating that the signal is specific to Alsin (Figure 10B, right panels).

To further characterize the localization of Alsin, fractionation experiments were performed on extracts from rat cerebellum. As shown in Figure 10C, Alsin is present in both soluble and pelletable pools, with an enrichment in the P3 fraction (see lane 3). This fraction corresponds to the microsomal or small

membranes and Rab5 has been shown to be enriched in P3 also (Lee *et al.*, 2001);

(data not shown). Alsin is also found in the LP1 fraction indicating that a portion

of the protein is associated with synaptosomal membranes. To ensure that the

membrane integrity was not perturbed by the fractionation procedure, we

investigated the pattern of the synaptical protein synaptophysin. Synaptophysin

was found completely in membrane fractions, similar to previous observations

(Sheng and Pak, 2000), indicating that membrane structures were not disturbed by

this protocol.

A

AB   −   +

Alsin —

180 —

120 —

    1   2

C

	P2	S2	P3	S3	LP1	LS1	LP2	LS2

Alsin —

Synp —

  1   2   3   4   5   6   7   8

B

    7DIV   14DIV   14DIV
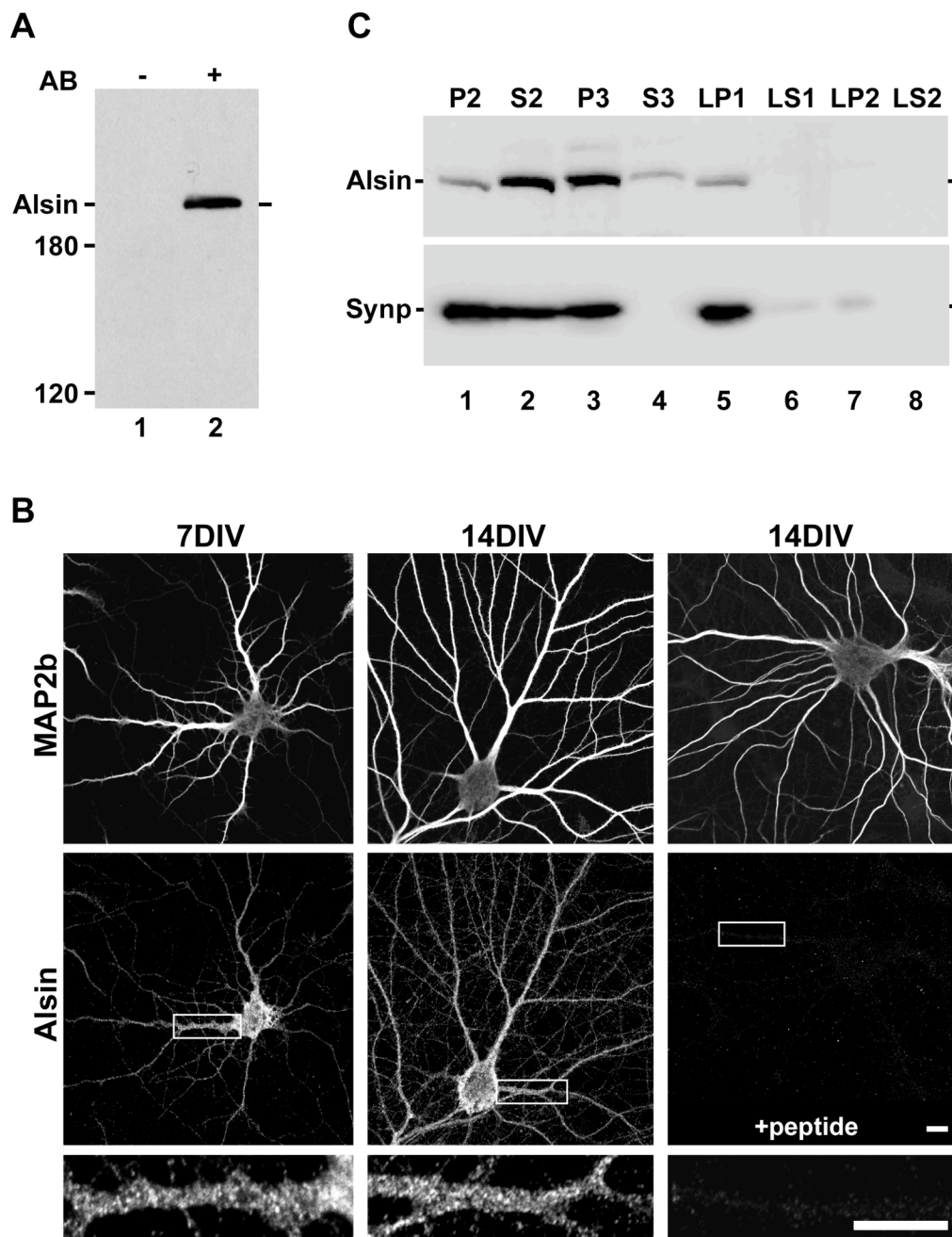
MAP2b

Alsin

+peptide

Figure 10. Alsin localizes to punctate membrane structures. A) Alsin antiserum immunoprecipitates Alsin from rat cerebellum. Rat cerebellum lysate was incubated in the presence of affinity-purified Alsin (lane 2) or pre-immune antisera (lane 1) and precipitated by the addition of protein-A sepharose. Immunoprecipitated material was separated by SDS-PAGE and the presence of Alsin was determined by Western blot analysis. B) Alsin localizes to cytoplasmic punctate membrane structures in hippocampal neurons. Rat embryonic hippocampal neurons were isolated and maintained *in vitro* for seven days (panel A) or 14 days (panel B and C). Endogenous Alsin was detected by indirect immunofluorescence with polyclonal antiserum directed against Alsin. Dendrites were visualized by staining with MAP2b antibody. The bottom panel shows a higher magnification of the box indicated. Pre-incubation of the Alsin antibodies with antigenic peptide (Alsin $_{1360-1657}$, panel C) effectively competes away the signal indicating the specificity of the antibody. Cells shown are representative images of the overall population. C) Alsin is present in cytoplasm and membrane fractions in rat cerebellum. An extract of rat cerebellum was generated and fractionated as described in Experimental Procedures. The presence of Alsin and synaptophysin in the various fractions was determined by immunoblot analysis.

Alsin colocalizes with Rab5 and stimulates endosome-endosome fusion

Since Alsin demonstrated guanine nucleotide exchange activity toward Rab5 (Figure 8), the localization pattern of Alsin was compared to that of Rab5. As shown in Figure 11A, Alsin and Rab5 partially colocalized to small punctate membrane structures throughout NIH3T3 cells. These structures are likely endosomal, as Alsin was also observed to colocalize with EEA1 (early-endosomal antigen 1), a known marker of early endosomes (Figure 11B).

To examine if Alsin was capable of activating Rab5 *in vivo*, we took advantage of the fact that Rab5 activation stimulates endosome-endosome fusion, resulting in endosome enlargement (Stenmark *et al.*, 1994; Roberts *et al.*, 1999). Wild-type Rab5a and the Vps9 domain of Alsin were co-expressed in NIH3T3 cells as red fluorophore (RFP) and green fluorophore (GFP) proteins, respectively, and endosome dynamics were monitored by immunofluorescence.

Overexpression of the Vps9 domain of Alsin and wild-type Rab5a dramatically altered the appearance of Rab5a-positive endosomal structures (Figure 11C). Instead of the small Rab5-positive punctate structures seen with overexpression of Rab5 alone, greatly enlarged endosomal structures were present. This pattern has also been observed when an activated form (GTPase-deficient) of Rab5 (Roberts *et al.*, 1999; Tall *et al.*, 2001; Barbieri *et al.*, 2003) or the Rab5 exchange factor Rabex-5 (data not shown) is expressed in cells. The formation of the Rab5a-positive enlarged endosomes was dependent upon wild-type Rab5a and Alsin expression as they were largely absent upon co-expression of dominant-negative Rab5a (Figure 11D) or with wild-type Rab5a alone (data not shown). Interestingly, other structures were also seen which contained only the Vps9 domain of Alsin (Figure 11C). The exact nature of this compartment is unknown.

A Alsin | Rab5 | Merge

B Alsin | EEA1 | Merge

C Alsin-Vps9D | WT-Rab5 | Merge
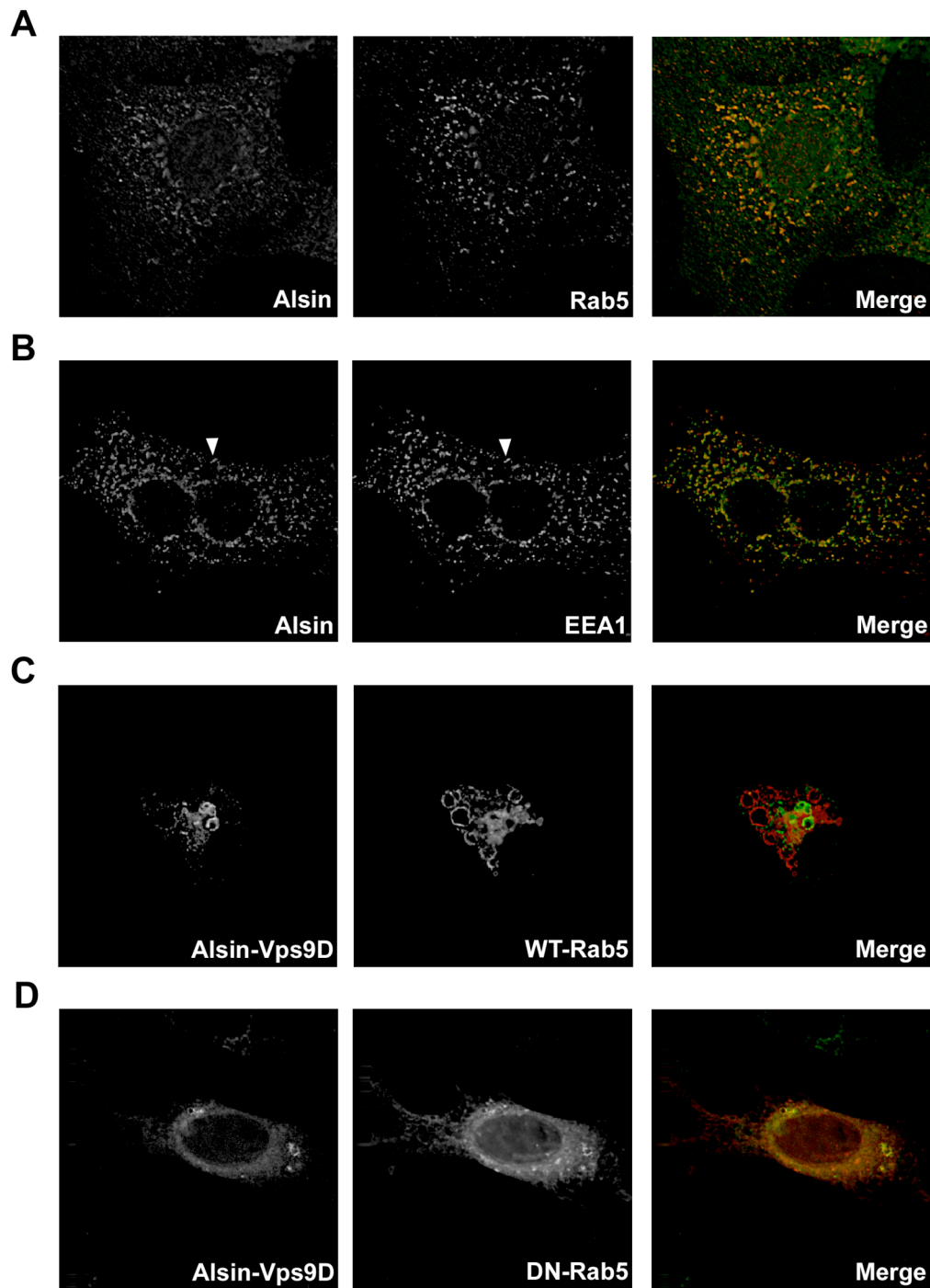
D Alsin-Vps9D | DN-Rab5 | Merge

Figure 11. Alsin colocalizes with Rab5 and stimulates endosome-endosome fusion. A) Endogenous Alsin colocalizes with Rab5. Approximately 80-90% confluent NIH3T3 cells were decorated with antibodies to Alsin and Rab5. B) Endogenous Alsin colocalizes with EEA1. Approximately 80-90% confluent NIH3T3 cells were decorated with antibodies to Alsin and EEA1. C) The Vps9 domain of Alsin stimulates endosome-endosome fusion. Subconfluent cells were co-transfected with GFP-Vps9 domain of Alsin and wild-type RFP-Rab5a and processed for microscopy 20-24 hrs later. D) Dominant-negative Rab5a blocks endosome-endosome fusion. Subconfluent cells were co-transfected with GFP-Vps9 domain of Alsin and dominant-negative RFP-Rab5a as in C).

Alsin colocalizes with Rac in membrane ruffles and lamellipodia

In the course of experimentation, it was observed that the endogenous Alsin staining pattern exhibited a dependence on cell density. When cells were plated at lower densities that promote cell migration, Alsin was present both at leading membrane edges and in a punctate staining pattern throughout the cell cytoplasm (Figure 12). Partial colocalization between Alsin, Rab5 (Figure 11A), and Rac (Figure 12A) to these punctate structures was also observed. More striking, however, was the overlap of Alsin and Rac in membrane ruffles. In many cells, colocalization at these sites was complete. Since Rac is known to play a role in actin remodeling at these sites (Hall, 1998; Kaibuchi *et al.*, 1999; Sah *et al.*, 2000), we asked whether Alsin and actin colocalized in membrane ruffles and lamellipodia. NIH3T3 cells expressing low levels of GFP-tagged Alsin were stained with rhodamine-conjugated phalloidin to label the actin cytoskeleton. As shown in Figures 12B and 12C, Alsin was present in actin-positive membrane ruffles and lamellipodia. Alsin colocalized with actin in membrane ruffles in two other cell types as well (data not shown). Although

Alsin localized to sites of actin remodeling, overexpression of Alsin alone did not

seem to stimulate these events (data not shown).

A

Alsin | Rac1 | Merge

B

Alsin | Actin | Merge
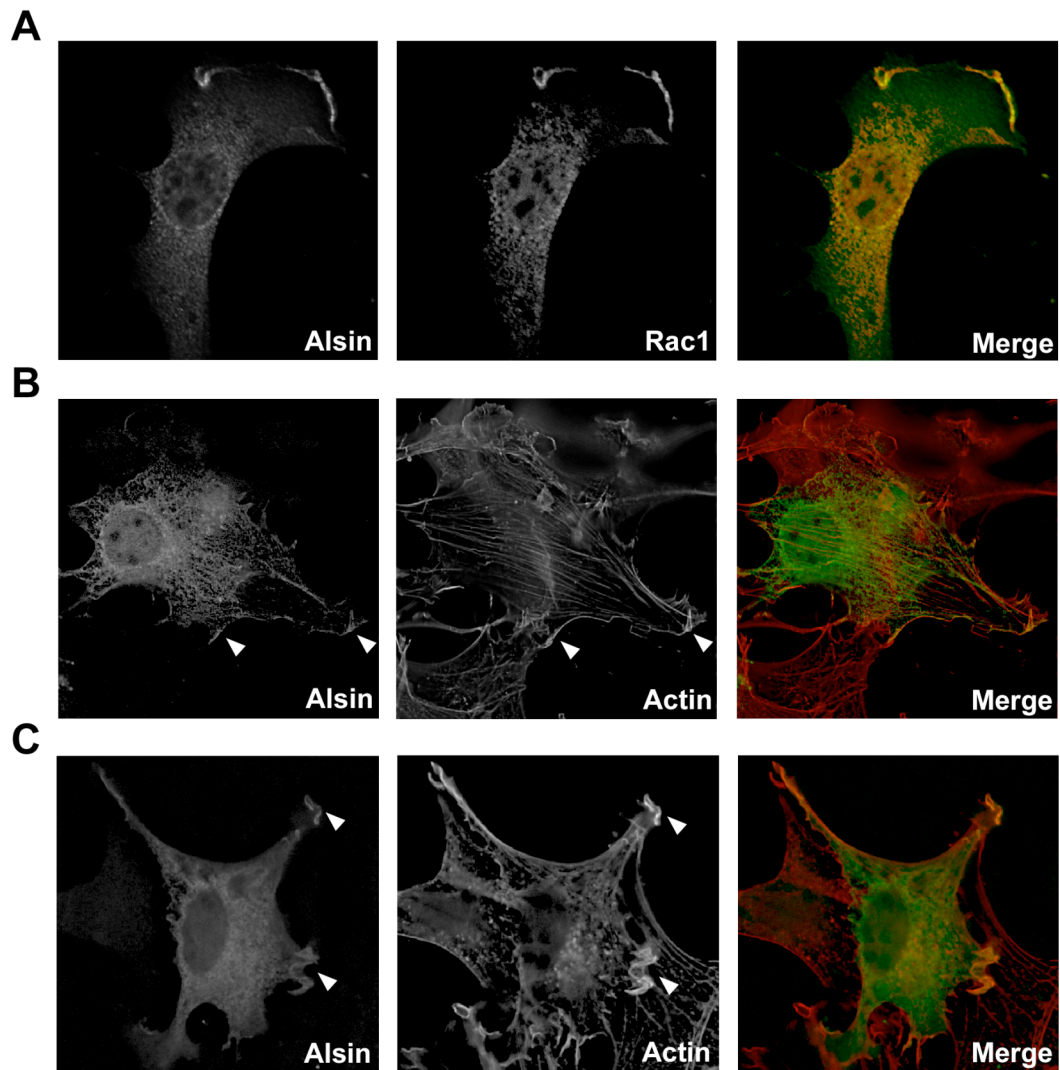
C

Alsin | Actin | Merge

Figure 12. Alsin colocalizes with Rac in membrane ruffles and lamellipodia. A) Endogenous Alsin colocalizes with Rac. Approximately 30-40% confluent NIH3T3 cells were stained with antibodies to Alsin and Rac1. At lower densities that promote cell migration, Alsin is observed at leading membrane edges in addition to the perinuclear region seen in cells at higher densities. Importantly, Rac and Alsin colocalize at both of these sites, with a marked enrichment at membrane edges. B, C) Alsin colocalizes with membrane ruffles and lamellipodia. GFP-tagged Alsin was transfected into approximately 30-40% confluent NIH3T3 cells and processed for immunofluorescence 20-24hrs later. Cells were decorated with rhodamine-phalloidin to label the actin cytoskeleton.

Alsin domain localization

To determine which domain(s) of Alsin were involved in membrane localization, a number of Alsin-GFP fusion constructs consisting of one or more domains were expressed in NIH3T3 cells and their subcellular localization was determined my fluorescent microscopy. Overexpression of the full-length Alsin-GFP construct showed a difference in localization when compared to endogenous Alsin. Although a portion of overexpressed Alsin was found in punctate membrane structures similar to those containing endogenous Alsin, the majority of overexpressed protein was observed primarily in the cytosol (Figure 13, panel A). The Alsin subdomain-GFP fusions were then used to dissect potential subcellular localization signals. The NH_2-terminal RCC1-like domain (RLD; Alsin $_{1-705}$, Figure 6A) of Alsin was found almost exclusively in the soluble cytoplasmic fraction, while a major portion of the DH/PH (Alsin $_{685-1026}$, Figure 6A) and Vps9 (Alsin $_{1360-1657}$, Figure 6A) domain GFP-fusion proteins were found primarily associated with intracellular structures (Figure 13, panel C and D). The GFP-Vps9 domain localized to membrane structures (Figure 13B, panel D) that

are likely enlarged endosomes similar to those observed upon overexpression of

Rab5 (Figure 11C) or another Rab5 exchange factor, Rabex-5 (data not shown).

The GFP-DH/PH (Alsin $_{685-1026}$, Figure 6A) domains fractionation pattern

revealed that this domain was present in bright punctate structures (Figure 13B,

panel C). The exact nature of these structures is unknown, but they are

reminiscent of an endosomal staining pattern. Mutations in *ALS2* that lead to the

disease phenotype have been found throughout the gene and are predicted to

encode prematurely truncated protein products (Hadano *et al.*, 2001; Yang *et al.*,

2001; Eymard-Pierre *et al.*, 2002; Gros-Louis *et al.*, 2003; Devon *et al.*, 2005). It

can be inferred from these mutations that Alsin protein lacking the Vps9 domain

is non-functional. To begin to determine the effects that loss in the Vps9 domain

has on Alsin function, we made two additional GFP fusion constructs of Alsin

lacking complete Vps9 domains and analyzed their subcellular localization. One

of the fragments lacked the MORN and Vps9 domains and is comprised of the

RCC1 repeats and DH/PH domains (Alsin $_{1-1026}$, see Figure 6A) only. The other

fragment was prematurely truncated at amino acid 1602 deleting approximately

half of the Vps9 domain (ΔVps9d; Alsin $_{1-1602}$, see Figure 6A). The ΔVps9d

construct closely resembles a recently identified mutational allele in *ALS2* (Gros-

Louis *et al.*, 2003). Both Alsin-GFP fusions that lacked a functional Vps9 domain

resembled were largely cytoplasmic (Figure 13, panel E and F), similar to that

seen with full-length Alsin (Figure 13, panel A). These data suggest that Alsin has

multiple localization signals that are able to contribute to cytoplasmic and/or

membrane distribution.
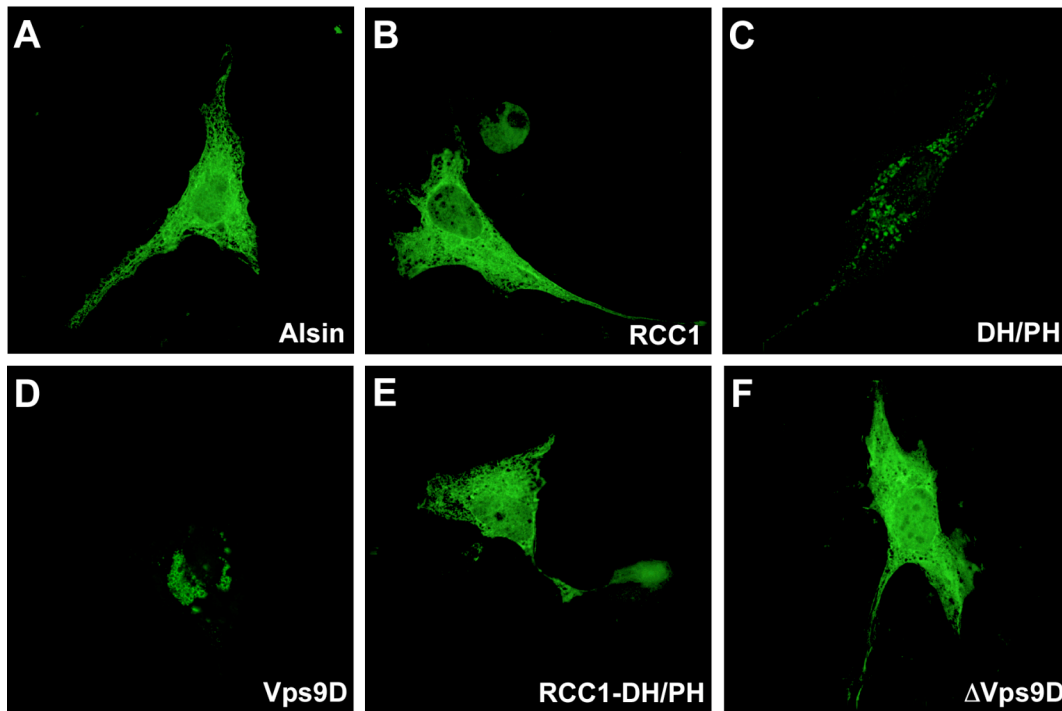
Figure 13. Localization of individual domains of Alsin.   Subconfluent NIH3T3 cells were transfected with full length Alsin fused to GFP (A), or GFP fusion constructs containing the Alsin RCC1-like domain (RLD; B), the DH/PH domains (C), the Vps9 domain (D), the RLD/DH/PH domains (E), or Alsin lacking the COOH-terminal half of the Vps9 domain (F). The fragments used are also shown in Figure 6A. The cells were processed for immunofluorescence 24 hrs later. Cells shown are representative of the overall population.

Discussion

The *ALS*2 gene product is a large protein that possesses many functional

domains that are implicated in cell signaling and membrane transport events. We

show here that the Vps9 domain of Alsin mediated an interaction with Rab5 and

acted as a specific guanine nucleotide exchange factor for Rab5 *in vitro* and *in vivo*. Similar to other Vps9 domain-containing proteins, Alsin exhibited exquisite specificity for Rab5 and did not enhance nucleotide release on the other Rab proteins tested. Alsin also showed a slight preference for the Rab5a isoform, but the significance of this observation is unclear. Recently, the Rab5 GEF activity of Alsin has been reported to require the presence of the MORN repeats in addition to the Vps9 domain (Otomo *et al.*, 2003). The results presented here demonstrate that the Vps9 domain alone can catalyze Rab nucleotide exchange. The specificity of Alsin action was also reflected by its colocalization with Rab5 on punctate structures in fibroblasts. A similar staining pattern was also observed with EEA1, suggesting that Alsin-positive structures are early endosomal in nature. When the localization of endogenous Alsin was examined in hippocampal neurons, the same punctate staining pattern was also observed. Overexpression of the Vps9 domain of Alsin with Rab5a resulted in the enlargement of Rab5a-positive structures, similar to the phenotype observed upon overexpression of an activated mutant of Rab5. Interestingly, the Alsin-Vps9 domain fragment also was present on enlarged endosomal-like compartments that were not decorated by Rab5. These Alsin-Vps9 domain positive-membranes may represent a unique endosomal structure. Further characterization of these compartments will be needed to define the potential role they may have in Alsin function.

In addition to its COOH-terminal Vps9 domain, Alsin possesses centrally located DH and PH domains, which are a hallmark of guanine nucleotide exchange factors of the Rho GTPase family (Zheng, 2001). It was found that a fragment of Alsin containing these domains (Alsin $_{685-1026}$) interacted specifically with Rac1 and that Alsin activated Rac1 *in vivo*, generating the GTP-bound form of the GTPase. Unfortunately, we were unable to observe *in vitro* guanine nucleotide exchange activity on Rac1 with Alsin $_{685-1026}$ alone (data not shown). This may be due to the requirement of a cofactor or post-translational modification on Alsin to promote exchange activity. This phenomenon has been observed with a number of Rac exchange factors including Ect2, mammalian Son-of-sevenless (mSos), P-Rex1, SWAP-70, and Dock180 (Scita *et al.*, 1999; Tatsumoto *et al.*, 1999; Lanzetti *et al.*, 2000; Brugnera *et al.*, 2002; Shinohara *et al.*, 2002; Welch *et al.*, 2002). With each of these GEFs, phosphorylation or interaction with other proteins and/or phosphatidylinositol (3,4,5)P3 was shown to be required for maximal nucleotide exchange activity in vitro. Another intriguing aspect of these results is the specificity of Alsin's interaction with Rac1. Though closely related, Rac3 showed little or no interaction with Alsin. This was somewhat surprising considering the high level of sequence identity shared by these two family members. However, differences in the distribution of Rac1 and Rac3 in the brain have been reported (Bolis *et al.*, 2003), as well as their ability to interact with downstream effectors to promote cell spreading and cell adhesion

(Haataja *et al.*, 2002). The Alsin-Rac1 interaction may reflect an additional level of functional specificity among the Rac isoforms.

In addition to the DH, PH, and Vps9 domains, Alsin possesses other domains that are likely to play an important functional role. For instance, the NH$_2$-terminal region of Alsin consists of five RCC1 repeats. Computational analysis predicts that this region is capable of adopting a seven-bladed propeller structure similar to that observed in RCC1 ((Bischoff and Ponstingl, 1991); see Figure 6B). It was originally suggested that this NH$_2$-terminal region of Alsin may function as a Ran GEF, because of its similarity to the RCC1 protein (Hadano *et al.*, 2001). Due to the ubiquitous presence of RCC1 repeats in many proteins of diverse function, it is likely that this region of Alsin is of structural importance rather than enzymatic importance. The potential propeller of Alsin may serve as a protein-protein interaction surface similar to the function of the seven-bladed propeller heterotrimeric G-protein β subunit (Wall *et al.*, 1995; Lambright *et al.*, 1996). Perhaps interaction with a cytoplasmic protein through this domain sequesters Alsin in the cytoplasm. This may play a role in regulating the Rac1 and Rab5 guanine nucleotide exchange activity of Alsin. Additionally, the beta propeller domain may bind back and interact with another domain of Alsin, serving to allosterically inhibit the Rac1 and Rab5 GEF domains. This may be reflected by the fact that overexpression of full-length Alsin was unable to stimulate Rab5-mediated endosome-endosome fusion (data not shown), whereas

the Vps9 domain alone possesses this activity. Further characterization of the

beta propeller domain and the proteins that interact with it should provide insight

into how it may regulate Alsin function.

How could a protein that specifically activates Rac1 and Rab5 be

important for motor neuron maintenance? Several hypotheses can be proposed.

First, Alsin may be involved in motor neuron maintenance by regulating actin

dynamics. Actin has been shown to be involved in a number of processes in

neurons, many of which provide structural integrity and include: dendritic spine

formation ((Dailey and Smith, 1996; Ziv and Smith, 1996; Fiala *et al.*, 1998) and

plasticity (reviewed in (Bonhoeffer and Yuste, 2002)), activity-dependent

formation of new active pre-synaptic terminals (Colicos *et al.*, 2001), axon

guidance (reviewed in (Gallo and Letourneau, 2000)), and cadherin-catenin

regulation of synaptic structural plasticity (Murase *et al.*, 2002; Togashi *et al.*,

2002). Actin has also been shown to be involved in receptor trafficking events in

neurons such as: clustering of post-synaptic receptors (Allison *et al.*, 1998; Hirai

and Launey, 2000), recycling of endocytic vesicles and subsequent transport to

the synaptic vesicle cluster (Shupliakov *et al.*, 2002), transport of exocytic

synaptic vesicles (Bernstein *et al.*, 1998), and regulation of synaptic vesicle fusion

(Morales *et al.*, 2000). Many processes that involve actin function are known to

be regulated by Rac (Hall, 1998; Kaibuchi *et al.*, 1999; Sah *et al.*, 2000).

Activation of Rac by Alsin could stimulate actin remodeling observed in all of the

aforementioned processes. Furthermore, it has been suggested that Rab5 may play a role in the formation of membrane ruffles (Spaargaren and Bos, 1999). Therefore, Alsin guanine nucleotide exchange activity on Rac1 or Rab5 could provide key upstream regulation of the actin pathway. An intriguing hypothesis is that Alsin activation of Rac1 and Rab5 are temporally distinct events resulting in transient but separate stimulation of actin dynamics. It is now being appreciated that perhaps as many as four different actin remodeling events are required for endocytosis (Qualmann *et al.*, 2000). Alsin, through Rac1 and Rab5 activation, may serve to regulate many of these events.

A second role for Alsin in motor neuron maintenance could involve the regulation of glutamate receptor endocytosis. It has been hypothesized that elevated levels of glutamate at the synaptic cleft trigger excessive activation of AMPA (α-amino-3-hydroxy-5-methyl-4-isoxazole propionic acid) receptors, the subsequent activation of NMDA (N-methyl-D-aspartate) receptors and Ca^{2+} influx (Julien, 2001). Motor neuron death due to ALS is generally thought to be apoptotic in nature, as mouse models show upstream caspase activation followed by cytochrome c release from the mitochondria (Kostic *et al.*, 1997; Li *et al.*, 2000; Pasinelli *et al.*, 2000; Vukosavic *et al.*, 2000; Guegan *et al.*, 2001). Moreover, inhibition of caspases and cytochrome c release and overexpression of anti-apoptotic proteins of the Bcl-2 family can prolong survival in these models (Kostic *et al.*, 1997; Li *et al.*, 2000; Zhu *et al.*, 2002). An overwhelming amount

of evidence exists showing that AMPA, NMDA, and metabotropic (mGlu)

glutamate receptors are cleared from the cell surface by endocytosis (Carroll *et al.*, 1999a; Carroll *et al.*, 1999b; Luscher *et al.*, 1999; Beattie *et al.*, 2000; Ehlers, 2000; Lin *et al.*, 2000; Man *et al.*, 2000; Wang and Linden, 2000; Dale *et al.*, 2001; Mundell *et al.*, 2001; Roche *et al.*, 2001; Snyder *et al.*, 2001; Xiao *et al.*, 2001; Zhou *et al.*, 2001; Lee *et al.*, 2002; Luis Albasanz *et al.*, 2002; Fourgeaud *et al.*, 2003; Nong *et al.*, 2003). Rab5 activation is required for the endocytosis of many plasma membrane receptors. Alsin regulation of Rab5 would provide a key point of regulation in the endocytic pathway. In addition, as mentioned above, Alsin activation of Rac1 and Rab5 could serve to regulate the actin dynamics required for endocytosis and other cellular functions. For example, stimulus-induced dendritic arbor growth not only requires glutamate receptor mediated synaptic transmission, but also an increase in Rac activity and modulation of the actin cytoskeleton (Li *et al.*, 2002; Sin *et al.*, 2002). If Alsin was involved in the endocytosis of glutamate receptors, a loss in Alsin function could be expected to cause an abundance of glutamate receptors at the cell surface, and subsequently, excessive activation through these receptors, triggering apoptosis.

Third, a loss of Alsin function may negatively impact neurotrophic factor signaling. Signaling events that initiate at distal dendrites and axons must be propagated to the cell body in order to mediate their effects on cellular homeostasis (Barker *et al.*, 2002; Chao, 2003). These signaling intermediates,

termed 'signaling endosomes' have been shown to contain Rab5 (Howe *et al.*, 2001). In addition, Rac activation has been observed in neurotrophic receptor signaling cascades (Huang and Reichardt, 2003). Therefore, through its regulation of Rac1 and Rab5, Alsin may be involved in the formation and maturation of neurotrophic receptor-containing signaling endosomes. In the absence of functional Alsin, internalization of activated receptors and their participation in neuronal retrograde signaling to the cell body may be lost, eventually leading to cellular apoptosis.

Since the disease-causing mutations in *ALS2* suggest that the Vps9 domain alone is required for Alsin function, the above hypotheses focus on pathways that require Rab5 and involve Rac1. However, a more central role for Rac1 activation in Alsin function should also be considered. In addition to its established role in regulating the actin cytoskeleton, Rac1•GTP also interacts with p35/cdk5 kinase (Nikolic *et al.*, 1998). Though the functional significance of this interaction is not clearly understood, p35/cdk5 is required for neurite outgrowth (Nikolic *et al.*, 1996) and synaptic vesicle endocytosis (Tan *et al.*, 2003) implicating a role for Rac1•GTP in both of these processes. Additionally, although it is well appreciated that phosphatidylinositides activate Rac1 through direct interaction with the PH domain of Rac1 GEFs, recent evidence has been presented that shows Rac1•GTP can positively regulate phosphatidylinositide production through its interaction with PI(3)K (Welch *et al.*, 2003). This suggests a potential role for

Alsin in the production of signaling lipids. Finally, Rac2•GTP has been

implicated in the generation of reactive oxygen species (ROS) by regulating the

assembly of the NADPH oxidase (Bokoch and Diebold, 2002). Although

primarily utilized in phagocytic leukocytes (Rac2), Rac1-mediated ROS

production has now been observed in other cellular contexts and is thought to play

a role in cell signaling (Bokoch and Diebold, 2002). Therefore, Alsin Rac1 GEF

activity may potentially link these processes and/or actin cytoskeleton remodeling

to membrane trafficking events regulated by the Vps9 domain. Further studies

will be required to determine which of these cellular events is perturbed when

Alsin function is lost in ALS2, juvenile-onset primary lateral sclerosis, and

infantile-onset hereditary spastic paraplegia.

Chapter 3. Cross-species characterization of the ALS2 gene and analysis of its pattern of expression in development and adulthood

Overview

Mutations in the *ALS2* gene that encodes Alsin cause autosomal recessive juvenile-onset amyotrophic lateral sclerosis (ALS2) and related conditions. Using both a novel monoclonal antibody and LacZ knock-in mice we demonstrate that Alsin is widely expressed in neurons of the CNS, including the cortex, brain stem and motor neurons of the spinal cord. Interestingly, the highest levels of Alsin are found in the molecular layer of the cerebellum, a brain region not previously implicated in ALS2. During development, Alsin is expressed by day E9.5, but CNS expression does not become predominant until early postnatal life. At the subcellular level, Alsin is tightly associated with endosomal membranes and is likely to be part of a large protein complex that may include the actin cytoskeleton. *ALS2* is present in primates, rodents, fish and flies, but not in the nematode worm or yeast, and is more highly conserved than expected among mammals. Additionally, the product of a second, widely expressed gene, ALS2 COOH-terminal like (ALS2CL), may subserve or modulate some of the functions of Alsin as an activator of Rab and Rho GTPases.

Introduction

Amyotrophic lateral sclerosis (ALS) is a neurodegenerative disorder that affects 0.5-3 per 100,000 individuals. It is characterized by the degeneration and death of large motor neurons in the cerebral cortex, brainstem and spinal cord, resulting in progressive muscle weakness, atrophy and death from respiratory paralysis usually within 3-5 years of symptom onset (Brown, 1995). The diagnosis of ALS requires the presence of both upper and lower motor neuron features with disease progression. While the majority of ALS cases are sporadic (SALS), 10% are familial (FALS) (Mulder *et al*., 1986). Four different FALS loci have been established by linkage analysis, but until recently only one mutated gene, Cu-Zn superoxide dismutase 1 (SOD1), had been identified. Mutations in SOD1 cause a dominant adult-onset form of ALS that comprises approximately 20% of FALS cases (Rosen *et al*., 1993); (Pramatarova *et al*., 1995). In 2001, two groups reported that mutations in the *ALS2* gene caused autosomal recessive juvenile onset ALS (ALS2) or the related condition juvenile primary lateral sclerosis (JPLS) in three families from Tunisia, Kuwait and Saudi Arabia (Hadano *et al*., 2001); (Yang *et al*., 2001). Since then, a total of nine recessive mutations have been described in the *ALS2* gene in ALS2, JPLS or infantile onset hereditary spastic paraplegia (IAHSP), that are spread widely across the entire coding sequence (Hadano *et al*., 2001); (Yang *et al*., 2001); (Eymard-Pierre *et al*., 2002); (Devon *et al*., 2003); (Gros-Louis *et al*., 2003).

All the mutations result in a similar clinical phenotype of an infantile onset of limb and facial muscle weakness, accompanied by bulbar or pseudobulbar symptoms, which generally progresses to paraplegia during childhood. This phenotype is suggestive of upper motor neuron damage, although there are as yet no reports of pathology in affected individuals. In the Tunisian family, lower motor neuron symptoms (muscular atrophy and EMG abnormalities) were also detected (Ben Hamida *et al.*, 1990), leading to a diagnosis of ALS. All the mutations described thus far are predicted to result in premature termination of translation, caused by a frameshift or nonsense mutation, and would therefore be expected to result in a complete loss of protein function. Consistent with this, Yamanaka et al recently demonstrated an absence of Alsin (both full length and truncated forms) in lymphoblasts from patients from four families (Yamanaka *et al.*, 2003).

The human *ALS2* gene is comprised of 34 exons located on chromosome 2q, and encodes a full-length cDNA of 6.5 kb. The *ALS2* cDNA is translated into a protein of 1657 amino acids, termed Alsin. In addition to the full-length cDNA, a short form of 2.6 kb was also detectable by Northern blot (Hadano *et al.*, 2001). This short form was predicted to be derived from alternative splicing at the 5' donor site after exon 4, thus corresponding to exons 1 to 4 followed by read-through into intron 4 (Hadano *et al.*, 2001); (Yang *et al.*, 2001). Of the nine mutations described so far, only the Tunisian family mutation (which lies in exon

3) would be predicted to affect both the full-length and short forms of *ALS2*. It has therefore been proposed that loss of full length Alsin leads to upper motor neuron degeneration, but that additional loss of the short form of Alsin might be required for lower motor neuron degeneration (Hadano *et al.*, 2001); (Yang *et al.*, 2001); (Leavitt, 2002). However, this hypothesis has yet to be substantiated, since there is no evidence for expression of the predicted short form of Alsin at the protein level (Otomo *et al.*, 2003); (Yamanaka *et al.*, 2003). Additionally, when a short form construct was expressed in cultured human cells, the protein was found to be unstable and rapidly degraded by the proteasome (Yamanaka *et al.*, 2003). It is unclear whether in vivo a transcribed mRNA is degraded before translation, or whether the short protein is rapidly processed.

The full-length Alsin protein contains several interesting domains that suggest membrane localization and roles in protein sorting and trafficking (Hadano *et al.*, 2001); (Yang *et al.*, 2001). Alsin contains a central Dbl-homology / Pleckstrin-homology (DH/PH) domain that is indicative of guanine nucleotide exchange (GEF) activity for the Rho GTPase family of proteins, and a COOH-terminal Vps9 domain implying Rab5 GEF activity. Indeed, Alsin has recently been shown to act as a GEF towards Rab5 (Otomo *et al.*, 2003); (Topp *et al.*, 2004) and Rac1 (Topp *et al.*, 2004). Rho and Rab5 family GTPase proteins have been implicated in a multitude of cellular functions, with the best characterized being regulation of the actin cytoskeleton (Rho) and protein trafficking through

early endosomes (Rab5). Additionally, Alsin contains regulator of chromatin condensation 1 (RCC1) domains at the NH_2-terminus, which may indicate Ran GEF activity or, since this motif has the potential to form a 7-bladed beta-propeller structure, may otherwise function as a protein-protein interaction domain (Topp *et al.*, 2004). Finally, the presence of eight membrane occupation and recognition nexus (MORN) motifs may indicate membrane attachment.

Towards further characterization of Alsin's normal function and its role in the pathology of ALS2, we have examined several aspects of *ALS2* and Alsin expression, from protein expression across species to subcellular localization. We predicted the sequence of Alsin's orthologues in five additional species from primates to insects, and have demonstrated Alsin expression in three mammalian species. We have also detected a previously unidentified second gene that shows substantial homology to the COOH-terminal half of *ALS2*. We have examined in detail the expression of the *Als2* gene and the Alsin protein in mouse neuronal and peripheral tissues, in adults and during development. This expression pattern was consistent with predictions based on transcription factor binding sites detected within the regulatory regions of the *ALS2* genomic DNA. Finally, we present data indicating that Alsin is enriched in fractions containing endosomal membranes and may be present in a large protein complex containing the actin cytoskeleton.

Materials and methods

Bioinformatics

ALS2 sequences in other species were identified by performing blastn,

tblastn or blast2sequences (Tatusova and Madden, 1999) similarity searches, with

default parameters, at the National Center for Biotechnology Information (NCBI)

website (www.ncbi.nlm.nih.gov/BLAST). Pairwise sequence alignments were

performed using Smith-Waterman alignment, using the BLOSUM62 matrix, a

gap opening penalty of 10 and a gap extension penalty of 0.5. Gene prediction

was performed using the GenomeScan (Yeh *et al.*, 2001) webserver

(http://genes.mit.edu/genomescan.html) using all known species of Alsin for the

required protein homology information. Multiple sequence alignment was

performed using ClustalX (v1.83) using the BLOSUM series matrix, a gap

opening penalty of 10, and a gap extension penalty of 0.2. Multiple sequence

alignments were visualized and manipulated using GeneDoc v2.6.02 (Nicholas,

1997) (http://www.psc.edu/biomed/genedoc). The neighbor-joining phylogenetic

tree was generated in ClustalX after exclusion of all positions with gaps, and was

viewed in TreeView (Page 1996)

(http://taxonomy.zoology.gla.ac.uk/rod/treeview.html). Domain structure was

identified by using reverse position specific (rps) blast at the NCBI website on the

Conserved Domain Database (Marchler-Bauer *et al.*, 2003) using an expect value

of 10. Domain architecture analysis was performed by searching the human Alsin

sequence using CDART (Conserved Domain Architecture Retrieval Tool) at the

NCBI website. Searches for motifs in untranslated regions were performed using

UTRscan (Pesole and Liuni, 1999). Searches for human disorders linked to the

ALS2CL locus were through OMIM via Entrez at the NCBI web-site

(www.ncbi.nlm.nih.gov/entrez/) and for phenotypes associated with the mouse

Als2cl locus through the Mouse Genome Informatics website

(www.informatics.jax.org/)

For analysis of regulatory regions, approximately 25 kb of genomic

sequence from human, chimp, mouse and rat *ALS2* genes (comprising 12kb

upstream of exon 1, exon 1, intron 1 and exon 2) were aligned using LAGAN or

Multi-LAGAN (Brudno *et al.*, 2003), with the user-defined parameters set as

follows: window length: 100 bp, percent identity: 75%, minimum level of

conservation to display: 50%, human as the base sequence. VISTA (Mayor *et al.*,

2000) provided plots and text summaries of the alignments. The alignments were

used as input for Consite (http://mordor.cgb.ki.se/cgibin/CONSITE/consite/) to

search for TFBS, with the following parameters: minimum specificity: 10 bits, TF

score threshold: 80%, window size: 100bp.

Polymerase chain reaction

Expression of the *ALS2CL* gene was tested on Human Multiple Tissue

cDNA Panels I and II (BD Biosciences). The same quantity of panel cDNA was

used in each reaction, and a 250 bp fragment was amplified using the Advantage

GC-2 Genomic PCR kit (BD Biosciences) using the primers forward: 5' GAA

CGC AGT CAC CCT CTT TGG 3' and reverse: 5' ATC AAA GGT GTG GAC

ATT GTG G 3'. Control glyceraldehydes-3-phosphate dehydrogenase (GAPDH)

PCR was performed with primers supplied with the cDNA panels.

Preparation of tissue homogenate and cell lysate

Wild-type adult mice (mixed C57Bl/6 and 129Sv/ImJ) were anaesthetized

by intraperitoneal injection of 0.5 mg/g avertin (2,2,2 tribromoethanol), terminally

perfused through the ascending aorta with 200 mls phosphate-buffered saline

(PBS) (7.2), and the required tissues harvested and snap frozen in liquid nitrogen.

Proteins were extracted from frozen tissues by homogenization for 10 seconds in

sucrose buffer (11% sucrose, 20 mM Tris (7.2), 1 mM $MgCl_2$, 0.5 mM EDTA, 5

mM of the protein inhibitor phenylmethane sulphonyl fluoride (PMSF)),

sonication for 10 sec, followed by microcentrifugation at 8,000 rpm for 5 min at

4°C and collection of the supernatant. For preparation of lysates from cultured

cells, cells were washed twice in ice cold PBS, and were then scraped from the

plate surface into 1 ml of PBS. The cells were pelleted by centrifugation for 10

min at 3,000 rpm at 4°C and were then lysed in 300 μl Triton lysis buffer (140

mM NaCl, 1% Triton X-100, 20 mM Tris (7.2), 0.5 mM EDTA, 10% glycerol, 5

mM PMSF) on ice for 20 min. The lysate was centrifuged for 1 min at 14,000

rpm at 4°C and the supernatant removed. For all samples, the total protein

concentration was determined by Lowry ELISA.

Antibodies

A construct expressing the NH$_2$-terminus of mouse Alsin (residues 1 to

364) fused to glutathione S-transferase was generated in the vector pGEX-6P-3

(Pharmacia). The purified Alsin NH$_2$-terminus fusion protein was used as the

immunogen to inject Balb/C mice. The mice were given 100 μg of the fusion

protein in Freund's complete adjuvant subcutaneously and then two additional

injections of 100 μg of the fusion protein in Freund's incomplete adjuvant at 14-

day intervals. Three days before cell fusion, the mice received an intravenous

injection of 100 μg of the fusion protein via the tail vein. Splenocytes were fused

with NS-1 myeloma cells, and hybridomas were selected and cloned. To identify

clones specific for the fusion protein, primary screening of hybridoma culture

supernatant was performed by ELISA using 96-well plates coated with the fusion

protein. 38 ELISA positive hybridomas were obtained. Western blotting was

used to select one of these, N-Alsin-24, for further use.

Western blot analysis

Protein homogenate or lysate was denatured by boiling for 5 min in 1x

sample loading buffer (0.1 M Tris (6.8), 10% glycerol, 1% SDS, 8% β-

mercaptoethanol) run on 7.5% acrylamide SDS-PAGE gels and transferred onto

PVDF membranes. For cross-species analysis, cerebella from mouse, rat and cow

were homogenized and fractionated as described below and supernatant from the

160,000 xg spin was subjected to SDS-PAGE. All Western blotting was

conducted using the purified N-Alsin-24 monoclonal antibody (1:500 dilution),

followed by detection using enhanced chemiluminescence (Amersham). For

competition studies, a 10-times molar excess of antigen was incubated with the N-

Alsin-24 antibody for two hrs at room temperature before diluting in milk.

Equivalent protein loading was assessed by subsequent glyceraldehyde-3-

phosphate dehydrogenase (GAPDH) (Chemicon) immunoblotting of the PVDF

membranes. A mouse neuronal tissue pre-made Western blot was purchased from

Zyagen Laboratories.

X-Gal staining

In order to study the expression of the *Als2* gene at the cellular level,

transgenic mice were generated that expressed the *lacZ* gene under the control of

the *Als2* promoter (R.S. Devon et al., in preparation). Wild-type and hemizygous

transgenic adult male mice from two independent lines (F1 C57Bl/6 x 129Sv/ImJ)

were anaesthetised by intraperitoneal injection of 0.5 mg/g avertin (2,2,2

tribromoethanol) and terminally perfused through the ascending aorta with 200

mls 2% paraformaldehyde, 0.2% glutaraldehyde in 0.1 M PBS (7.4). Following

perfusion, tissues were removed and post-fixed at 4°C for an additional hr in the same fixative. To study developmental stages, the F2 progeny of intercrosses between two hemizygous transgenics were dissected at multiple developmental stages and the embryos were immersion-fixed in 2% paraformaldehyde, 0.2% glutaraldehyde in 0.1 M PBS (7.4) at 4°C for 2-3 hrs. The embryonic yolk sac from each embryo was harvested for genotyping. At days E9.5, E12.5 and E14.5, entire embryos were fixed, at days E16.5 and E18.5 just the head, and at day P7 the brain was removed and fixed. For each age one wild-type and two hemizygous transgenic animals were examined. After fixation, all tissues were transferred to 30% sucrose in PBS at 4°C overnight. Tissues were then frozen on dry ice and sectioned at 25 μm on a cryostat. Embryonic and adult peripheral tissue sections were thaw-mounted onto glass slides (Fisherbrand Superfrost Plus). Adult brain tissue sections were collected free-floating and mounted on glass slides afterwards. The mounted and free-floating sections were washed three times for 10 min at room temperature in X-Gal wash buffer (2 mM $MgCl_2$, 0.01% sodium deoxycholate, 0.02% Nonidet-P40 (NP-40), in PBS). Staining was carried out in 1mg/ml X-Gal (5-bromo-4-chloro-3-indolyl-β-d-galactoside, Gibco), 5 mM potassium ferrocyanide, and 5 mM potassium ferricyanide in X-Gal wash buffer at room temperature overnight, under agitation in the dark. After staining, sections were washed three times for 10 min in PBS, followed by a brief rinse in distilled water, air-dried and coverslipped with DPX (BDH). Some

sections were counterstained with 0.25% Neutral Red (ICN) in distilled water (containing 50 µl glacial acetic acid per 100 ml) for 30 sec at room temperature.

Immunohistochemistry

Tissue processing was carried out as described above except that for fixation, 4% paraformaldehyde in 0.1 M PBS (7.4) was used. Immunohistochemistry with the N-Alsin-24 antibody (dilution 1:1000) was performed using the Animal Research Kit (Dako, K3954) as described in the manufacturer's protocol. As a control for immunostaining, the antibody was pre-absorbed with a ten-fold molar excess of either N-Alsin-24 antigen or an unrelated antigen, overnight at 4°C. Absorption with the antigen abolished immunostaining, while absorption with the unrelated antigen had no effect on staining pattern or intensity. To identify cell types expressing the *lacZ* product, X-Gal staining was combined with immunohistochemistry. Following X-Gal staining the sections were treated for 30 min with 0.5% H_2O_2 in PBS, containing 0.3% Triton X-100 (PBS-T), transferred into 5% skimmed milk in PBS-T for 30 min, and incubated overnight at room temperature with the primary antibodies NeuN (Chemicon, MAB377, dilution 1:100-200) and GFAP (DAKO, Z 0334, dilution 1:5000). Sections were next treated with the appropriate biotinylated secondary antibody (Vector Lab; 1:200) for 2 hrs at room temperature, followed by incubation in avidin-biotinylated horseradish peroxidase complex (ABC Elite,

Vector Lab; 1:1000) for 1 hr at room temperature. Peroxidase labeling was

visualized by incubation in 0.05% 3,3-diaminobenzidine (Pierce) containing

0.01% H_2O_2 in 0.05 M Tris (7.6). When the brown staining product developed,

the reaction was stopped by transferring the sections into PBS. Sections were

then rinsed in distilled water, air-dried and coverslipped with DPX (BDH).

Additional controls for immunostaining were performed by omitting the primary

antibody.

Cerebellum fractionation and characterization

Mouse cerebella were lysed in lysis buffer (0.32 M sucrose, 5 mM Tris

(7.5), 0.5 mM $CaCl_2$, 1 mM $MgCl_2$, protease inhibitor cocktail) and homogenized

(30 strokes) in a 15 ml Dounce homogenizer. Homogenate was then lysed by

light sonication or passage through 18- and 25-gauge needles. (The fractionation

pattern of Alsin was the same with both lysis methods). The homogenate (WC)

was centrifuged at 500 xg for 10 min to remove unlysed cells and debris (P1).

The resultant lysate (S1) was then centrifuged for 15 min at 10,000 xg to generate

a pellet (P2) and supernatant (S2) fraction. This S2 supernatant was then

centrifuged at 160,000 xg for 2 hrs to generate a pellet (P3) and supernatant (S3)

fraction. Supernatants and WC were isolated and added to an equal volume of 2x

urea/sample buffer (20% glycerol, 10% β mercaptoethanol, 6% sodium dodecyl

sulfate (SDS), 6 M urea, 125 mM Tris (6.8), 0.02% bromophenol blue) and pellets

were resuspended in 2 volumes 2x SDS-sample buffer. Equivalent amounts of each subcellular fraction were analyzed by Western blotting with antibodies to Alsin (N-Alsin-24, 1:1000), Transferrin receptor (Zymed, 1:1000), actin (Sigma Aldrich, 1:2000), NaK-ATPase (Novus Biologicals, 1:2000), and Rab5 (BD Bioscience, 1:100).

P3 association experiments were performed by incubating 40 μl S2 (generated as above) with 10 μl of one of the following: H_2O, 5 M NaCl, 6 M urea, 0.5 M Na_2CO_3 (11), 5% sodium deoxycholate, 5% Tween-20, 5% CHAPS, 5% NP-40, 5% Triton X-100. Samples were incubated on ice for 30 min with light vortexing every few minutes, and then centrifuged at 160,000 xg for 2hrs. Supernatant was isolated and added to 50 μl 2x SDS-sample buffer (same as above, without urea) and pellets were resuspended in 100 μl 2x SDS-sample buffer. An equal volume of sample for all fractions was analyzed by Western blotting with the N-Alsin-24 antibody (1:500).

Results

Identification of *ALS2* in primates, rodents, fish and insects

Human (Accession no. NM_020919), mouse (NM_028717) and Drosophila (NM_141090) Alsin have been described previously (Hadano *et al*., 2001), (Yang *et al*., 2001). Using bioinformatics approaches, we have now predicted *ALS2* from the chimpanzee (*Pan troglodytes*), rat (*Rattus norvegicus*),

puffer fish (*Fugu rubripes*), zebrafish (*Danio rerio*) and mosquito (*Anopheles gambiae*). Nucleotide sequence data are available in the Third Party Annotation Section of the DDBJ/EMBL/GenBank databases under the accession numbers TPA: BK005190-BK005194. Pairwise comparisons between Alsin sequences in each species are shown in Figure 14A.

The chimpanzee Alsin sequence was assembled from four clones (accessions AACZ01057807.1, AADA01247766.1 , AACZ01057805.1, and AACZ01057804.1) in the whole genome shotgun (WGS) database and three sequences from the trace archive (ti|244355573, ti|368654191, and ti|254583660). Chimpanzee Alsin is 1657 amino acids long, the same length as human Alsin, and is extremely similar: 1653 amino acids are identical (99.8%) and 1656 amino acids are similar (99.9%). The only non-conservative amino acid change (R1283G) is surprising since a glycine at this position is conserved among all other vertebrates, and it is possible that this in fact reflects a C/G substitution error in the primary genomic sequence.

The rat *ALS2* sequence was predicted from the rat chromosome 9 genomic sequence AABR030686212.1 and the trace archive sequence ti|155354063. The 34 exon/33 intron genomic structure of the *ALS2* gene is identical between rat, mouse and human. The rat predicted protein is 1657 amino acids long and is very highly conserved with human, showing 91.4% identity and 95.0% similarity. This is considerably more highly conserved than expected since the average

identity between human and rat is 88% (Makalowski and Boguski 1998). The majority of the sequence variation occurs outside predicted domain regions, with 63 of the 143 non-identities (44%), including a six amino acid deletion, occurring in a 212 amino acid stretch between amino acids 264 and 475, in between two RCC1 repeats (Yang *et al*., 2001). Of note, the RefSeq proteins XP_343575 and XP_343576 are both annotated to be rat Alsin but the protein is split into two due to erroneous prediction of splice sites, and also includes an additional exon between exons 13 and 14 that is not present in human or mouse *ALS2*.

The puffer fish *ALS2* sequence was predicted from the Fugu rubripes WGS assembly SCAFFOLD_69, CAAB01000069.1. There was insufficient sequence homology to identify the extreme 5' end of the Fugu gene using the tblastn approach. Moreover, no expressed sequence tags (ESTs) or cDNA sequences could be identified spanning this region. Therefore the predicted Fugu *ALS2* sequences are still incomplete at this end (corresponding to exons 1 and 2). Fugu *ALS2* is comprised of 34 exons like its mammalian counterparts, although the length of some exons is different. In the absence of empirical data it is not possible to verify whether these represent genuine differences or rather errors in the prediction. The distance spanned in genomic DNA by Fugu Alsin from the start of exon 3 to the stop codon is 9.7 kb, compared with 65.5 kb for the corresponding sequence in human, a 6.7-fold compaction, slightly less than the observed average 7.5 to 8-fold compaction in the Fugu genome relative to human

(Miles *et al.*, 1998); (McLysaght *et al.*, 2000). The Fugu Alsin protein is 1639 amino acids long (with a predicted 8 NH_2-terminal amino acids missing) and exhibits 59.0% identity and 73.3% similarity with human. This level of conservation between human and Fugu agrees with the average across the proteome; it has been shown that the modal degree of sequence similarity between human proteins and their Fugu orthologues is 70% (Aparicio *et al.*, 2002).

The zebrafish *ALS2* sequence used was predicted from the working draft sequence of clone DKEY-33M14 (accession BX571704.3). Similarly to Fugu, there was insufficient sequence homology to identify sequence corresponding to human exons 1 and 2, and also the terminal exon 34, so the cDNA sequence is incomplete at the extreme 5' and 3' ends. The zebrafish Alsin sequence is 1590 amino acids long (with a predicted 19 amino acids missing) and exhibits 50.5% sequence identity and 65.0% similarity with human Alsin. Interestingly, intron 4 appears to be missing in zebrafish: the conservation with human is poor in this region but the sequence that would correspond to human exons 4 and 5 is contiguous (zebrafish cDNA bp 149 to 1468). This implies that zebrafish *ALS2* does not have the potential to encode a short isoform comparable to that proposed in human and mouse (Hadano *et al.*, 2001); (Yang *et al.*, 2001)since this short isoform requires translational read-through into intron 4. This is the only known species in which intron 4 is missing.

The mosquito *ALS2* sequence was predicted from the WGS sequence of

chromosome 3L, AAAB01008986.1. The 4170 bp cDNA sequence is split into eight exons, spanning only 5.8 kb in genomic DNA. The full length predicted peptide is 1390 amino acids long, and exhibits 23.0% identity and 37.1% similarity with human Alsin.

A partial multiple alignment of all eight species, and a phylogenetic tree generated from this alignment, are shown in Figures 14B and 14C. The COOH-terminal alignment shown is the most highly conserved region of the protein, and includes the Vps9 domain, in which 78 of the 95 residues (82%) are identical or similar across all vertebrates. Considerable evidence points to this domain being essential for Rab5 regulation of endosomal fusion (Horiuchi *et al*., 1997); (Barbieri *et al*., 1998); (Tall *et al*., 2001). The two most highly conserved residues in the Vps9 domain, according to the Protein Families (PFAM) database entry PF02204, are also identical in Alsin among all identified species (a proline at amino acid 1592 and an aspartic acid at amino acid 1624). However, it can be seen from Figure 14B that the cross-species conservation in Alsin extends well beyond the boundaries of the Vps9 domain itself, to regions that contain no known domain or motif. It is likely that these regions contain previously unrecognized, functionally important sequences, and this entire region exhibits significant similarity to the consensus of the recently defined Clusters of Orthologous Groups protein family, KOG0231 ("Junctional membrane complex protein Junctophilin and related MORN repeat proteins"). In contrast to the

COOH-terminus of the protein, the NH_2-terminal region, spanning the RCC1

repeats, is not highly conserved at the sequence level, although similarity with

RCC1 repeats is detectable in each case.

An analysis of the domain architecture of Alsin revealed that Alsin is the

only known protein that possesses its particular complement of domains, i.e.

RCC1, DH/PH, MORN and Vps9 (Hadano *et al.*, 2001); (Yang *et al.*, 2001),

although all these domains are found in other proteins, either in isolation or in

combination with other domains (data not shown). There are no potential Alsin

pseudogenes in the human or mouse genomes, and it is thus likely that Alsin plays

a unique role in coupling the activation of specific Rab and Rho GTPases.

A

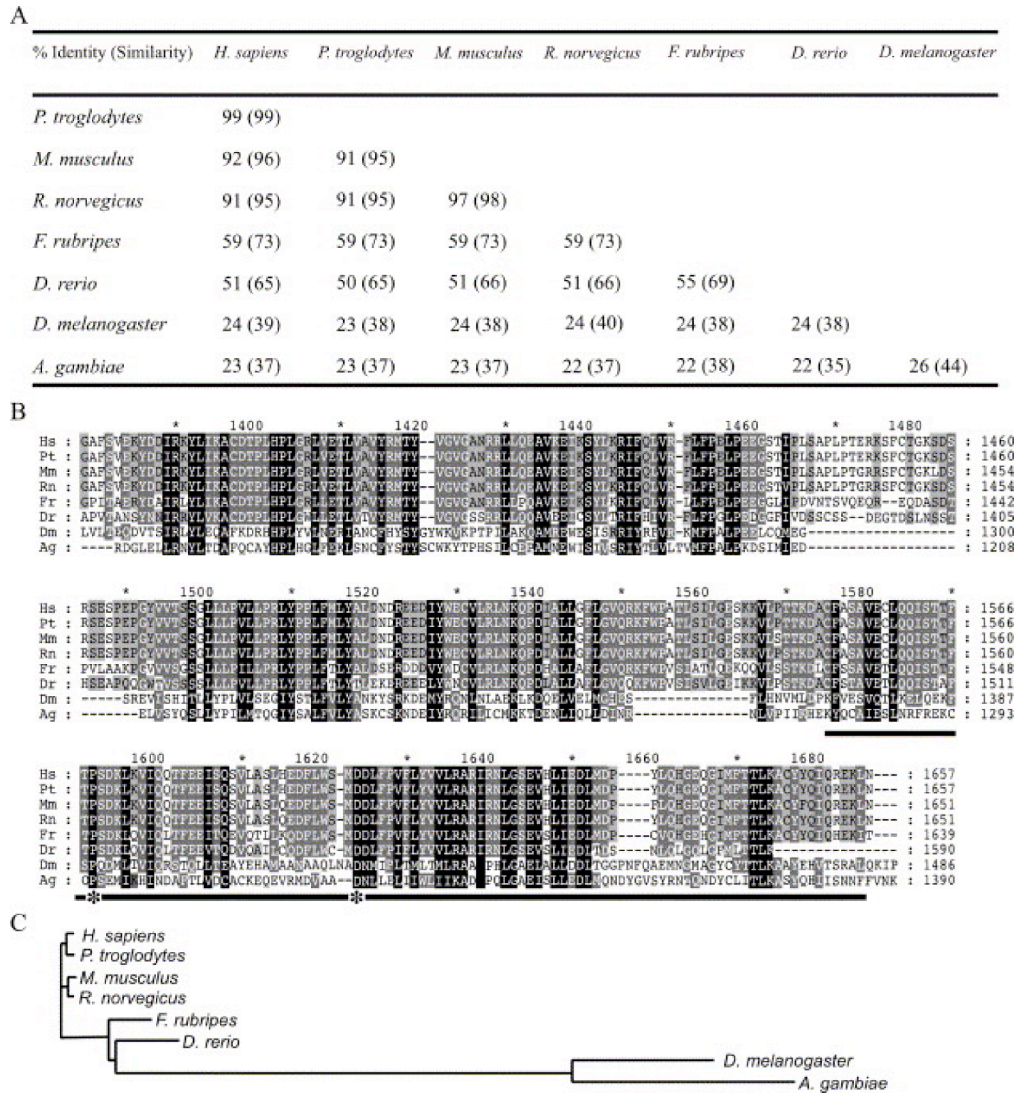| % Identity (Similarity)	H. sapiens	P. troglodytes	M. musculus	R. norvegicus	F. rubripes	D. rerio	D. melanogaster
P. troglodytes	99 (99)						
M. musculus	92 (96)	91 (95)					
R. norvegicus	91 (95)	91 (95)	97 (98)				
F. rubripes	59 (73)	59 (73)	59 (73)	59 (73)			
D. rerio	51 (65)	50 (65)	51 (66)	51 (66)	55 (69)		
D. melanogaster	24 (39)	23 (38)	24 (38)	24 (40)	24 (38)	24 (38)	
A. gambiae	23 (37)	23 (37)	23 (37)	22 (37)	22 (38)	22 (35)	26 (44)

B

C

Figure 14. Comparison of Alsin sequence across species. A) Percentage identity and similarity in pairwise alignments. B) Cross-species multiple sequence alignment of the COOH-terminus of Alsin, containing the Vps9 domain (underlined region). Hs = *Homo sapiens*, Pt = *Pan troglodytes*, Mm = *Mus musculus*, Rn = *Rattus norvegicus*, Fr = *Fugu rubripes*, Dr =*Danio rerio,* Dm = *Drosophila melanogaster*, Ag = *Anopheles gambiae*. Black shading indicates identity or similarity across all eight species, dark grey shading across six or seven (generally vertebrates only) and light grey shading across three or four (generally mammals only). Asterisks indicate residues completely conserved among all proteins containing the Vps9 domain. C) Phylogram showing divergence of Alsin sequences across evolution. Horizontal line lengths represent evolutionary time.

Transcription factor binding sites predict *ALS2* expression in neurons, testis and kidney

Cross-species homology in non-coding regions of the *ALS2* orthologues in human, chimp, mouse and rat were used to search for putative transcription factor binding sites (TFBS). Experimental evidence has shown that TFBS tend to occur within 5 kb upstream of the transcriptional start site and within intron 1 (Levy and Hannenhalli, 2002). We thus selected approximately 25 kb of non-coding sequence (comprising 12 kb upstream of exon 1 through to the 3' end of exon 2) in each species. It was found that across this region, the chimp sequence aligned to the human sequence with 98% identity; the chimp sequence was therefore excluded from further analysis since it would not be informative. Pairwise alignments of human:mouse and human:rat sequence were searched for vertebrate TFBS, using automatically defined appropriate conservation cutoffs of 68% for human-mouse and 66% for human-rat.

Twenty seven putative TFBS were identified on the + (cis) strand from the human-mouse alignment, and twenty-eight from the human-rat. Of these, 12 TFBS were common to both alignments, all of which were located within intron 1. The two alignments also showed two similar patterns of conserved sequence at approximately 1250 and 750 bp upstream of exon 1, but at below the previously stipulated conservation cut-off values. The conservation cut-off was therefore reduced to 50%. This resulted in the identification of three additional TFBS,

bringing the total to fifteen sites present in the human, mouse and rat. The TFBS identified, along with their sequence and position in the human sequence, are shown in Table 1.

Of these 15 TFBS, eight (c-fos, n-myc, c-rel, p65, NF-κB, ARNT, Tal1β, USF) are very widely or ubiquitously expressed, and are therefore not informative. Hepatic leukemia factor (HLF) and Hen-1 however are of particular interest since they may in part control expression of Alsin in the nervous system. HLF is expressed primarily throughout the brain in adulthood, and its expression increases markedly with synaptogenesis, suggesting a role in the maintenance of differentiated neurons (Hitzler *et al.*, 1999). Hen-1 is specific to the embryonic nervous system, is expressed mainly in the neuroepithelium of embryos from E9.5 to E14.5 and is likely to function in neurogenesis (Brown and Baer, 1994).

HFH-3 and Sox-5 may be involved in *ALS2* expression in the periphery. HFH-3 (hepatocyte nuclear factor-3 /forkhead homolog family) expression is restricted to the epithelium of the renal distal convoluted tubules (Overdier *et al.*, 1997), and Sox-5 expression is restricted to post-meiotic germ cells, particularly round spermatids (Denny *et al.*, 1992). Thing1-E47 and the FREAC transcription factors are important during development (Pierrou *et al.*, 1994); (Hollenberg *et al.*, 1995). Taken together these data predict expression of *ALS2* during development and in the CNS in adult animals.

Putative transcription factor binding sites common to human, mouse and rat *A L S 2* genomic sequences, the DNA consensus sequence of each, and the position in which they were found in human *A L S 2* genomic sequence (base +1 corresponds to the first base of exon 1). Sites corresponding to Sox-5, c-FOS and Hen-1 were revealed when the conservation cut-offs were reduced below 68% (human-mouse) and 66% (human-rat). Sites corresponding to Sox-5, c-FOS and Hen-1 were revealed when the conservation cut-offs were reduced below 68% (human-mouse) and 66% (human-rat).

Table 1. Putative transcription factor binding sites common to human, mouse and rat ALS2.

Transcription Factor	Sequence	Position
Sox-5	TAACAAA	-350 to -344
c-FOS	ATGAATCA	-19 to -12
Hen-1	AATCAGCTGATC	-16 to -5
c-REL	GTGAAATTCC	+358 to +367
NF-κB	GTGAAATTCC	+358 to +367
p65	GTGAAATTCC	+358 to +367
HFH-3	TTATATTTGGCT	+910 to +921
HLF	TGTTCCATAAGG	+1472 to +1483
FREAC-2	CATGTGTAAACATT	+5436 to +5449
Thing1-E47	ACTCTGGTTT	+5536 to +5545
FREAC-4	GGAAACAG	+11059 to +11056
Tal1β-E47S	GAAACAGATGGA	+11060 to +11071
ARNT	CACTTG	+11906 to +11911
n-MYC	CACTTG	+11906 to +11911
USF	CACTTGT	+11906 to +11911

A truncated COOH-terminal Alsin-like gene

In the genomes of the human, mouse and rat, a second gene was detected that corresponds to an Alsin-like gene, which is similar to the COOH-terminal half of Alsin, and contains a RhoGEF domain, MORN motifs and a Vps9 domain in the same arrangement as full length Alsin. This gene has been termed ALS2 C-terminal like (*ALS2CL*; HUGO Gene Nomenclature Committee approved). In humans, *ALS2CL*, presently annotated as hypothetical gene FLJ36525, maps to chromosome 3p21.3. This gene is predicted to encode three different protein isoforms, of 953 amino acids (isoform 1; NP_667340), 762 amino acids (isoform 2; NP_877575) and 300 amino acids respectively (isoform 3; NP_877576), which arise from alternative splicing (Figure 15A). Isoform 1 exhibits 33.8% identity

and 51.9% similarity to the aligned COOH-terminal region of Alsin. In the mouse, the *ALS2CL* gene RN49018 (Mitchem *et al.*, 2002) is located on chromosome 9, in a region that shows evidence of conservation of synteny with human chromosome 3p21.3. It encodes a protein of 952 amino acids (accession NP_666340). In the rat, the ALS2CL protein (accession XP_236654) is also 952 amino acids long, and the gene maps to chromosome 8q32. Both the mouse and rat ALS2CL protein sequences exhibit a high level of similarity with human ALS2CL (89.4% and 90.1% respectively), and less similarity with the aligned COOH-terminal region of Alsin (51.7% and 51.8% respectively) so it seems likely that these three truncated Alsin proteins are orthologues of each other. At the time of submission, no human disorders had been mapped to the human *ALS2CL* locus, nor were any mouse phenotypes associated with mutations at the mouse locus.

We have tested the expression of *ALS2CL* by semi-quantitative RT-PCR on human cDNAs from multiple tissue sources and found that it was expressed in every tissue tested (Figure 15B). Highest levels were observed in the kidney and pancreas, moderate levels in the heart, lung, liver, spleen and colon, and, in contrast to Alsin, low levels in the brain and testis. Additionally, *ALS2CL* matches ESTs from a very wide range of peripheral and neuronal tissues, both adult and embryonic, which suggests that its expression pattern is widespread or even ubiquitous. Mouse *ALS2CL* is highly enriched (comprising 2.5% of clones)

in a jejunal and colic lymph node cDNA library (dbEST Library ID.9958). The

predicted size of the protein encoded by *ALS2CL* is 105 kDa, but there is as yet no

evidence for expression of ALS2CL at the protein level. Neither of the COOH-

terminal antibodies previously described that have been tested against multiple

tissues (pAB-ALS21082 (Yamanaka *et al.*, 2003) and HPP1024 (Otomo *et al.*,

2003) is directed against peptide sequences that are sufficiently conserved with

ALS2CL to cross-react, so it is not surprising that ALS2CL has not been

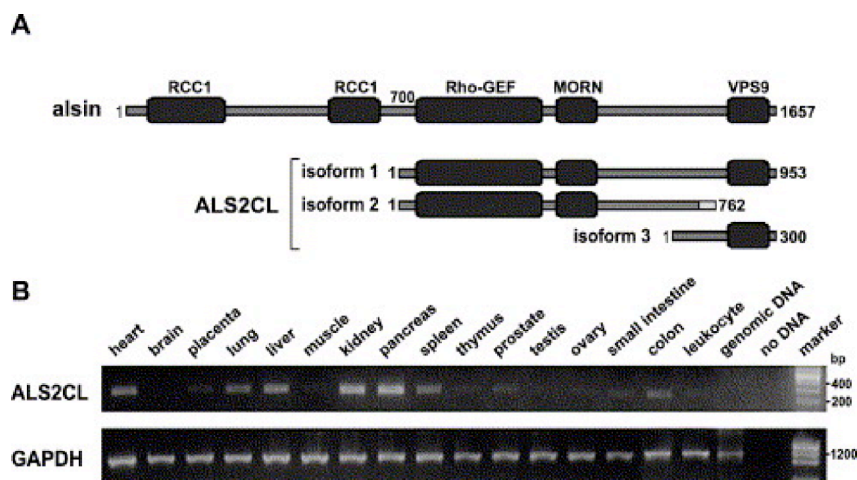previously detected by immunoblotting.

Figure 15. Structure and expression of ALS2CL. A) Domain structure of full-length Alsin and the three isoforms of human ALS2CL. Isoform 3 is identical to the COOH-terminal 300 amino acids of isoform 1; isoform 2 is identical to the first 729 amino acids of isoform 1 but has an alternative COOH-terminus. B) ALS2CL PCR on a panel of human cDNA samples after 25 cycles of amplification. GAPDH PCR was performed as a control for the cDNA templates.

In adult mouse, Alsin is predominantly expressed in the CNS

A monoclonal antibody, N-Alsin-24, was raised in mice against an NH$_2$-terminal fragment of mouse Alsin (amino acids 1 to 364). This antibody recognized a band corresponding to the expected size of full length Alsin (~185 kDa) in Western blots of mouse tissue homogenate (Figure 16), and specifically recognized a ~220 kDa band in blotted lysates of HeLa cells transfected with a full length *Als2*-EGFP fusion construct (Figure 16A). Additionally, recognition of the 185 kDa band was abolished by pre-incubation of N-Alsin-24 with a 10-times molar excess of Alsin antigen, but not with the same excess of an unrelated antigen of a similar size (Figure 16B, panels ii and iii).

Immunohistochemical analysis with the N-Alsin-24 antibody showed Alsin expression in all areas of the mouse brain (Figures 16A, C), including areas likely to be important for ALS2 pathology, such as the brain stem and spinal cord. Interestingly in this regard, expression was also slightly higher in cortex and medulla than in other brain regions. The highest levels of expression were seen in cerebellum. Within the periphery, Alsin expression was sparse, although it was expressed in testis at levels comparable with cortex, and also at lower levels in kidney and liver (Figure 16D). No Alsin expression was detected in heart, lung, spleen or skeletal muscle.

Additionally, smaller Alsin bands were sometimes observed: at ~30-35 kDa (Figure 16A), and ~60 kDa (in the liver, Figure 16D). Both of these bands

were present in samples after freezing and thawing, but were not seen when fresh tissue samples are used (Figure 16B). They were both effectively competed-out with Alsin antigen (data not shown) and are therefore presumed to be genuine Alsin cleavage products. We did not detect a band corresponding to the 44 kDa predicted Alsin short form (Hadano *et al.*, 2001); (Yang *et al.*, 2001). A strong band at approximately 50 kDa was observed in all non-neuronal tissues. This band is presumed to correspond to cross-reactivity with mouse IgG, since i) it is the expected size, ii) its intensity was dramatically reduced if tissue samples were perfused with PBS to remove blood prior to harvesting (data not shown), and iii) it was not competed out by Alsin antigen (Figure 16B).

Consistent with the finding that the *ALS2* gene sequence is present and highly conserved among other mammals, we were able to demonstrate expression of Alsin by Western blotting in cerebellum extracts from mouse, rat and cow (Figure 16E). The antibody reacted poorly with human Alsin, and we are currently generating a second antibody that would allow us to determine the pattern of expression of Alsin in human tissues.
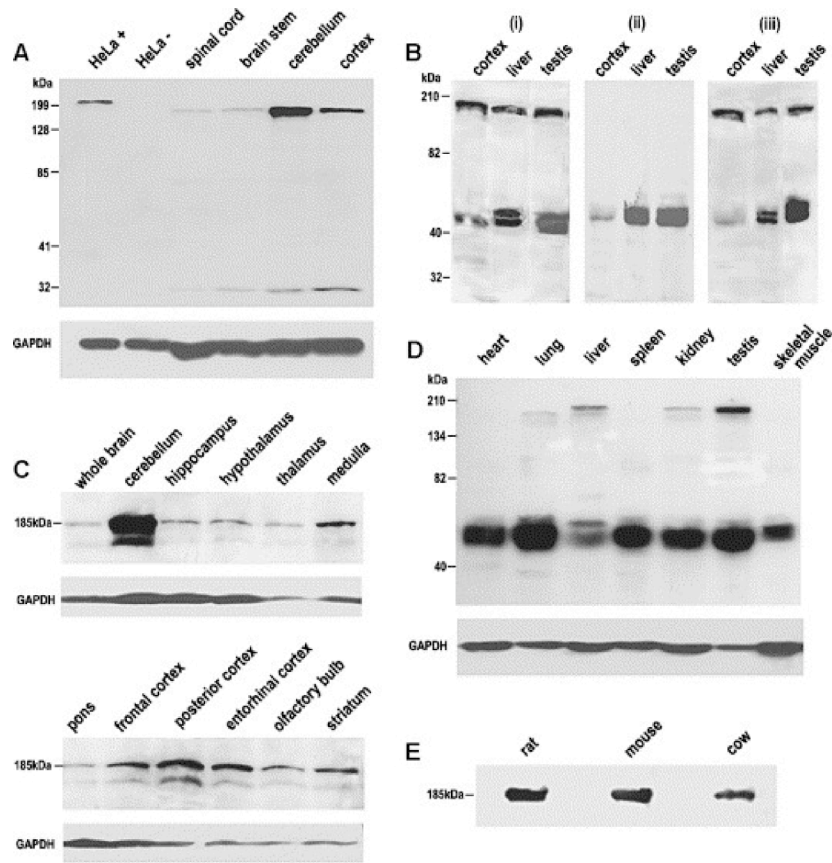
Figure 16. Alsin expression in mouse tissues. Subsequent blotting with an antibody against GADPH was used to quantify the relative loading. A) Mouse neuronal tissues (20 μg total protein) and HeLa cells plus or minus transfection with a full length Als2-EGFP fusion construct (expected size 220 kDa). B) Competition assay to prove specificity of N-Alsin-24. i) Cortex, liver and testis homogenate (30 μg total protein) probed with N-Alsin-24. ii) and iii) The same homogenates probed with N-Alsin-24 after pre-incubation of the antibody with an excess of N-Alsin-24 antigen (ii) or an unrelated antigen of a similar size (iii). C) Mouse neuronal tissues (75 μg total protein). D) Mouse peripheral tissues (60 μg total protein). E) Cerebellar S3 lysates from rat (10 μg), mouse (10 μg) and cow (30 μg) probed with N-Alsin-24.

Als2 is highly expressed in cerebellar granule cells and alpha motor neurons of the spinal cord

In order to study the detailed cellular expression pattern of *Als2*, we generated mice transgenic for the *lacZ* gene under the control of the endogenous

Als2 promoter (R.S. Devon et al., in preparation). Staining for β-galactosidase activity therefore revealed the cells in which *Als2* is expressed. No staining was observed in wild-type animals (data not shown).

The β-galactosidase staining pattern in adult hemizygote transgenic mice showed strong regional variations (Figure 17A) and correlated well with the expression pattern observed by Western blotting. Compared to peripheral organs, the brain and spinal cord were the predominant sites of β-galactosidase activity. In the spinal cord, staining was especially strong in the large motor neurons of the ventral horn (Figure 17B, C), the cell type predominantly affected by neurodegeneration in ALS. Interestingly and unexpectedly, the most intense region of staining was in the granular layer of the cerebellum (Figures 17A, D, L). Cerebellar Purkinje cells were negative, and expression in the molecular layer and white matter was weak (Figures 17D, L). The choroid plexus was a second brain area with very strong expression. Moderate expression was found in the hypothalamus, amygdala, hippocampus, piriform and cingular cortices and in the septum (Figures 17E, F, G).

To identify the cell types expressing β-galactosidase, X-Gal staining was combined with Neutral Red counterstaining (Figures 17C-F) or immunohistochemistry for the astroglial marker glial fibrillary acidic protein (GFAP) or the neuronal marker NeuN. Immunostaining with NeuN and GFAP demonstrated colocalization of β-galactosidase activity with neurons (Fig. 17G)

but not with astroglia (Figure 17H). Association with neurons could also be demonstrated in sections counterstained with Neutral Red as shown for the alpha motor neurons of the spinal cord (Figure 17C), hippocampal layer CA1 (Figure 17E) and cingular cortex (Figure 17F).

Immunohistochemical staining with the N-Alsin-24 antibody was strongest in the cerebellar cortex and weak in other areas of the brain. The staining intensity was highest in the molecular layer and moderate in the granule layer, while Purkinje cells and white matter remain unstained (Figure 17M). In the molecular layer, intense staining of the neuropil was apparent but the bodies of stellate and basket cells were not stained. Absorption of the antibody with the N-Alsin-24 antigen abolished immunostaining (Figure 17N) while incubation with an unrelated antigen did not reduce the staining (Figure 17O).

In peripheral tissues, β-galactosidase activity varied greatly. It was strongest in testis (seminiferous tubules, Figure 17I) and kidney (convoluted tubules and weaker in glomeruli, Figure 17J), weak or not observable in heart (Figure 17K), lung, and small intestine (not shown).
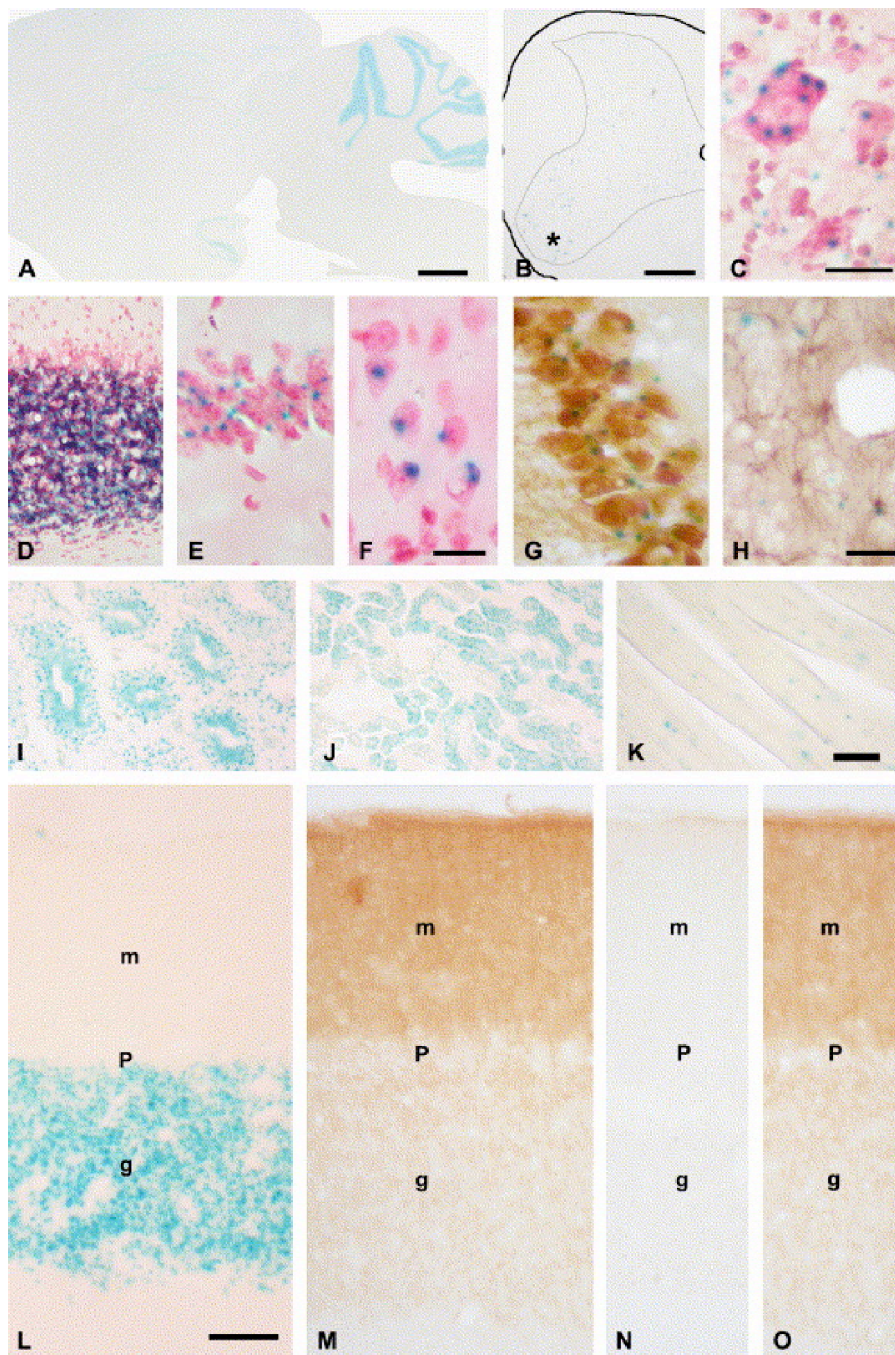
Figure 17. Expression of *lacZ* (under control of *ALS2* promoter) in adult transgenic mouse brain and organs. A) Low power microphotograph of a sagittal section demonstrating that β-galactosidase staining is most intense in cerebellum and the pyramidal layer of the hippocampus. B) Low power microphotograph of a coronal section through the spinal cord showing that lacZ expression is limited to gray matter. The asterisk indicates the ventral horn where the motor neurons are visible as blue dots. Boundaries of the white matter are outlined. C) Shows *lacZ* expression in spinal cord alpha motor neurons, counterstained with Neutral Red, in high power microphotographs. D-F) High power microphotographs of sections counterstained with Neutral Red indicating association of *lacZ* expression with neurons in D) the cerebellar granular layer, E) the hippocampal CA1, and F) the cingulate cortex. G) Combination of NeuN immunohistochemistry and β-galactosidase staining in hippocampus showing close association of lacZ expression with neurons, but not with GFAP-stained astroglia cells H). I-K) Shows *lacZ* expression in testis I), kidney J) and heart K). Calibration bars in A) 1mm; in B) 300 µm; in C) 20 µm; in F) for D) 100 µm, for E) 50 µm and for F) 20 µm; in H) for G) and H) 20 µm; and in K) for I) and J) 100 µm and for K) 25 µm. L-O) Comparison of Alsin immunohistochemical staining and lacZ expression in the cerebellar cortex. L) β-galactosidase staining shows that lacZ is strongly expressed in the granule layer (g). Purkinje cells (P) and molecular layer (m) lack expression. M) Alsin immunohistochemistry shows strong staining in the molecular layer (m), moderate staining in the granular layer (g), while Purkinje cells (P) and white matter remained unstained. N) Absorption with the antigen abolished immunostaining. O) Incubation of the antibody with an irrelevant antigen did not diminish the staining. Calibration bar: 50 µm.

Brain expression of *Als2* becomes predominant in early postnatal life

Alsin expression during development was studied using immunoblotting and also using β-galactosidase expression in the transgenic animals. Alsin expression was seen using both methods at every developmental stage tested, from E9.5 to E18.5 (Figure 18). Immunoblotting showed that Alsin was expressed at low levels at E9.5, but was upregulated by E10.5, and was then expressed at a constant level throughout the rest of development (Figure 18A). Lysates from E9.5 to E16.5 were of whole embryo, whereas the E18.5 lysate was of head only, and the same amount of total protein was loaded in each lane. The apparent decrease of expression in the E16.5 embryo is thus consistent with declining expression outside the head by this age.

Transgenic embryos at E9.5 and E12.5 showed weak to moderate X-Gal staining, while the WT embryos remained unstained (Figure 18A, B). In tissue sections of early embryonic stages (E9.5 - E14.5), β-galactosidase activity was very weak in the developing brain, being limited to choroid plexus, meninges and ventricle endothelium (Figures 18C-G) at E12.5. At E14.5 (Figures 18H-O) neuronal expression was first observed in regions relevant to ALS - the medulla oblongata, pons and spinal cord (Figure 18L). At E18.5, weak expression appeared in the forebrain, but β-galactosidase activity did not reach adult levels until P7. At P7, the hippocampal pyramidal cell layer and the granule cells of the dentate gyrus were strongly positive (Figure 18P). Moderate expression was found in amygdala, striatum, midbrain and in large neurons of the neocortex (Figure 18Q). The cerebellum lacked detectable β-galactosidase activity (Figure 18R and S), reflecting the late postnatal development of this region.

In contrast to its expression in the adult, *Als2* expression was more widespread in the periphery during development. At early stages, β-galactosidase activity was moderate in connective tissue, chondroid tissue, musculature and some organs, and by E12.5 moderate X-Gal staining was visible in tissue next to developing bone and cartilage (Figure 18G, Meckels cartilage of the tongue) and weak staining could be seen in heart and liver. At E14.5 and E16.5, β-galactosidase activity was strong in connective tissue around organs and bone (Figure 18K), and moderate in heart (Figure 18N), liver (Figure 18O), lung and

olfactory epithelium (Figure 18M). Even at E18.5, X-Gal staining in muscle
(Figure 18T), chondroid (Figure 18U) and connective tissue was stronger than in
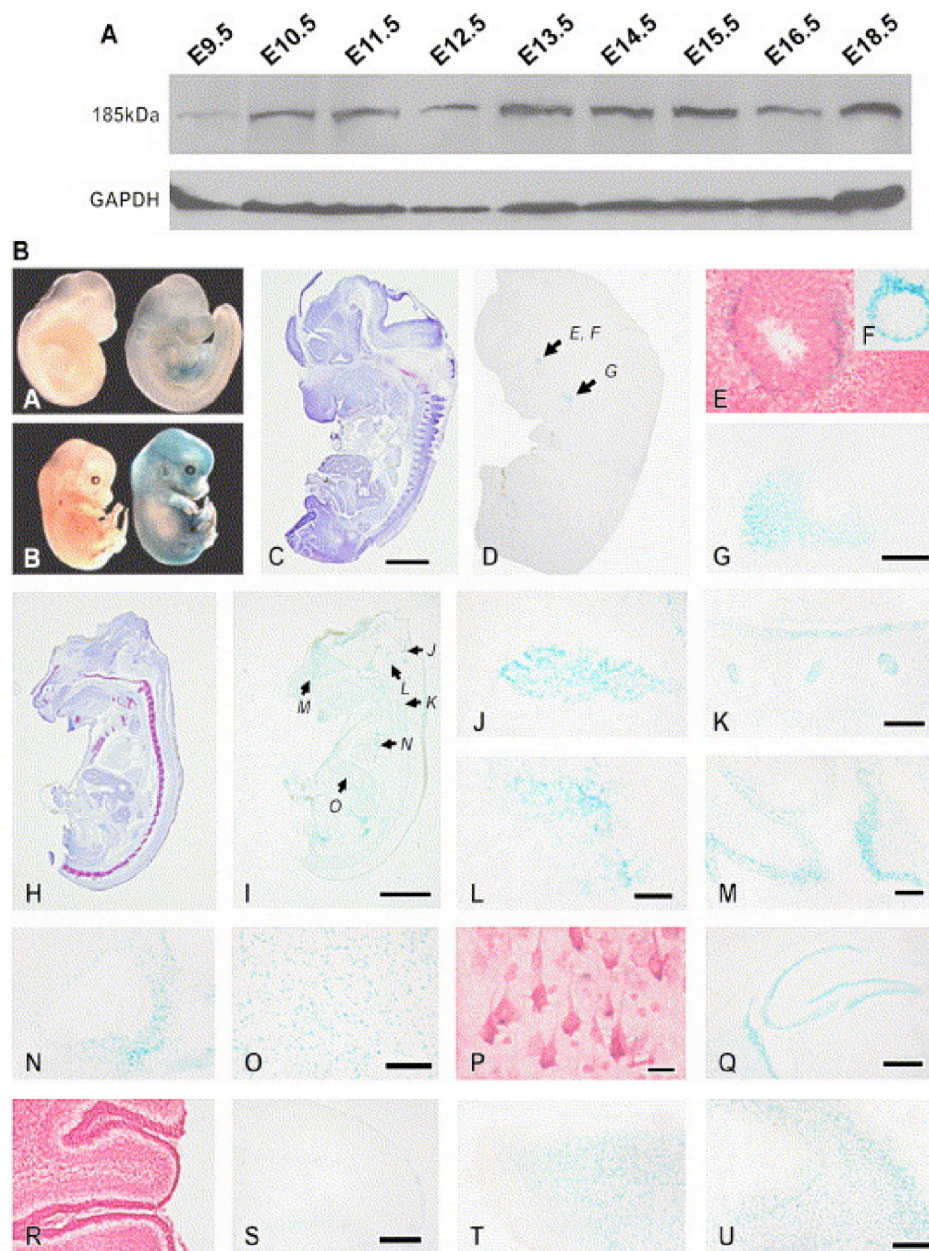the brain.

Figure 18. Expression of Alsin in development. A) Alsin expression during mouse development from E9.5 to E18.5. 50 μg whole mouse embryo homogenate (head only for E18.5) was probed with N-Alsin-24. B) Expression of *lacZ* in embryonic transgenic mouse brain and organs. A, B) *lacZ* expression in wild-type (left) and transgenic (right) embryos at E9.5 and E12.5. C) Sagittal section of an E12.5 embryo, stained with Cresyl Violet compared to D) *lacZ* expression. E-G) High power photomicrographs demonstrating E12.5 *lacZ* expression in the epithelium of the optic recess of the diencephalon (E and F, F is counterstained with Neutral Red) and G) the tissue surrounding Meckels cartilage in the tongue. H) Sagittal section of an E14.5 embryo, Cresyl Violet and I) *lacZ* expression. Arrows in I) indicate the areas enlarged in the following high power photographs. J) Choroid plexus, K) developing chondroid tissue of vertebrae, L) neuronal expression in the brainstem, M) olfactory epithelium, N) heart and O) liver. P-S) On P7, β-galactosidase staining is found in cortical (P) and hippocampal neurons (Q). Neuronal *lacZ* expression reaches almost adult levels, with the exception of the cerebellum where levels are still low (R, Neutral Red and S, lacZ). T and U) Peripheral *lacZ* expression on E18.5 in muscular tissue of the tongue T) and chondroid of the skull U). Calibration bars in C) for C) and D) 1 mm; in G) for E) and F) 100 μm and for G) 200 μm; in I) for H and I) 500 μm; in K) for J) 100 μm and K) 200 μm; in L) 100 μm; in M) 100 μm; in O) for N) 200 μm and O) 100 μm; in P) 20 μm; in Q) 500 μm; in S) for R) and S) 200 μm; and in U) for T) and U) 100 μm.

Alsin is enriched in an endosomal membrane fraction

The subcellular localization of Alsin was further characterized using differential centrifugation. Since Alsin is highly expressed in cerebellum (Figure 16A, C), this portion of the brain was used as starting material. Mouse cerebellum was homogenized and subjected to three sequential centrifugations at 500 xg, 10,000 xg and 160,000 xg. The presence of Alsin and marker proteins in the resultant pellet and supernatant fractions was determined by Western analysis. As shown in Figure 19A, the vast majority of Alsin was associated with the high-speed pellet fraction (P3, lane 6). This fraction was enriched in endosomal membranes as a large portion of the endosomal Rab5 GTPase also associated with P3 material (Figure 19A, see discussion). The plasma membrane markers, NaK-ATPase and transferrin receptor were found in the lower speed pellet fractions P1

and P2 (Figure 19A lanes 2 and 4) as expected for larger membranes. The same fractionation pattern was also observed using rat cerebellum as source material. In this case, quality antibodies were available for rat endoplasmic reticulum and Golgi marker proteins, the majority of which partitioned with the lower speed P1 and P2 fractions (not shown). To determine the fractionation pattern of cytoskeletal elements the same fractions were probed for the presence of actin. Both soluble and pelletable forms of actin were found in all fractions following differential centrifugation. This result indicated that the pelletable fractions also contained large protein complexes, including cytoskeletal elements.

To further characterize the nature of Alsin's P3 association, the S2 fraction was treated with a variety of reagents prior to the final 160,000 xg centrifugation. Pretreatment of the S2 fraction with harsh ionic detergent (deoxycholate) was the only condition that completely extracted Alsin from this pelletable material (Figure 19B, lane 5). Other detergents such as CHAPS, NP-40, and Triton X-100, were able to extract only a portion of Alsin from the pelletable fraction (lanes 7, 8, and 9), while salts, low pH, and the mild detergent Tween-20 were ineffective as solubilization agents (lanes 2-3, and 6). Taken together, these data suggest that Alsin P3 association in this cerebellum fractionation is indicative of a stable interaction with a membrane-associated protein(s), potentially endosomal in nature. This interpretation is consistent with indirect immunofluorescence

localization studies in cell culture systems, which indicate that Alsin is associated

with endosomal structures (Otomo *et al.*, 2003); (Topp *et al.*, 2004). However, at

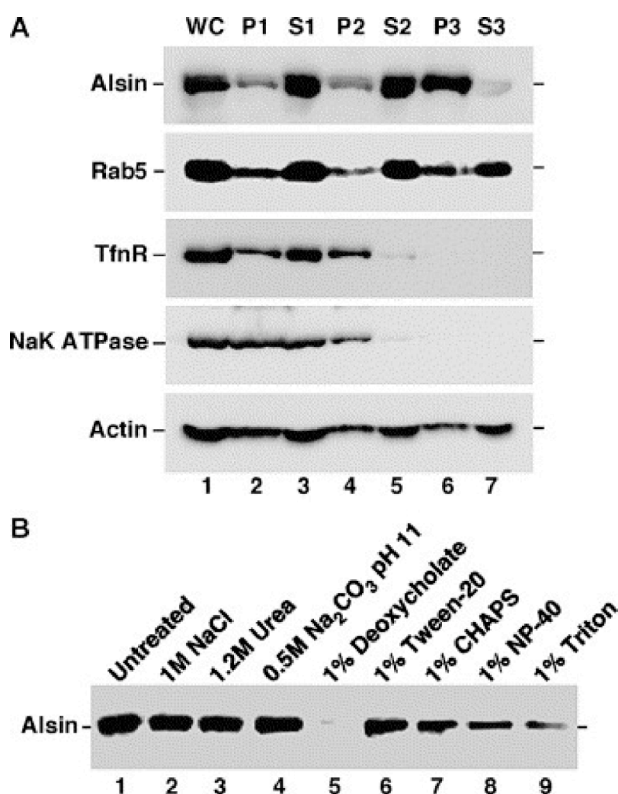this point an additional association with a large protein complex cannot be ruled

out.

Figure 19. Alsin fractionation pattern in cerebellum. A) Mouse cerebellum was separated by differential centrifugation and equal amounts of the resultant supernatant (S) and pellet (P) fractions were analyzed by Western blotting with antibodies to Alsin, actin, transferrin receptor, NaK-ATPase, and Rab5. WC = initial homogenate, P1/S1 = pellet and supernatant from initial spin (500 xg), P2/S2 = pellet and supernatant from low-speed (10,00 xg) centrifugation, P3/S3 = pellet and supernatant from high-speed (160,000 xg) centrifugation. (B) S2 sample was treated with the reagents indicated and subjected to centrifugation at 160,000 xg to generate a pellet (P3) fraction. The presence of Alsin in an equal amount of the P3 fractions was determined by Western blotting.

Discussion

The monoclonal antibody and lacZ transgenic mice described here provide

two useful new tools to study the expression pattern of the *Als2* gene and Alsin

protein. The N-Alsin-24 antibody we have generated is the first anti-Alsin

monoclonal antibody described, and is also the first Alsin antibody free of apparent cross-reactivity with multiple proteins (Otomo *et al.*, 2003); (Yamanaka *et al.*, 2003); (Topp *et al.*, 2004). The transgenic mice express *lacZ* under the control of the endogenous *Als2* promoter and other possible regulatory elements in the *Als2* locus, and therefore permit detailed analysis of the cellular pattern of *Als2* expression in adulthood and throughout development.

Using the multiple approaches of Western blotting, immunohistochemistry and X-Gal staining in transgenic mice, we have shown that Alsin is primarily expressed in neurons of the CNS in adulthood. Consistent with the pathology observed in ALS (Brown, 1995) and the clinical phenotypes described for patients with *ALS2* mutations (Ben Hamida *et al.*, 1990); (Gascon *et al.*, 1995); (Lerman-Sagie *et al.*, 1996); (Devon *et al.*, 2003); (Gros-Louis *et al.*, 2003), expression was observed in the brain stem and spinal cord, with especially high levels in motor neurons, which are the first cells to undergo neurodegeneration. Interestingly though, the highest level of expression was in the densely-packed neurons of the granular layer of the cerebellum, a finding that is consistent with all previously published Northern (Hadano *et al.*, 2001) and Western (Otomo *et al.*, 2003); (Yamanaka *et al.*, 2003) blot results. The cerebellum has not been previously implicated as a site of ALS2 pathology, although it is clear that in the presence of upper motor neuron symptoms, cerebellar functions are difficult to assess, and any cerebellar phenotype may be masked. An understanding of cerebellar

involvement may lead to important new insights in the molecular pathogenesis of ALS and a detailed assessment of cerebellar pathology in human ALS2, JPLS and IAHSP cases is warranted.

During development, *Als2* expression was observed at all stages examined, from E9.5 onwards. *Als2* expression did not become prominent in the brain however until E16.5, and did not reach adult levels until P7. This raises the possibility that Alsin performs different functions during development and in adulthood. The adult cerebellar expression pattern was still not visible at P7, although this is not surprising since the cerebellar granule cell layer develops when granule cell neuroblasts migrate inwards through the molecular and Purkinje cell layers during the first three weeks of life (Goldowitz and Hamre, 1998).

Within the cerebellum, the obvious difference between the pattern of X-Gal staining (indicating the cell types in which the *Als2* mRNA is expressed) and Alsin immunostaining (indicating the location of the Alsin protein) may fortuitously provide detailed insight into Alsin's *in-vivo* subcellular localization. The X̃ staining suggests that the *Als2* mRNA is expressed in the small glutamatergic granule cells, whereas the immunohistochemical staining may reflect the transport of the majority of the Alsin protein into the granule cell axons that reach into the molecular layer. Once in the molecular layer, the unmyelinated granule cell axons bifurcate to form the parallel fibers that make connections with

Purkinje cell dendrites and the stellate/basket cells (Voogd and Glickstein, 1998).

The high level of Alsin in these axons may indicate that it plays an important role

in the cross-talk between different cellular components of the cerebellum.

The differential centrifugation fractionation pattern of Alsin in cerebellar

cell lysate has shed additional light on its potential function. The presence of

Alsin in a high-speed pellet fraction is consistent with Alsin's association with a

subcellular membrane and/or large macromolecular protein complex and is

consistent with previous reports of endosomal localization (Otomo *et al.*, 2003);

(Yamanaka *et al.*, 2003); (Topp *et al.*, 2004). This association is very stable, is

only disrupted by treatment with strong ionic detergents and is largely resistant to

Triton X-100 treatment. One hallmark of f-actin associated proteins is their

inability to be extracted with Triton. The data presented here are most consistent

with Alsin being associated, in part, with a large protein complex, possibly the

actin cytoskeleton. It is well known that actin and actin-binding proteins are

required for endocytosis (Qualmann et al. 2000); (Schafer 2002). Additionally,

presence of active guanine nucleotide exchange domains for the two small

GTPases Rac1 and Rab5 (Topp *et al.*, 2004) further implicates a role for Alsin in

regulating actin polymerization (Rac1) and endocytic protein traffic (Rab5).

Precisely defining a role for Alsin in actin cytoskeleton reorganization and

endocytosis is one focus of our future studies.

We did not see evidence for the existence of the proposed short form of

Alsin protein, which is consistent with previous findings (Otomo *et al*., 2003);

(Yamanaka *et al*., 2003). Northern blot and RT-PCR suggest that the short

product of *ALS2* exists at the mRNA level in humans (Hadano *et al*., 2001);

(Yang *et al*., 2001). The two ESTs detectable by blastn that traverse the boundary

between exon 4 and intron 4 (accession numbers AI243773 and BF993329)

provide further evidence for this. There is as yet no evidence for the short form in

the mouse, either in previously published data or within the EST database,

although there is considerable sequence similarity between human and mouse

across the whole of the portion of intron 4 corresponding to the short form

3'UTR, including a 375 bp element in the human sequence that shows 62%

identity with mouse. There are no known untranslated region motifs within this

conserved sequence. At the protein level however, there are no known PROSITE

motifs detected within the short stretch of amino acids that would be translated

from intron 4 before a stop codon is reached (25 in human or 30 in mouse), and

this sequence is not conserved across species, which is in marked contrast to the

92% similarity observed across the rest of the protein. Overall, it is intriguing that

there is evidence for the existence of the short form at the mRNA level (in human

at least), but not at the protein level. This raises the possibility that the short form

mRNA is important, perhaps for regulation of translation of the full length *ALS2*

mRNA, and that its absence in the Tunisian ALS2 family is indeed responsible for

the observed lower motor neuron degeneration. This phenomenon may be specific to mammals since the lack of intron 4 in the zebrafish would result in an inability to transcribe an equivalent short form in this species.

We predicted the sequence of the *ALS2* genes in five different species (chimpanzee, rat, puffer fish, zebrafish and mosquito) in order to facilitate a deeper understanding of the residues and motifs required for Alsin function, to map TFBS for expression profile prediction, and to provide a foundation for future functional studies in model organisms such as the rat and zebrafish. The tissue specificities of the seven informative TFBS detected showed remarkable concordance with the experimental expression pattern that we observed, highlighting the usefulness of this predictive approach.

At the sequence level, Alsin is unexpectedly highly conserved between human and rodents (Makalowski and Boguski, 1998), but exhibits an average level of conservation between human and Fugu (Aparicio *et al.*, 2002). There is considerably greater conservation across species in the COOH-terminal half than the NH$_2$-terminal half of the protein, and the greatest conservation of all is seen in the Vps9 domain at the extreme COOH-terminus. The COOH-terminal half of Alsin contains both the Rho and Rab-GEF domains, which indicates that GEF-activity is critical for Alsin function. This is also is consistent with the observation that the COOH-terminus of the protein is essential for function in man since a mutation in the Vps9 domain (Gros-Louis *et al.*, 2003) gives rise to

the same, if not a more severe, phenotype in patients, than a mutation found at the NH$_2$-terminus (Hadano *et al.*, 2001); (Yang *et al.*, 2001). The relatively poor conservation of the NH$_2$-terminus corroborates speculation that the RCC1 repeats play a structural role rather than an enzymatic one (Topp *et al.*, 2004). The beta-propeller structure they form is likely to be important for protein-protein interaction, rather than acting as a GEF for Ran, the nuclear localization of which is difficult to reconcile with recent data on Alsin's Rac1 and Rab5 GEF activities and cytoplasmic localization.

Interestingly, Alsin could not be detected in the nematode worm, *C. elegans*, or in either yeast species *S. cerevisiae* or *S. pombe*. The genomes of all three of these species have been completely sequenced, so it is unlikely that this finding is due to an insufficiency of data. Since Alsin is present in insects, it must have been present in the common ancestor of all coelomates, prior to the divergence of deuterostomia (containing vertebrates) and protostomia (containing insects), between 670 (Ayala *et al.*, 1998) and 1200 (Wray *et al.*, 1996) million years ago. Most human neurological disease genes have an orthologue in both *Drosophila* and *C. Elegans*, although examples are known which, like Alsin, are found only in *Drosophila* (for instance, parkin and SCA2) (Rubin *et al.*, 2000). Overall, only 30% of *Drosophila* proteins have putative orthologues in the worm (Rubin *et al.*, 2000).

During the course of the cross-species investigations we detected a second gene, *ALS2CL*, which shows considerable sequence similarity and an identical domain structure to the COOH-terminal half of Alsin, containing the Rho-GEF, MORN and Vps9 domains. RTPCR and EST evidence suggest that this gene is widely, if not ubiquitously, expressed. The existence of ALS2CL may have profound implications for the proposed function of Alsin and the effect of its deletion in human patients or in an animal model since the ability to coordinately regulate members of the Rho and Rab GTPase families may not be unique to full length Alsin. It is possible that ALS2CL plays a more general role in the activation of these proteins, whereas the presence of the RCC1 repeat beta-propeller lends an added specificity to full-length Alsin. Further investigation of the subcellular localization and potential for GEF activity of ALS2CL is warranted.

Chapter 4. Alsin Rab5 GEF activity is required for IGF-1 receptor trafficking and signal transduction

Overview

The *ALS2* gene product, Alsin, is mutated in hereditary juvenile forms of amyotrophic lateral sclerosis (ALS) and primary lateral sclerosis (PLS), and in infantile-onset ascending hereditary spastic paraplegia (IAHSP). Alsin is a large protein with several domains predicted to function in signaling and/or trafficking events. We and others have previously shown that Alsin catalyzes guanine nucleotide exchange (GEF) on Rac1 and Rab5, small monomeric GTPases of the Ras superfamily. In light of these activities and Alsin's localization to endocytic structures, we hypothesized that Alsin functions in receptor endocytosis and signaling. To test this, PC12 cells stably expressing wild-type (WT) and ΔVps9d Alsin (Alsin lacking an intact Rab5 GEF domain) were monitored for their ability to signal in response to various growth factors. We found that ΔVps9d Alsin specifically impaired IGF-1 signal transduction, but not that induced by EGF or NGF stimulation. Expression of WT Alsin potentiated this signaling. Furthermore, Alsin was required for normal IGF-1 signal transduction. Primary cells from mice deficient for Alsin (-/-) exhibited a marked decrease in signaling with IGF-1, but not EGF. Since IGF-1 signal transduction requires receptor

internalization, our results implied that Alsin Rab5 GEF activity is necessary for this process. Immunofluorescence experiments were performed to examine IGF-1 internalization. Expression of ΔVps9d Alsin impaired IGF-1R endocytosis, while expression of WT Alsin stimulated this process. The ability of IGF-1 to serve as a potent survival factor is well established and it is possible that impairment of IGF-1 signaling would inhibit this function. Indeed, cells expressing ΔVps9d Alsin showed reduced protection from serum withdrawal-induced apoptosis by IGF-1, yet NGF protection was unaffected. These data demonstrate that Alsin Rab5 GEF activity is required for normal IGF-1 receptor trafficking and IGF-1-mediated signal transduction. Mutant Alsin proteins that perturb IGF-1 receptor endocytosis and signaling compromise cell survival and identify a potential cause for the motor neuron degeneration observed in juvenile ALS.

Introduction

Amyotrophic lateral sclerosis (ALS) is a heterogeneous group of neurological disorders that result from motor neuron degeneration and usually lead to death (Brown, 2001); ((Rowland and Shneider, 2001). Although ALS is predominantly sporadic, familial ALS accounts for approximately 10% of the total cases of this disease (Mulder *et al.*, 1986). Eight independent chromosomal loci have been described and two specific genes have been identified that are mutated in familial forms of ALS (Bruijn *et al.*, 2004). The first affected gene

described, SOD1, encodes a Cu-Zn superoxide dismutase, which possesses free

radical scavenger activity (Rosen *et al.*, 1993). Interestingly, much work has over

the past decade has shown that the SOD1 mutations that lead to ALS result in a

toxic gain-of-function (reviewed in (Cleveland and Rothstein, 2001)). Several

hypotheses have been formulated to explain mutant SOD1 toxicity including: (1)

toxicity due to formation of intracellular aggregates, (2) abnormal trafficking and

axonal strangulation due to disruption of neurofilaments, (3) calcium-mediated

apoptosis by glutamate excitotoxicity, and (4) disruption in retrograde axonal

transport, though the exact mechanism of action(s) is unknown (reviewed in

(Bruijn *et al.*, 2004)).

The second affected gene identified, *ALS2*, is mutated in a rare and

recessive juvenile form of ALS, ALS2 (Hadano *et al.*, 2001); (Yang *et al.*, 2001).

Mutations in the *ALS2* gene product, Alsin, lead not only to ALS2, but also to

juvenile primary lateral sclerosis (JPLS) and infantile-onset ascending hereditary

spastic paralysis (IAHSP) (Hadano *et al.*, 2001); (Yang *et al.*, 2001); (Eymard-

Pierre *et al.*, 2002); (Devon *et al.*, 2003); (Gros-Louis *et al.*, 2003). Alsin

possesses several interesting domains including an RCC1-like (RLD) beta

propeller domain, MORN repeats, Dbl homology (DH), Pleckstrin homology

(PH), and Vps9 domains (Hadano *et al.*, 2001); (Yang *et al.*, 2001). Mutations in

ALS2 that have been described are all expected to result in prematurely truncated

forms of Alsin that are lacking one or more of these domains. A common feature

of these truncations is the absence of the Vps9 domain, suggesting that activity of this domain is required for Alsin function. However, it is possible that these truncated forms of Alsin are unstable (Yamanaka *et al.*, 2003).

Immunofluorescence and fractionation techniques have shown that endogenous Alsin is present on small membrane structures, which are likely endosomes (Otomo *et al.*, 2003); (Yamanaka *et al.*, 2003); (Topp *et al.*, 2004); (Devon *et al.*, 2005). We and others have shown that Alsin is a guanine nucleotide exchange factor (GEF) for Rab5 (Otomo *et al.*, 2003); (Topp *et al.*, 2004), with activity mapping to the Vps9 domain (Topp *et al.*, 2004). In addition, Alsin possesses GEF activity for Rac1 that is mediated by the DH and PH domains (Topp *et al.*, 2004); (Kanekura *et al.*, 2005). No known functions have been reported for the RLD or MORN repeats although it has been argued that upon overexpression the RLD may serve to localize Alsin to endosomes (Yamanaka *et al.*, 2003), or it may negatively regulate Alsin membrane localization (Otomo *et al.*, 2003); (Topp *et al.*, 2004).

It is well appreciated that growth factors such as ciliary neurotrophic factor (CNTF), brain-derived neurotrophic factor (BDNF), nerve growth factor (NGF), vascular epidermal growth factor (vEGF), insulin-like growth factor 1 (IGF-1), and glial-derived neurotrophic factor (GDNF) all provide trophic support for motor neurons (Seeburger and Springer, 1993); (Bohn, 2004). In addition, retrograde adeno-associated delivery of GDNF, vEGF, and IGF-1 have been

shown to postpone onset, delay progression, and prolong survival in mouse models of ALS (Wang *et al.*, 2002); (Azzouz *et al.*, 2004); (Kaspar *et al.*, 2003), presumably by activating cell signaling cascades through their cognate cell surface receptors. In many cases, signaling has been shown to require ligand-mediated receptor endocytosis (EGF: (Vieira *et al.*, 1996); nerve growth factor (NGF): (Riccio *et al.*, 1997); BDNF: (Watson *et al.*, 1999); IGF-1: (Chow *et al.*, 1998); (Lin *et al.*, 1998); and reviewed in (Sorkin and von Zastrow, 2002), and (Baass et al., 1995)) a process regulated by Rab5 (Zerial and McBride, 2001). In the case of the neurotrophins NGF and BDNF, data supports the hypothesis originally put forth by Mobley and colleagues (Beattie *et al.*, 1996) that signal transduction by these growth factors occurs via the formation of organelles termed "signaling endosomes" (reviewed by (Ginty and Segal, 2002)). We have previously postulated that Alsin Rac1 and Rab5 GEF activity may serve to positively regulate growth factor signaling through the trafficking of activated receptors (Topp *et al.*, 2004). If this hypothesis is correct, it could be expected that mutations in Alsin leading to ALS result from a defect in the formation of growth factor-induced signaling endosomes.

In this study, we have investigated the role Alsin plays in cell signaling mediated by the growth factors EGF, NGF, and IGF-1. We find that Alsin specifically regulates IGF-1R endocytosis and signaling. Overexpression of Alsin lacking an intact Vps9 domain (ΔVps9d) disrupts endocytic trafficking of the

IGF-1R and drastically impairs IGF-1 signal transduction. EGF- and NGF-mediated signaling were not affected by ΔVps9d expression, indicating that Alsin specifically regulates IGF-1. In addition, cells lacking Alsin exhibit impaired IGF-1-mediated, but not EGF-mediated signaling. Defects in signaling are associated with a decrease in IGF-1 protection of cells upon serum withdrawal, demonstrating that Alsin function is required for IGF-1-mediated cell survival. Taken together, these data show that Alsin regulates the IGF-1 signal transduction pathway by positively modulating the intracellular trafficking of the IGF-1 receptor, and identifies a mechanism for the neurodegeneration associated with juvenile ALS.

Material and methods

Reagents

PC12 cells were a kind gift of C. McMurray (Mayo Clinic). NIH-3T3 cells stably expressing the human IGF-1R (NWTb3: (Blakesley *et al.*, 1995)) were a generous gift of D. LeRoith (NIH). Recombinant IGF-1 was from R&D Systems or Sigma. Recombinant EGF and NGF were purchased from Sigma. GFP-Alsin, GFP-ΔVps9d, and RFP-Rab5a (DN) plasmids were described previously (Topp *et al.*, 2004). The GFP-EEA1 FYVE domain fusion (amino acids 1252-1411; (Hunyady *et al.*, 2002)) was a generous gift of T. Balla (NIH). This construct was used to generate DSRed-EEA1 (FYVE domain), which was

also used in our studies. Alexa-conjugated transferrin ligands (568, 488) and

biotinylated IGF-1 were from Molecular Probes and GroPep, respectively.

Formaldeyde and Triton for immunofluorescence techniques were from Tousimis

and Pierce Biotechnology, Inc., respectively. Monoclonal phospho-tyrosine (P-

Tyr-102) antiserum and polyclonal antibodies to IRS-1, IGF-1R (alpha subunit),

Akt, phospho-Akt, ERK1/2, and phospho-ERK1/2 were from Cell Signaling.

Monoclonal IGF-1R (beta subunit) antiserum was from Lab Vision. Monoclonal

antibodies to GFP (A.V.) were purchased from BD Biosciences. Polyclonal

glucose-6-phosphate dehydrogenase antiserum was from Sigma. Alexa secondary

antibodies were from Molecular Probes. Horseradish peroxidase-conjugated

secondary antibodies were from Amersham Biosciences. SuperSignal West

Femto Sensitivity substrate was purchased from Pierce Biotechnology, Inc. All

other products were from Sigma unless otherwise noted.

Cell Culture

PC12 cells were maintained in a 37°C, 10% CO_2 environment and

cultured in Dulbecco's modified essential medium (DMEM with high glucose;

Mediatech) supplemented with 10% horse serum (Invitrogen), 5% fetal bovine

serum (Invitrogen), penicillin (100 units/ml) and streptomycin (100 μg/ml)

(Mediatech). NWTb3 cells (NIH-3T3 cells stably expressing the human IGF-1R)

were grown in a 37°C, 5% CO_2 environment and cultured in DMEM (high

glucose) supplemented with 10% fetal bovine serum, penicillin (100 units/ml), streptomycin (100 μg/ml), and G418 (0.5 mg/ml, Invitrogen). Cultures were routinely passaged twice a week.

Primary mouse embryonic fibroblasts (MEFs) from wild-type and Alsin-deficient (-/-) mice (Devon et al., in preparation) were isolated by flushing out bone marrow from femurs and allowing cells to grow out in media (DMEM with high glucose, 10% fetal calf serum, 2mM glutamine, penicillin (100 units/ml), and streptomycin (100 μg/ml). Stocks of cell pellets were frozen down at -80°C using standard procedures. Thawed MEFs were maintained in a 37°C, 5% CO_2 environment and cultured in DMEM (high glucose) supplemented with 10% fetal bovine serum, penicillin (100 units/ml), streptomycin (100 μg/ml), and L-glutamine (2 mM). Cultures were split once to twice a week.

Generation of the GFP-Alsin and GFP-ΔVps9d stable cell lines was as described previously (Melikian and Buckley, 1999). PC12 cells were plated in 6 well plates. The next day (when cells were approximately 50% confluent), the cells were washed once with 1ml Optimem (Invitrogen), and each well transfected with 2 μg GFP-Alsin or GFP-ΔVps9d plasmids using Lipofectamine 2000 (Invitrogen) in 1 ml Optimem. 20-24 hrs later, media was aspirated and replaced with 1.5 ml normal medium. An additional 24 hrs later, the cells were removed and plated into 4 15 cm plates containing normal growth medium supplemented with 0.5 mg/ml G418. The media was replaced every 3-4 days for 2 weeks, when

individual colonies were selected and expanded. RNA and protein expression
(Figure 20) was confirmed by QPCR and SDS-PAGE/Western blotting with GFP
mA.V. antibody (1:500-1000). Cultures were maintained in normal growth
medium containing G418 (0.5 mg/ml) and routinely passaged twice a week.

Ligand Stimulations and Westerns

PC12 stimulations were performed following the protocol of Mobley and
colleagues (Howe *et al.*, 2001). PC12 parent and stable cell lines were plated on
10 cm plates. The next day (when cells were approximately 60-80% confluent),
the cells were washed once with PBS, and switched to minimal medium (DMEM
+ 1% horse serum). The following day (16-20 hrs later), cells were removed from
plates with phosphate-buffered saline (PBS). Cells were centrifuged and
resuspended in 5-6 mls (per 10 cm plate) PGBH (10 mM HEPES (7.5), 1 mg/ml
BSA, 1 mg/ml glucose, in PBS). Cells were then dispensed into 1ml aliquots and
rotated end-over-end at 37°C for 15 min to equilibrate prior to the addition of
growth factor (IGF-1 at 100 ηg/ml; NGF at 50 ηg/ml; EGF at 100 ηg/ml; the 0
min timepoint was removed at this step, and received no growth factor). At the
timepoints indicated, samples were immediately moved to ice and subjected to
centrifugation. Cell pellets were then resuspended in 100-125 μl SDS-sample
buffer (20% glycerol, 10% β-mercaptoethanol, 6% sodium dodecyl sulfate (SDS),

125 mM Tris (6.8), 0.02% bromphenol blue) and boiled at 95°C for 5 min. Prior to loading, samples were sonicated to shear DNA.

For MEF stimulations, cells were plated in 6 well plates. 1-2 days later, media was aspirated and cells washed 3 times with 1 ml DMEM. The medium was replaced with DMEM. The next morning (14-16 hrs later), the medium was aspirated and cells stimulated (in DMEM) with 100 ηg/ml IGF-1 or 100 ηg/ml EGF for 5 min (the medium was not changed for the 0 min timepoint). Plates were immediately moved to ice, medium aspirated, and washed 2 times with 1 ml PBS. Cells were then scraped from the plate in 1 ml PBS and centrifuged. Cell pellets were resuspended in 30-50 μl urea/SDS-sample buffer (6 M urea, 10% β-mercaptoethanol, 6% SDS, 0.125 M Tris (6.8), 0.02% bromphenol blue) and heated for 10 min at 65°C. Prior to loading, samples were sonicated in a water sonicator bath.

IRS-1 Immunoprecipitations

PC12 parent and stable cell lines were plated on two 10 cm plates. The next day (when cells were approximately 70-80% confluent), plates were washed once with minimal medium (DMEM with 1% horse serum), replaced with minimal medium, and incubated overnight. The next day (~16-20 hrs later), medium was aspirated and cells stimulated with 100 ηg/ml IGF-1 (in minimal medium) for 5 min (the medium was not changed for the 0 min timepoint). Plates

were immediately moved to ice and the medium aspirated. Cells were collected

with PBS and centrifuged. Cell pellets were resuspended in 0.5 ml lysis buffer

(20 mM Tris (8), 137 mM NaCl, 1% NP-40, 10% glycerol, 2 mM EDTA, 1 mM

sodium orthovanadate, 50 mM β-glycerolphosphate, 10 mM NaF, 1X protease

inhibitor mixture: N-tosyl-ʟ-phenylalanine chloromethyl ketone, N^a-p-tosyl-ʟ-

lysine chloromethyl ketone, phenylmethylsulfonyl fluoride, leupeptin, trypsin

inhibitor) and proteins extracted on ice for 10 min. Lysate was then centrifuged at

16,000 Xg for 10 min. Protein concentration was determined using the BCA

Protein Assay Kit (Pierce Biotechnology, Inc.) and 0.8 mg of lysate was

immunoprecipitated with 6.4 μl IRS-1 pAb or 1.6 μg control pAb (glucose-6-

phosphate dehydrogenase) by rotating end-over-end at 4°C for 2 hrs. 75 μl

protein-A sepharose was added and the incubation continued end-over-end at 4°C

for an additional 1 hr 15 min. Beads were pelleted, washed 3 times with lysis

buffer, and proteins eluted with 30 μl urea/SDS-sample buffer. Samples were

heated at 65°C for 10 min and centrifuged prior to loading.

SDS-PAGE and Western Blotting

Samples were separated by SDS-PAGE (8-12%) and transferred to

nitrocellulose. For both PC12 and MEF stimulations, 4-10 μl was analyzed with

the following antibodies: Akt (1:1000), phospho-Akt (1:1000), ERK1/2 (1:750),

phospho-ERK1/2 (1:750). Blots were developed by enhanced

chemiluminescence and visualized using the AutoChemi Darkroom and Labworks

Image Acquisition and Analysis Software (UVP). For activation of signaling

proteins (Akt, ERK1/2), data are presented as the level of phosphorylated

phospho-protein divided by the total level of phospho-protein.

For IRS-1 immunoprecipitations, 3 μl and 12.5 μl were analyzed with

antibodies to IRS-1 and phospho-tyrosine. Samples were quantitated and are

presented as tyrosine-phosphorylated IRS-1 divided by total IRS-1.

For determining relative levels of IGF-1R, PC12 cells from parent and

stable cell lines were removed from plates with PBS. Cell pellets were

resuspended in lysis buffer (see above) and proteins extracted on ice for 10-30

min. The lysate was then centrifuged at 16,000 xg for 10 min. Relative protein

levels in the supernatants were determined using the BCA Protein Assay Kit

(Pierce Biotechnology, Inc.) and 10-20 μg protein was subjected to SDS-PAGE

and Western blotting with antibodies to the alpha (1:1000) and beta subunits

(1:1000) of the IGF-1R.

QPCR c-fos Assays

PC12 parent and stable cells were plated in normal growth medium in 6

well plates. The next day, cells were switched to minimal media (DMEM + 1%

horse serum). 16-20 hrs later, the cells were stimulated with IGF-1 (100 ηg/ml)

or EGF (100 ηg/ml) for 0-120 min. Total RNA from each timepoint was

analyzed for rat *c-fos* mRNA expression by quantitative polymerase chain

reaction (QPCR). RNA was isolated from cells using the RNeasy Mini Kit

(Qiagen) following the manufacturer's animal cell protocol. RNA concentrations

were measured using a Beckman DU 800 spectrophotometer, diluted to 25 ηg/ml

and further quantitated using Ribogreen RNA Quantification kit (Invitrogen).

QPCR was performed using Applied Biosystems guidelines.

A 71 bp amplicon of rat *c-fos* was generated using forward primer

TGGAGCCGGTCAAGAACATT, reverse primer

TGCCGGAAACAAGAAGTCATC and HPLC purified dual-labeled probe 5`-56-

Fam-CAACATGGAGCTGAAGGCTGAACCCT 3BHQ_1-3` synthesized by

Integrated DNA Technologies. The 25 μl TaqMan reaction volume contained

125 ηg RNA, 2x One Step RT-PCR TaqMan Universal Mix (Applied

Biosystems), 400 ηM forward and reverse primers and 100 ηM probe. Samples

were amplified in triplicate using an iCycler IQ (BioRad). Cycling parameters

were 50°C for 2 min, 95°C for 10 min and 40 cycles of 95°C for 15 sec and 60°C

for 1 min.

A 71-mer single-stranded oligonucleotide, sequence identical to the

amplicon, was synthesized and page-purified (Integrated DNA Technologies).

Serial dilutions of the oligonucleotide were utilized in obtaining a cDNA

reference standard curve. The oligonucleotide's concentration (μg/ml) and length

were factored into the calculated copy number of *c-fos*. Amplification was

measured in real time by determining the first detected fluorescence signal over baseline or the threshold cycle number (Ct). The Ct of standards (y axis) were plotted against corresponding copy number (10^2 to 10^8) and copy numbers derived for all reversed transcribed RNA samples as an approximation of mRNA copies. Results were normalized to RNA amounts determined by the Ribogreen assay and expressed as rat *c-fos* copies per ηg of RNA.

Radioactive Cell Surface IGF-1 Labeling

PC12 parent and stable cells were plated in 12 well plates in normal growth medium. The next day, medium was replaced with minimal medium (DMEM + 1% horse serum). The following day (~16-20 hrs later), medium was removed and cells washed with 1 ml cold binding medium (100 mM HEPES, (7.9), 120 mM NaCl, 5 mM KCl, 1.2 mM $MgCl_2$, 1 mM EDTA, 15 mM sodium acetate and 5 mg/ml BSA) as described previously (Kato *et al.*, 1993). Binding curves were performed using 22,000 cpm $[I^{125}]$IGF-1 (approximately 10 pM) and increasing amounts of unlabeled IGF-1 (0.05 – 200 ηM) in 0.5 ml binding medium. Cells were incubated 5 hrs on ice. Binding of IGF-1 was quantified by removing unbound ligand with cold PBS and solubilizing cells in 0.2 N NaOH. The amount of $[I^{125}]$IGF-1 bound to cell surface IGF-1 receptors was determined by counting cell lysates in a gamma counter (Isodata100).

Immunofluorescence

NWTb3 cells (NIH-3T3 cells stably expressing the human IGF-1R) were plated in 12 well plates in normal growth medium. The next day, cells were transfected with 1.5-2 μg DNA (GFP-Alsin, GFP-ΔVps9d, wild-type and dominant-negative RFP-Rab5a, DSRed-EEA1 (FYVE domain) and GFP-EEA1 (FYVE domain)) using Lipofectamine 2000 (Invitrogen). 4-6 hrs later, cells were washed 5 times with Dulbecco's PBS (DPBS, Mediatech) and removed from the plate with 0.2 ml Trypsin. For each transfection, cells were diluted to 4-5 ml in normal growth medium and 0.5 ml was plated on 12mm glass coverslips. The next day, medium was aspirated and cells washed 2-3 times with DPBS. Cells were then incubated with minimal medium (DMEM with 0.2% FBS) overnight. The next day, medium was aspirated and cells stimulated with 100 ηg/ml IGF-1 (in minimal medium) for 10-30 min as indicated. Medium was aspirated, and cells processed for immunofluorescence as previously described (Henley *et al.*, 1998). Briefly, cells were fixed for 20 min (0.1 M PIPES (6.95), 1 mM EGTA, 3 mM MgSO$_4$, 3% formaldeyde), washed 3 times (3 min each) with DPBS, and permeabilized with 0.1% Triton (in PBS) for 2 min. The coverslips were then washed 3 times (5 min each) with DPBS and blocked for at least 60 min in blocking solution (5% goat serum, 5% glycerol, 0.04% sodium azide, in DPBS). Primary antibody (IGF-1R alpha Cell Signaling) was added and incubated for 2-3 hrs at room temperature or overnight at 4°C. After washing with DPBS (3 times,

5 min each), secondary antibodies (Alexa647 anti-rabbit 1:200, Alexa594 anti-rabbit 1:500, Alexa488 anti-rabbit 1:500) were added and incubated at room temperature in the dark for 1-2 hrs. The coverslips were washed with DPBS (3 times, 5 min each) and mounted using the Prolong Antifade Reagent (Molecular Probes). Images were acquired and processed as described previously (Topp *et al.*, 2004).

For ligand internalization experiments, the above protocol was followed except the ligands were conjugates (transferrin (Alexa488 and Alexa568), added at 5 μg/ml in DMEM + 0.2% BSA for 30 min; biotin: IGF-1, added at 100 ηg/ml in DMEM + 0.2% FBS for 5-30 min). For transferrin internalization, the plates (containing coverslips) were immediately moved to ice. Medium was aspirated and cells washed once with ice-cold DPBS. Cell surface-bound transferrin was stripped with ice-cold acetic acid (3.5, in DPBS) for 1 min. Cells were neutralized by repeated washing with ice-cold Hanks balanced salt solution (HBSS; Mediatech). Upon neutralization, cells were fixed and coverslips mounted (without permeabilization) as described above. For biotin: IGF-1 internalization, the plates (containing coverslips) were immediately moved to ice. Medium was aspirated and cells washed once with ice-cold DPBS. Cell surface-bound IGF-1 was stripped with ice-cold stripping solution (0.2 M acetic acid (2.65), 0.5 M NaCl) twice for 2 min, and once for 1 min. Cells were then neutralized by repeated washing with ice-cold Hanks balanced salt solution

(HBSS; Mediatech). Upon neutralization, cells were fixed, permeabilized, and incubated with Alexa594-conjugated streptavidin (1:500) for 1-2 hrs prior to mounting.

For PC12 cell immunofluorescence, cells from parent and stable cell lines were plated in normal growth medium on poly-lysine-coated coverslips (BD Bioscience). The next day, the medium was aspirated and the cells were washed twice with DPBS prior to replacement with minimal medium (DMEM + 1% horse serum). The next day (~16-20 hrs later), medium was aspirated and cells processed for immunofluorescence as described above.

Survival and Apoptosis Assays

Approximately 10,000 PC12, GFP-Alsin, and GFP-ΔVps9d cells were plated in 96 well plates with DMEM, DMEM + growth factor, or normal growth medium. 44-48 hrs later, cell survival was monitored using the CellTiter96 Aqueous 1 solution assay (Promega). Percent survival for each condition is shown after normalization with normal growth medium.

Acknowledgements

Results

Alsin Rab5 GEF activity is required for IGF-1-mediated signaling

PC12 cell lines stably transfected with GFP-Alsin (wild-type, WT) or GFP-ΔVps9d Alsin were generated (Alsin lacking the last 55 amino acids; see Figure 20). Cell lines were chosen that expressed low, but similar levels of GFP-WT or GFP-ΔVps9d Alsin protein (Figure 20). PC12 cells were utilized as they are an accepted neuronal model system and possess endogenous receptors for the ligands EGF, NGF (neurotrophic growth factor, related to BDNF) and IGF-1. The ΔVps9d Alsin truncation closely resembles a previously described mutation (Gros-Louis *et al.*, 2003). Alsin lacking an intact Vps9 domain does not colocalize with dominant-negative Rab5a, while WT Alsin and other Rab5 exchange factors do (Topp *et al.*, 2004); (data not shown). In addition, new structural information on the Vps9 domain reveals that ΔVps9d Alsin lacks the entire surface required for interaction with Rab5 (Delprato *et al.*, 2004). If Alsin Rab5 GEF activity is required for appropriate receptor endocytosis and signaling, ΔVps9d Alsin would be expected to affect both of these processes.
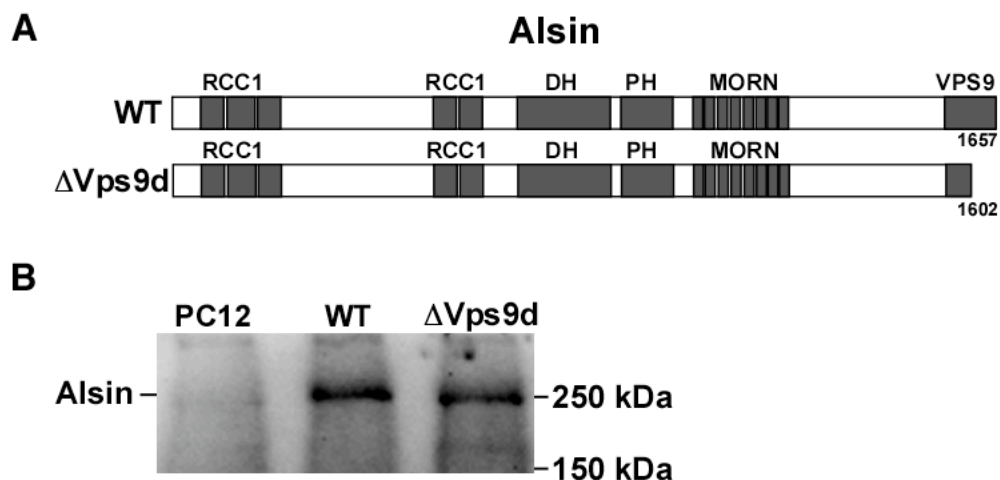
Figure 20. Generation of WT and ΔVps9d Alsin PC12 stable cell lines. A) Alsin constructs introduced into PC12 cell lines as described in Material and methods. B) Western analysis (antibodies to GFP) showing relative expression levels of stable cell lines used in these studies. Cell lines were chosen that expressed low, but equivalent levels of both WT and ΔVps9d Alsin.

To address whether Alsin regulates signaling by EGF, NGF, or IGF-1, serum-starved PC12 parent and stable cell lines were stimulated with EGF, NGF, and IGF-1 for 10 minutes. As expected, the addition of each ligand resulted in the activation of signaling molecules such as ERK1/2 and Akt. Surprisingly, cells expressing ΔVps9d Alsin dramatically impaired ERK1/2 phosphorylation upon stimulation with IGF-1, but not with EGF or NGF (Figure 21A). ΔVps9d expression didn't simply delay the activation, as ERK1/2 phosphorylation was decreased out to 30 minutes (Figure 21B). Similar experiments with EGF showed that cells expressing ΔVps9d Alsin had equivalent levels of ERK1/2 activation as parent PC12 cells from 5-30 minutes of stimulation (data not shown). In addition to the MAPK pathway, IGF-1 is also known to signal via PI(3)K/Akt. Similar to

the effect observed in ERK1/2 phosphorylation, ΔVps9d decreased Akt activation

upon IGF-1 stimulation (Figure 21C). Interestingly, we also noticed an increase

in Akt phosphorylation with IGF-1 in cells expressing WT Alsin (Figure 21C).
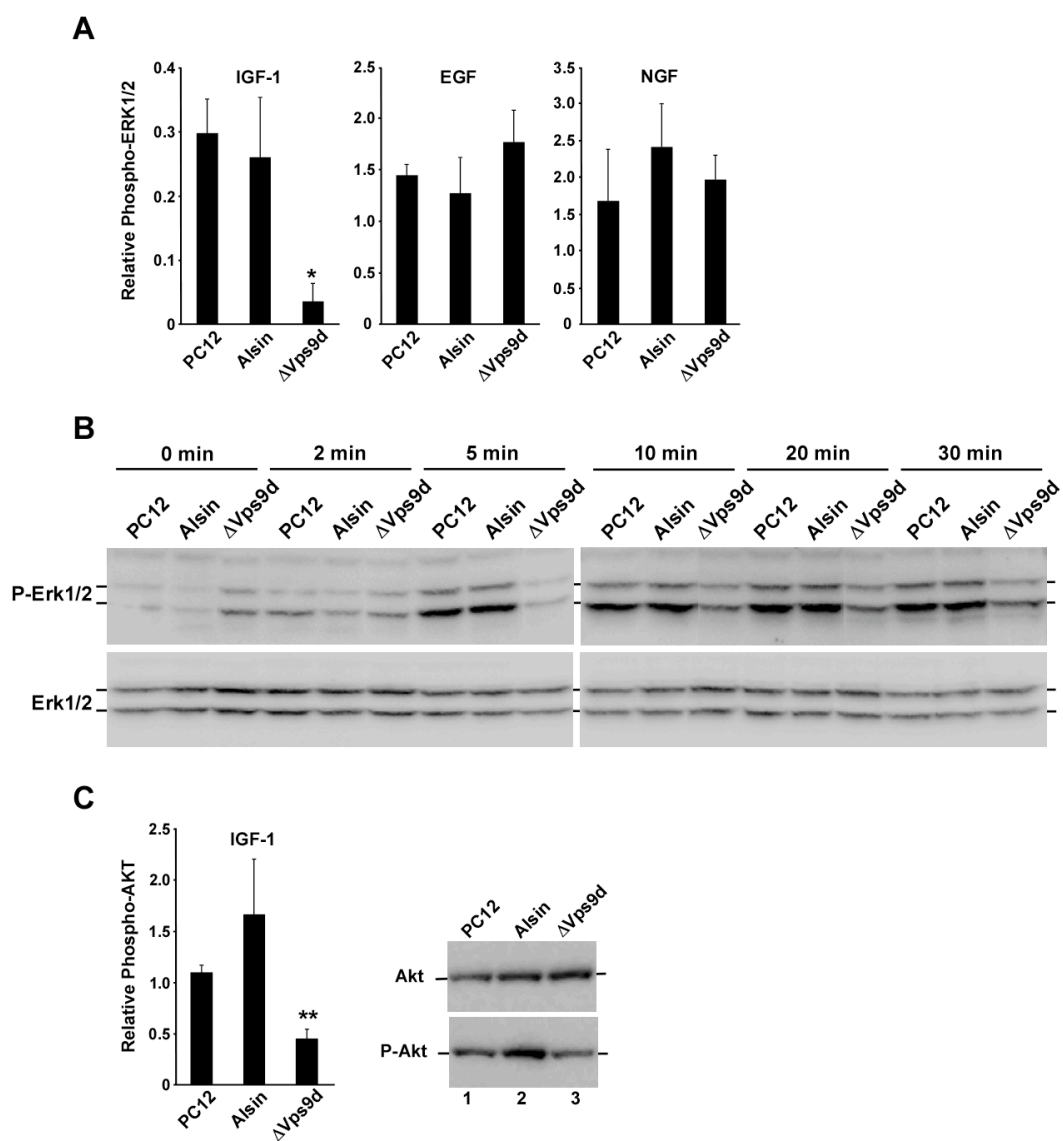
Figure 21. ΔVps9d Alsin expression specifically impairs IGF-1-mediated signaling. A) PC12 and Alsin stable cell lines (see Figure 20) were serum-starved and stimulated with EGF (100 ηg/ml), NGF (50 ηg/ml), and IGF-1 (100 ηg/ml) for 10 minutes. Cell pellets were resuspended in SDS-sample buffer and analyzed for ERK1/2 activation by SDS-PAGE and Western blotting with antibodies to total ERK1/2 or phosphorylated ERK1/2. Densitometry analysis (phosphorylated ERK1/2, normalized to total ERK1/2) is shown with each sample representing at least three separate stimulations. Two-tailed t tests were performed indicating that the differences in ERK1/2 activation for PC12 and ΔVps9d Alsin were statistically significant ($P = 1.81 \times 10^{-4}$, *). Results in this and all other figures are considered to be statistically significant if $P < 5.00 \times 10^{-2}$. B) Similar experiments to A) except stimulations were performed with IGF-1 (100 ηg/ml) in a timecourse (0-30 minutes). Shown is a representative example of an experiment performed at least three times. C) Similar experiments were performed as in A) except stimulations were for five minutes and samples were analyzed for Akt activation. Two-tailed t tests were performed indicating that the differences in Akt activation for PC12 and ΔVps9d Alsin were statistically significant ($P = 8.06 \times 10^{-4}$, **).

We used Western blotting and cell surface ligand binding experiments to ensure that discrepancies in receptor level and localization were not responsible for the differences in signaling observed with ΔVps9d Alsin expression. Multiple antibodies to both the alpha and beta subunits of the receptor showed that each cell line had equivalent whole cell levels of IGF-1R (Figure 22A; data not shown). To address surface localization of the receptor, radio-active $[I^{125}]$IGF-1 was added to serum-starved cells in the presence and absence of excess unlabeled competitor. Control PC12, WT and ΔVps9d cell lines exhibited similar IGF-1 binding characteristics (Figure 22B). In addition, indirect immunofluorescence with antibodies to both subunits revealed that the cell lines had similar levels and localization of IGF-1R when subjected to serum starvation (Figure 22C; data not shown). These data show that the effects observed in the IGF-1 signaling pathway with WT and ΔVps9d Alsin expression were not due to receptor level

and localization prior to stimulation, but instead to transmission of the signal from

ligand-bound receptor to signaling intermediate.

A
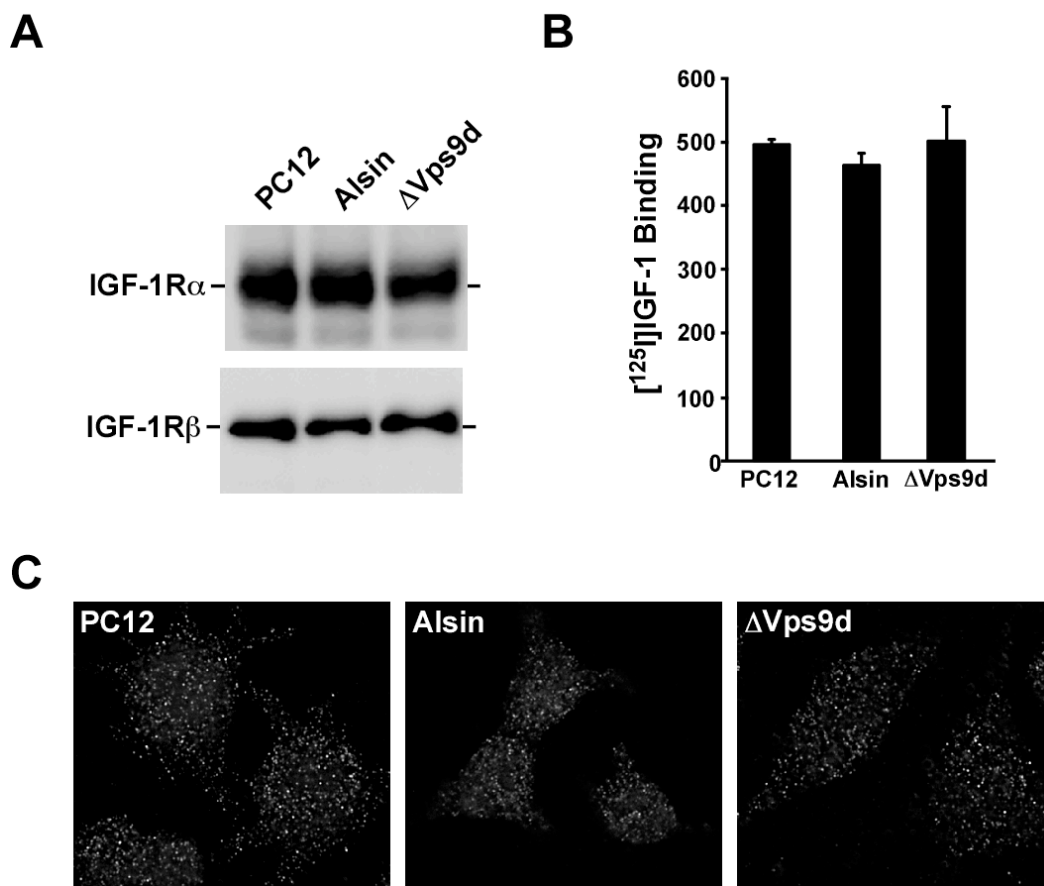

IGF-1Rα–

IGF-1Rβ–

B

C

Figure 22. PC12 stable cell lines express equivalent levels of cell surface IGF-1R. A) Lysates from each cell line were generated and subjected to SDS-PAGE and Western blotting with antibodies to both the alpha and beta subunits of the IGF-1R. B) Cell surface binding analysis for each cell line. Serum-starved PC12 parent and stable cell lines were incubated with [I^{125}]IGF-1 on ice (inhibits internalization of the receptor) to determine the level of IGF-1 receptors at the plasma membrane. C) Serum-starved PC12 parent and stable cell lines were processed for indirect immunofluorescence with antibodies to the alpha subunit.

Upon IGF-1 interaction with its cognate receptor, activated IGF-1R phosphorylates the key upstream signaling molecules, IRS-1 and Shc (Butler *et al.*, 1998). In particular, IRS-1 possesses at least 20 potential tyrosine phosphorylation residues, several of which are phosphorylated in response to IGF-1 stimulation (Myers *et al.*, 1994). As expected, a five minute incubation with IGF-1 caused IRS-1 phosphorylation in control PC12 cells (Figure 23). However, in cells expressing ΔVps9d Alsin, IRS-1 phosphorylation was dramatically reduced (Figure 23). This was not due to an absence of IRS-1 protein in cells (compare input levels). In addition, it was observed that ΔVps9d Alsin expression decreased Shc activation in response to IGF-1 (data not shown). Taken together, these data strongly support the hypothesis that Alsin regulates IGF-1 signaling at a step between ligand binding and activation of upstream signaling molecules in PC12 cells.
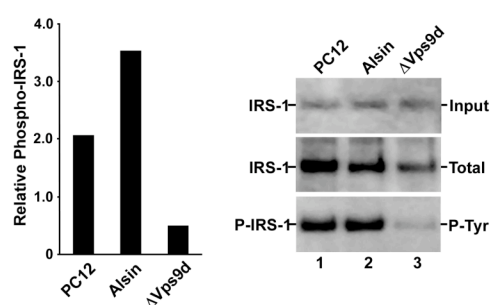

Figure 23. ΔVps9d Alsin blocks IGF-1-mediated signaling to IRS-1. Serum-starved PC12 parent and stable cell lines were stimulated with IGF-1 (100 ηg/ml) for five minutes. Extracts were generated and subjected to immunoprecipitation with IRS-1 antiserum. Immunoprecipitates and input material (extract) were analyzed by SDS-PAGE and Western blotting with antibodies to IRS-1 and phosphorylated tyrosine. The experiment was performed in duplicate and results from one of the experiments are presented. Shown is a graph in which the levels of phosphorylated IRS-1 were normalized to total IRS-1 (in immunoprecipitate).

Alsin Rab5 GEF activity is required for IGF-1R endocytosis

Based on the above results, we postulated that ΔVps9d-Alsin was

affecting IGF-1 signaling by altering IGF-1R trafficking to endosomes. Previous

studies have shown that IGF-1-mediated signaling requires endocytosis (Chow *et*

al., 1998) in a dynamin- and beta-arrestin-dependent manner (Lin *et al.*, 1998);

(Povsic *et al.*, 2003). In order to better visualize IGF-1R trafficking, indirect

immunofluorescence was performed on an NIH-3T3 cell line that overexpresses

the human IGF-1R (NWTb3). This line expresses approximately 400,000

receptors per cell and exhibits normal IGF-1-mediated signal transduction

(Blakesley *et al.*, 1995). Although much is known about IGF-1R signal

transduction, little is known as to the endocytosis and trafficking of the IGF-1R.

To determine the hallmarks of IGF-1R trafficking, IGF-1R movement was

monitored by immunofluorescence after IGF-1 stimulation. A GFP-tagged

version of the EEA1 FYVE domain was used to mark the PI(3)P-positive

endosomal structures (Hunyady *et al.*, 2002); (Gillooly *et al.*, 2000). IGF-1R was

found on the cell surface of unstimulated cells (Figure 24A). Upon IGF-1

stimulation a portion of the IGF-1R became associated with PI(3)P-positive

endosomes by 20 minutes. By 30 minutes post stimulation nearly all of the

PI(3)P-positive structures were also decorated with the IGF-1R (Figure 24A). As

previously shown (Lin *et al.*, 1998), mutant dynamin that blocks IGF-1 mediated

signaling also inhibited IGF-1R endocytosis (data not shown). To address

whether WT or ΔVps9d Alsin expression affects IGF-1R endocytosis, cells were transiently transfected with each prior to IGF-1 stimulation. ΔVps9d expression effectively blocked accumulation of IGF-1R in perinuclear endosomal structures (Figures 24B). By comparison, overexpression of WT Alsin resulted in a similar staining pattern to untransfected cells, with the accumulation of receptors on large perinuclear structures (Figures 24C). Quantitation revealed that WT Alsin and ΔVps9d Alsin enhanced and impaired, respectively, IGF-1 receptor trafficking to these endosomes (Figure 24D). Interestingly, cells expressing WT Alsin had an increase in peripheral membrane ruffling in the presence of IGF-1 (Figure 24C). We found previously that Alsin was present in membrane ruffles, but it did not by itself stimulate their formation. Data here suggests that Alsin can potentiate this process, but it requires IGF-1 stimulation to do so.
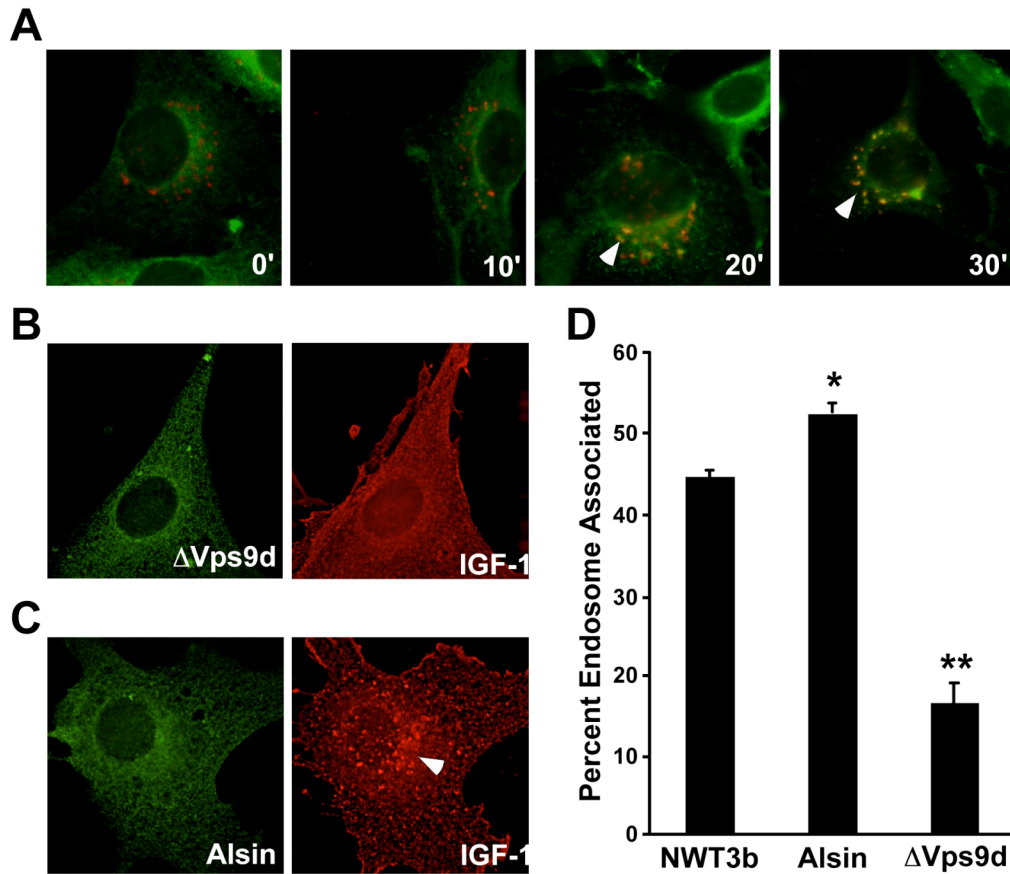
Figure 24. ΔVps9d Alsin inhibits, while WT Alsin stimulates IGF-1R endocytosis. A) IGF-1R colocalizes with perinuclear PI(3)P-positive endosomes after 20-30 minutes of stimulation. Serum-starved NWTb3 cells (NIH3T3 cells stably expressing the human IGF-1R) transfected with GFP-EEA1 FYVE domain (domain that specifically interacts with PI(3)P) were stimulated with IGF-1 (100 ηg/ml) for 0-30 minutes. Cells were processed for indirect immunofluorescence with antibodies to the alpha subunit of the IGF-1R. B) ΔVps9d Alsin blocks perinuclear endosomal trafficking of IGF-1R. NWTb3 cells transiently transfected with GFP-ΔVps9d Alsin were serum-starved and stimulated with IGF-1 (100 ηg/ml) for 30 minutes. Note the absence of receptor in the endosomal compartment as compared to that observed in (A). C) WT Alsin stimulates IGF-1R endocytosis. NWTb3 cells transiently transfected with GFP-Alsin (WT) were treated as in B). Note the enlargement of IGF-1R-positive endosomes and IGF-1R localization to peripheral ruffles. D) Quantitation of receptor accumulation in perinuclear endosomes. Cells were counted from three separate stimulations (30 minutes with IGF-1 at 100 ηg/ml; > 60 cells per sample). Two-tailed t tests reveal that WT Alsin increases endocytosis ($P = 1.29 \times 10^{-3}$ (*)), while ΔVps9d decreases endocytosis ($P = 9.42 \times 10^{-5}$ (**)), as monitored by perinuclear IGF-1R trafficking. Arrowheads in (A) and (C) point to endocytic structures containing IGF-1R.

In addition to the receptor trafficking experiments, endocytosis assays were performed with biotinylated IGF-1. Application and internalization of this ligand followed by acid stripping of the cell surface-bound IGF-1 allows visualization of IGF-1-positive endocytic structures. After 10 minutes of stimulation, IGF-1 accumulated in small structures characteristic of endosomes (Figure 25A, untransfected cell). Similar to what was observed with the receptor, IGF-1 association with these endosomes was inhibited by expression of ΔVps9d Alsin (Figure 25A, transfected cell). WT Alsin expression caused the formation of somewhat enlarged IGF-1-positive endocytic structures after 10 minutes of stimulation and internalization (Figure 25B), which became further enlarged after 30 minutes (Figure 25C). These data, coupled with the receptor trafficking data, demonstrate that Alsin Rab5 GEF activity is required for the trafficking of IGF-1R through the endocytic pathway.
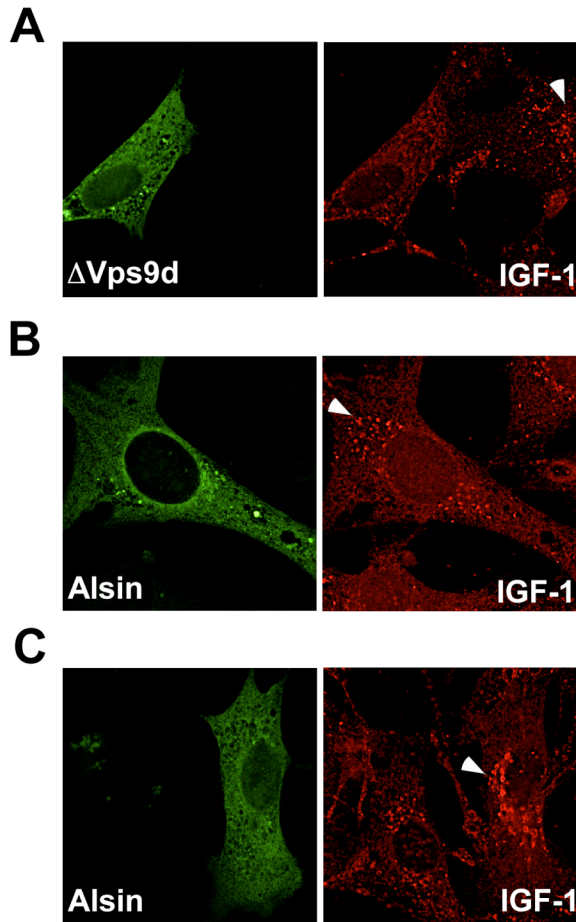
Figure 25. ΔVps9d Alsin impairs, while WT Alsin stimulates IGF-1 internalization. A) NWTb3 cells transiently transfected with GFP-ΔVps9d Alsin were serum-starved and stimulated with biotin-conjugated-IGF-1 (100 ηg/ml) for 10 minutes. Cell-surface bound IGF-1 was acid-stripped allowing visualization of internalized ligand. At 10 minutes, IGF-1 is present in structures reminiscent of early endosomes which is blocked by ΔVps9d Alsin expression (compare transfected to untransfected cell, with arrowhead pointing to endosomal structure in untransfected cell). B, C). NWTb3 cells transiently transfected with GFP-Alsin (WT) were serum-starved and stimulated with IGF-1 (100 ηg/ml) for 10 (B) or 30 (C) minutes. At each time point the size of IGF-1-positive endosomes is increased (compared transfected to untransfected cells), with this enlargement being most obvious at 30 minutes of stimulation. The arrowheads in (B) and (C) point to the enlarged endosomes containing IGF-1 that are formed with WT Alsin expression.

Since ΔVps9d Alsin is unable to bind and catalyze GTP loading on Rab5, expression of Rab5 that is defective in GTP-binding (dominant-negative) should phenocopy this result. Expression of dominant-negative (DN) Rab5a also blocked IGF-1R trafficking to endocytic structures (Figure 26). This indicates that the defect in IGF-1R endocytosis with expression of ΔVps9d Alsin is likely due to its inability to activate Rab5a. To determine whether ΔVps9d Alsin affects IGF-1R endocytosis specifically, we studied receptor-mediated endocytosis of

transferrin. While DN Rab5a reduced transferrin internalization, ΔVps9d Alsin

had no effect (Figure 27).
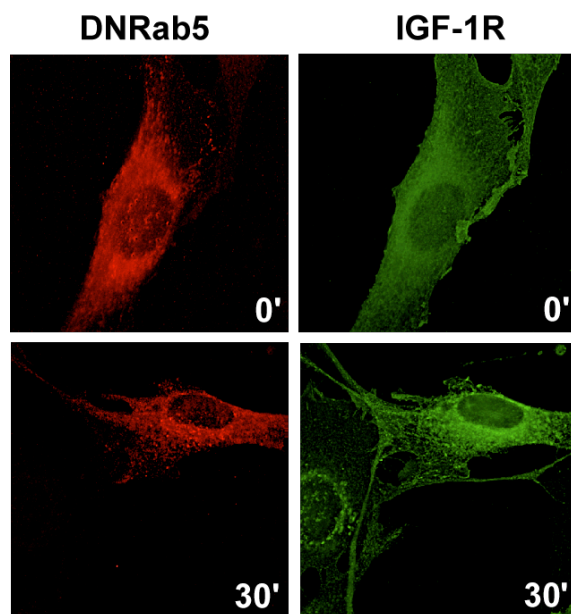
Figure 26. Dominant-negative Rab5 blocks IGF-1R trafficking. NWTb3 cells transiently transfected with dominant-negative Rab5 were serum-starved, stimulated with IGF-1 for 0 or 30 minutes, and processed for immunofluorescence as described in Figure 24.
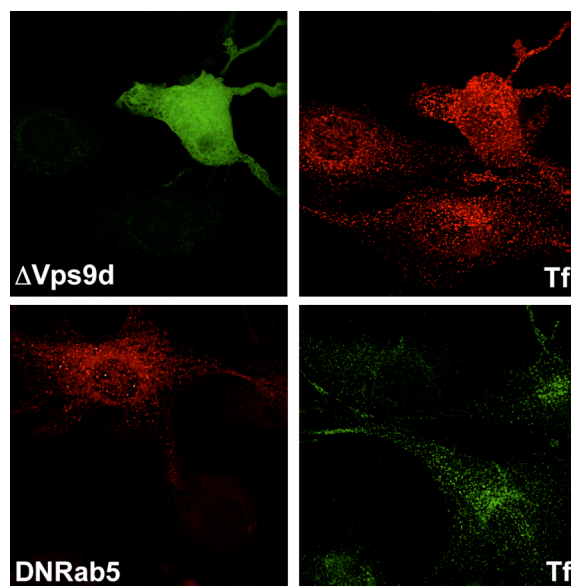
Figure 27. ΔVps9d Alsin does not inhibit transferrin receptor-mediated endocytosis. NWTb3 cells transiently transfected with GFP-ΔVps9d Alsin or dominant-negative RFP-Rab5 were labeled with fluorescent transferrin for 30 minutes. Cell-surface-bound transferrin was removed by acid-stripping allowing the visualization of internalized transferrin. Although Rab5 activation is required for transferrin endocytosis, ΔVps9d Alsin expression had little effect on this process, indicating that its effect on IGF-1R endocytosis is specific

Loss-of-Alsin function impairs IGF-1-mediated signaling

The above studies with ΔVps9d Alsin showed that overexpression of Alsin

lacking an intact Vps9 domain specifically impairs IGF-1 signaling by inhibiting

endocytosis of the IGF-1 receptor. This suggests that ΔVps9d Alsin behaves as a

dominant-negative. If Alsin is required for these processes, cells deficient for

Alsin may be expected to yield similar results. To test this, we studied IGF-1-

mediated signaling in MEFs from WT and Alsin knockout (-/-) mice (Devon et

al., in preparation). WT MEFs exhibited a robust increase in Akt phosphorylation

upon the addition of IGF-1 (Figure 28). However, Alsin (-/-) MEFs only partially

activated Akt (Figure 28). Similar experiments demonstrated that both WT and

Alsin (-/-) MEFs display equivalent levels of phosphorylated Akt in response to

EGF (Figure 28). In addition, when compared to WT MEFS, Alsin (-/-) MEFs

exhibited a decrease in ERK1/2 activation in response to IGF-1, but not EGF

(data not shown). These data demonstrate that the signaling defects observed

with expression of ΔVps9d Alsin also exist in Alsin (-/-) cells, and that Alsin is

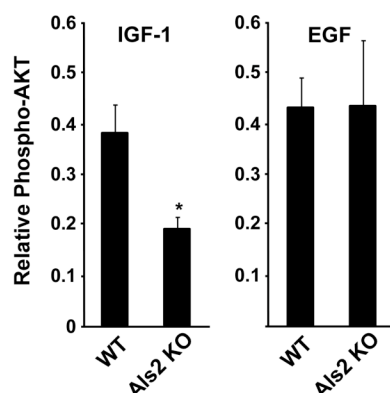required for normal IGF-1-mediated signal transduction.

Figure 28. Alsin-deficient MEFs exhibit defects in IGF-1-mediated signaling. WT MEFs or MEFs lacking Alsin (-/-) were serum-starved and stimulated with IGF-1 (100 ηg/ml) or EGF (100 ηg/ml) for five minutes. Akt activation was determined by SDS-PAGE, Western blotting, and densitometry as described above (Figure 21) for PC12 cells. Results are the average of three stimulations. Differences in Akt activation are statistically significant for IGF-1 ($P = 1.02 \times 10^{-2}$ (*), but not EGF ($P = 9.79 \times 10^{-1}$).

Alsin Rab5 GEF activity is required for IGF-1-mediated survival

One of the most distal events in signal transduction cascades is the transcriptional activation of specific target genes. QPCR analysis was used to determine the impact Alsin expression had on IGF-1 stimulated gene activation. As shown in Figure 29A, cell lines expressing WT and ΔVps9d Alsin increased and decreased, respectively, the transcription of *c-fos* as compared to PC12 cells. Three different ΔVps9d Alsin stable cell lines exhibited similar effects in *c-fos* transcription in response to IGF-1 (data not shown). In addition, as observed with ERK1/2 and Akt activation, EGF-stimulated *c-fos* levels were unaffected by WT or ΔVps9d Alsin expression (data not shown). Taken together, these data show that Alsin Rab5 GEF activity is required for IGF-1-induced transcriptional events.

IGF-1 is known to be a potent survival factor for cells that undergo apoptosis after serum withdrawal. Although multiple signaling cascades are involved in IGF-1 mediated cell survival, the PI(3)/K/Akt pathway is the most

prominent(D'Mello *et al.*, 1997). IGF-1 signal transducers promote survival

directly by phosphorylation and subsequent inactivation of pro-apoptotic factors

such as Bad and also by increasing synthesis of downstream target genes

including the anti-apoptotic protein Bcl-2 (Vincent and Feldman, 2002). We

hypothesized that defects in IGF-1 signal transduction observed with ΔVps9d

overexpression would translate to an inability of IGF-1 to protect cells upon

serum removal. To test this, we studied IGF-1-mediated survival in PC12 parent

and Alsin stable cell lines. Previously, it was observed that 1 ηM IGF-1 and 100

ηg/ml NGF were effective in protecting PC12 cells from serum withdrawal-

induced apoptosis (Forbes *et al.*, 2002). As shown in Figure 29B, PC12 parent

cells, as expected, were protected from serum withdrawal by both NGF and IGF-

1. However, death from serum removal was not protected by IGF-1 in cells

expressing ΔVps9d Alsin (Figure 29B). Intriguingly, NGF was able to protect

these cells, indicating that ΔVps9d Alsin specifically inhibits IGF-1-mediated

survival (Figure 29B). In addition, cells expressing WT Alsin exhibited an

increase in IGF-1 protection (as compared to PC12 parent cells) when

normalizing to DMEM alone (Figure 29C). These data indicate that the effects

observed with IGF-1- mediated signaling with both WT Alsin and ΔVps9d Alsin

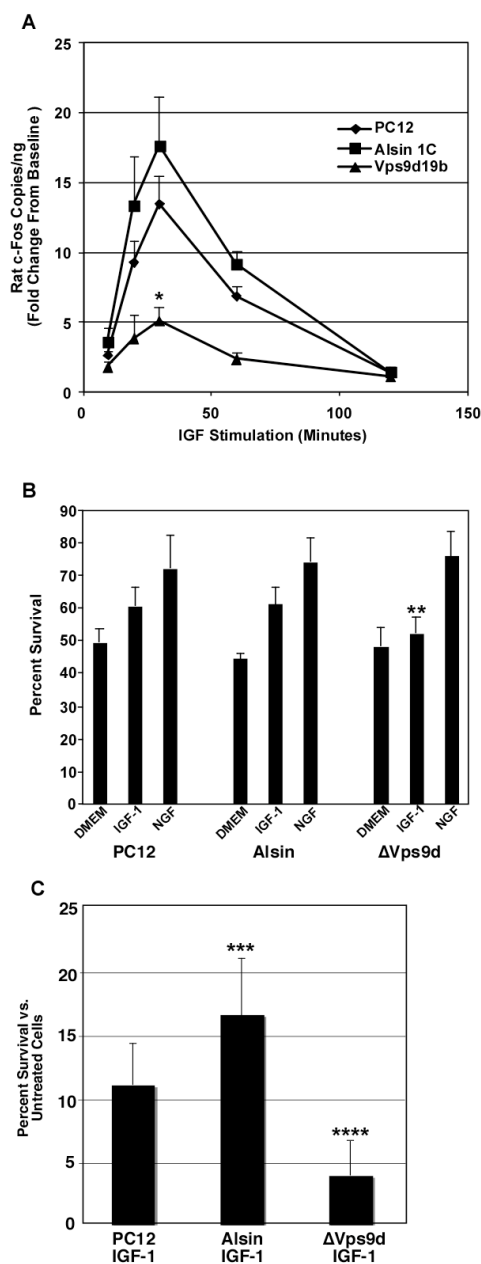expression correlate with IGF-1 protection from serum withdrawal.

A

B

C

Figure 29. ΔVps9d Alsin inhibits IGF-1-mediated survival. A) Serum-starved PC12 parent and Alsin stable cell lines were stimulated with IGF-1 (100 ηg/ml) for 0-120 minutes and *c-fos* transcription monitored as described in Materials and methods. ΔVps9d expression drastically impairs *c-fos* transcription (P = 1.91X10^{-2} (*, two-tailed t test), when comparing 30 minute samples to PC12 cells), while Alsin increases *c-fos* transcription, similar to that observed in Akt activation. B) Survival assays (MTT-based, see Materials and methods) were performed after 44-48 hrs treatments with DMEM alone, DMEM + IGF-1 (1 ηM), DMEM + NGF (100 ηg/ml), or normal growth medium (DMEM + 10% horse serum, 5% FBS). Results shown are the average of eight separate samples (two independent experiments done in quadruplicate). Two-tailed t test analysis reveals that IGF-1-mediated survival is impaired in ΔVps9d cell line as compared to PC12 parent cells (P = 8.68X10^{-3} (**)). Intriguingly, NGF-mediated survival in ΔVps9d cells is not statistically significant from that observed in PC12 parent cell. C) WT Alsin increases while ΔVps9d Alsin decreases IGF-1-mediated survival. Shown is IGF-1-mediated survival normalized to DMEM alone. The WT Alsin increase (P = 1.32X10^{-2} (***)) and ΔVps9d decrease (P = 3.06X10^{-4} (****)) in IGF-1 protection are both significant from that observed in PC12 parent cells, respectively. NGF protection by this analysis reveals that the differences for either WT Alsin or ΔVps9d expression (when compared to PC12 parent cells) are not statistically significant.

Discussion

Data presented here show that Alsin specifically regulates IGF-1 signal transduction by stimulating endocytosis of the IGF-1 receptor. Alsin does not affect signaling mediated by other growth factors such as EGF or NGF, demonstrating that Alsin functions specifically to couple IGF-1 receptor endocytosis and signaling. Overexpression of a mutant version of Alsin that lacks an intact Vps9 domain had a dominant-negative phenotype, and impaired IGF-1-mediated signal transduction. This inhibition of signaling resulted in a decrease in IGF-1 stimulated mitogenicity and serum withdrawal-induced survival, suggesting that the Rab5 GEF activity of Alsin is essential for its regulation of the IGF-1 pathway.

In addition to the ΔVps9d Alsin overexpression studies, it was also observed that IGF-1-mediated ERK1/2 and Akt activation was impaired in primary fibroblasts deficient for Alsin (-/-). This demonstrates that Alsin function is required for appropriate IGF-1 signal transduction, likely through endocytic trafficking of the IGF-1 receptor. Although receptor endocytosis has not been studied in primary fibroblasts herein, similar experiments have been conducted in neurons lacking Alsin (-/-). These studies have shown that Alsin is required for IGF-1 stimulated retrograde transport of IGF-1R (Devon et al., in preparation). Specifically, the IGF-1 receptor is not appropriately targeted to the cell body and

appears to be trapped in a vesicular or early endosomal intermediate (Devon et al., in preparation). These studies in combination with our current studies with ΔVps9d Alsin strongly support the hypothesis that Alsin function is required for IGF-1R endocytosis and signal transduction.

Regulation of IGF-1R endocytosis monitored by both receptor trafficking and IGF-1 ligand internalization required Alsin with an intact Vps9 domain. Previously, we reported that overexpression of another Vps9 domain family member, Rin1, stimulated EGF internalization (Tall *et al.*, 2001). This also required a functional Rab5 GEF domain since a naturally occurring splice variant lacking a significant portion of the Vps9 domain inhibited EGF uptake (Tall *et al.*, 2001). Since Rab5 is known to regulate endosomal fusion of plasma membrane-derived vesicles, it is possible that blocking endosomal fusion (by inhibiting Rab5 activation) results in the recycling and release of ligand at the cell surface. However, it is also possible that inactive Rab5 sequesters endocytic machinery downstream of vesicle fission that is nevertheless required for internalization. Additionally, Rab5 has been shown to interact with the angiotensin receptor (Seachrist *et al.*, 2002) and Rab5 function has been implicated in the sequestration of ligand into clathrin-coated pits (McLauchlan *et al.*, 1998). This suggests that activation of Rab5 may be required prior to vesicle formation and/or fission. Further work is required to determine the precise step in which Rab5 activation occurs in the endocytic process.

We found that ΔVps9d Alsin expression in PC12 cells inhibited IGF-1 signaling at an early step in the pathway, namely IRS-1 and Shc tyrosine phosphorylation. Studies have shown that IGF-1R internalization is required for Shc activation (Chow *et al.*, 1998); (Leahy *et al.*, 2004), but the role of receptor internalization in IRS-1 activation is not well understood. Results from studies using tissue or adipocytes on the related insulin receptor have suggested that IRS-1 tyrosine phosphorylation occurs primarily on endosomes (reviewed in (Baass *et al.*, 1995); (Bevan *et al.*, 1996)). Another group has shown that IRS-1 activation does not require IGF-1R internalization, implying that this step occurs at the plasma membrane (Chow *et al.*, 1998). The reason for this discrepancy is unknown but may involve differences in IGF-1 receptor levels in the various model systems in these studies. It has been postulated that early steps in the endocytic pathway may serve to stabilize the interaction between some growth factors and their receptors (Sorkin and Von Zastrow, 2002), and thus maintain the receptors in an activated state. Indeed, multiple adaptors and intermediate signaling molecules including Shc and PI(3)K are present on endosomes (Sorkin and Von Zastrow, 2002); (Foti *et al.*, 2004). Interestingly, during endocytosis, IGF-1 remains bound to its receptor much longer than the related ligand, insulin, perhaps because this interaction is stable at lower pH (Zapf *et al.*, 1994). Since the interaction between IGF-1 and IGF-1R occurs on endosomes, it is likely that these structures are competent for signal transduction. Indeed, we have observed

that endosomes containing IGF-1 and its receptor are positive for phosphorylated

IGF-1R and Shc, demonstrating that signaling occurs from endosomes (J.D. Topp

and B.F. Horazdovsky, unpublished observations). These studies provide a

platform for the future work required to delineate the temporal and spatial

regulation of IGF-1 signal transduction.

It is generally accepted that tyrosine phosphorylated IRS-1 and Shc

regulate signaling via the PI(3)K/Akt and MAPK pathways, respectively (Butler

et al., 1998). However, activated IRS-1 may be capable of stimulating the MAPK

cascade since it interacts directly with an upstream signaling molecule in this

pathway, Grb2 (Adams *et al.*, 2000). We found that in cells lacking Alsin (-/-) or

in cells overexpressing ΔVps9d Alsin both ERK1/2 and Akt signaling were

affected. This suggests that Alsin function is required for a common and early

step in the IGF-1 signal transduction pathway that is upstream of Shc and IRS-1

phosphorylation. In the currently accepted model of endocytosis, Rab5 activation

is required for docking and subsequent fusion of clathrin-coated pit derived

endocytic vesicles with endosomes, suggesting that endosomal fusion is required

for activation of these molecules.

Based on these data and those presented in this study, we propose three

models for Alsin regulation of IGF-1 signal transduction, each of which include

Alsin Rab5 GEF activity positively regulating endosomal delivery of IGF-1:IGF-

1R containing vesicles. In the first model, the adaptor molecules IRS-1 and Shc

are present on endosomes and are phosphorylated when vesicles containing

activated IGF-1R fuse with the endosomes. In this model, endosomal delivery of

receptor is thus required for IRS-1 and Shc activation. In the second model, IRS-

1 and Shc are phosphorylated at the cell surface in response to IGF-1 stimulation

and incorporated into budding vesicles with activated IGF-1R. These vesicles

then undergo continual rounds of internalization and recycling back to the cell

surface; it should be noted that high levels of recycling have been observed for

IGF-1 (Zapf *et al.*, 1994). Upon recycling of the vesicles, IGF-1 could be

released which would cause phosphatase-mediated inactivation of the now

unoccupied IGF-1R, thus decreasing the interaction between the IGF-1R and IRS-

1 and Shc. In this model, Rab5 activation would be expected to drive activated

IGF-1R-containing vesicles deeper into the endocytic pathway, thus increasing

the half-life of phosphorylated IGF-1R and its associated adaptor proteins. Since

the interaction between IGF-1 and its receptor is observed at lower pH than the

related ligand insulin and its receptor (Zapf *et al.*, 1994), it is plausible that

endosomes provide the most favorable platform for IGF-1 signal transduction. In

the third model, Alsin Rab5 GEF activity is required for IGF-1R

autophosphorylation. Perhaps endocytosis serves to effectively concentrate the

IGF-1R, which is needed to maximally activate the receptor tyrosine kinase

activity. Studies with mutant receptors have shown that receptor internalization

and autophosphorylation while connected, can occur independently. For instance,

Smith and colleagues reported of a naturally occurring IGF-1R splice variant that

exhibits autophosphorylation twice the level of wild-type receptor yet isn't

efficiently internalized (Condorelli *et al.*, 1994).

The ability of IGF-1 to protect various cell types from serum withdrawal-

induced apoptosis is well appreciated (Rukenstein *et al.*, 1991); (Parrizas *et al.*,

1997); (D'Mello *et al.*, 1997). Our studies suggest that Alsin is required for IGF-1

anti-apoptotic function and provide a mechanism for Alsin-related disease

manifestation. It has been proposed that low levels of IGF-1 or a loss of

sensitivity to IGF-1 may be responsible for the progression and perhaps, even the

initial development of neurodegenerative disease (Trejo *et al.*, 2004). One study

conducted on 13 patients with ALS revealed that serum levels of IGF-1 were

approximately 35% lower than the levels of age-matched controls (Torres-

Aleman *et al.*, 1998), implying that deficiency in IGF-1 correlates with the

diseased state. Our results with Alsin suggest that in addition to a reduction in

IGF-1 ligand bioavailability, ALS may also be the result of an inability to

appropriately transduce the IGF-1 survival signal.

This study marks the first known genetic links between receptor

endocytosis, signal transduction, and neurodegeneration. Alsin is required for

IGF-1R endocytosis and subsequent IGF-1-mediated signaling. Intriguingly, the

ability of IGF-1 to serve as a treatment for sporadic ALS is becoming more

recognized as the subcutaneous injection of recombinant IGF-1 is in Phase III

clinical trials (ALS Association, 2004). Importantly, previous clinical trials have

suggested that IGF-1 may slow the rate of progression and is well tolerated by

patients (reviewed in (Dore *et al.*, 1997)). In addition, recent advances have been

made in recombinant adeno-associated viral (AAV) therapy. Gage and colleagues

have reported that retrograde delivery of IGF-1, in which the virus is taken up by

motor neurons and transported to the cell body for sustained expression, prolongs

survival and delays ALS progression even when delivered at the onset of

symptoms (Kaspar *et al.*, 2003). These findings, coupled with the apparent safety

of this viral method for patients, demonstrates that recombinant AAV may be a

useful therapy for sporadic ALS (Boillee and Cleveland, 2004). Our studies with

Alsin help to explain why IGF-1 treatment is beneficial and also genetically and

functionally identify a novel mode of neurodegeneration. Future work is required

to determine the precise mechanism by which Alsin regulates the IGF-1 signal

transduction pathway both in the diseased and healthy state, and should lead to a

greater understanding of ALS progression and potential methods of treatment.

Chapter 5. Conclusions and future perspectives

Implications of the links between Alsin, IGF-1, and neurodegeneration

Our work has shown that Alsin is required for IGF-1R endocytosis and signal transduction. Inhibition of IGF-1R trafficking caused the impairment of IGF-1-mediated phosphorylation of the signaling molecules ERK1/2 and Akt. This inhibitory effect on signaling resulted in a decrease in the mitogenicity of IGF-1 and the ability of IGF-1 to protect cells from serum withdrawal-induced apoptosis. IGF-1-mediated signaling was affected in cells overexpressing a truncation of Alsin lacking an intact Vps9 domain and in cells lacking Alsin. These results suggest that the Rab5 guanine nucleotide exchange (GEF) activity of Alsin is essential for the IGF-1 signal transduction pathway.

These studies provide the first genetic and functional link between IGF-1 signal transduction and neurodegeneration. Based on the data generated from cells expressing dominant-negative Alsin (ΔVps9d) or in cells lacking Alsin, it can be inferred that Alsin function is required for IGF-1-mediated signaling by directing the appropriate trafficking of the IGF-1 receptor. Activated receptors and bound signaling molecules must be transported from the axon tip to the cell body where transcription occurs. This transport process likely involves signaling

endosomes. Although mainly characterized for the neurotrophin signaling

pathway (Sofroniew *et al.*, 2001), similar events are likely required for other

growth factors. Data showing that IGF-1-mediated signaling requires endocytosis

(Chow *et al.*, 1998) in a dynamin- and beta-arrestin- (Lin *et al.*, 1998), and now

Rab5- (Chapter 4) dependent manner, provides evidence that similar mechanisms

of signal transduction will occur in neurons.

Initially described in 1997 (Dudek *et al.*, 1997), the role for IGF-1 in

neuronal survival is now widely appreciated (reviewed in (Vincent and Feldman,

2002)). IGF-1 anti-apoptosis is mediated by phosphorylation and activation of the

signaling intermediates, Akt and ERK1/2 (Vincent and Feldman, 2002). Both the

PI(3)K and MAPK pathways are known to promote survival via transcriptional

activation of target genes, including anti-apoptotic proteins such as Bcl-2 and Bcl-

x (Vincent and Feldman, 2002). In addition, activated Akt directly phosphorylates

Bad and members of the Forkhead (FKH) transcription factor family, which

promotes their interaction with 14.3.3 proteins and prevents their pro-apoptotic

activity (Vincent and Feldman, 2002). Results presented here (Chapter 4) show

that ΔVps9d Alsin impairment of IGF-1-mediated signaling decreases both Akt

phosphorylation and transcription of target genes. Since both of these pathways

are affected, it is not surprising that IGF-1 is unable to protect cells expressing

ΔVps9d from serum withdrawal-induced apoptosis (Figure 29). Furthermore,

since phosphorylation of both Akt and ERK1/2 are decreased in primary

fibroblasts from mice deficient for Alsin (-/-) (Figure 28), it is likely that IGF-1-mediated survival will be similarly affected. These results support those obtained by Lefkowtiz's group who showed that beta-arrestin-dependent endocytosis of IGF-1R was required for IGF-1 anti-apoptotic activity (Povsic *et al*., 2003). Studies in sympathetic neurons revealed that the internalization and delivery to the cell body of kinase-active TrkA (NGF receptor) was necessary for NGF-mediated neuronal survival (Ye *et al*., 2003).

Taken together, these data provide a potential mechanism for the neurodegeneration associated with mutations in Alsin. This mechanism, named the IGF-1 signal transduction model of neurodegeneration, states that loss-of-Alsin function impairs the trafficking of protein complexes containing activated receptors and signaling intermediates. This would be expected to block the ability of IGF-1 to promote survival, making the cells more susceptible to apoptosis. Trejo et al. have proposed that defects in IGF-1 input to neurons or loss of sensitivity could promote progression, and perhaps the initial development, of neurodegenerative diseases such as ALS (Trejo *et al*., 2004). This hypothesis is supported by three pieces of evidence: (1) one study showed that patients with ALS have decreased serum levels of IGF-1 (Torres-Aleman *et al*., 1998); (2) in a clinical trial, IGF-1 delivered subcutaneously delayed progression of ALS (reviewed in (Dore *et al*., 1997)); and (3) retrograde delivery of IGF-1 to motor

neurons prolonged survival and delayed disease progression in mouse models of ALS, even with delivery after onset of symptoms (Kaspar *et al.*, 2003).

Our results provide the first functional evidence to substantiate the above hypothesis of neurodegeneration put forth by Torres-Aleman and colleagues (Trejo *et al.*, 2004). However, our studies also extend their hypothesis and show that appropriate transduction of the IGF-1 signal is required for the ability of IGF-1 to function as a survival factor. This might explain why IGF-1 treatment, while providing some therapeutic benefit, has only a small effect on patients with ALS (reviewed in (Bruijn *et al.*, 2004)). It is interesting to note that two previous studies showed that patients with ALS had a dramatic increase in IGF-1 binding sites in the ventral horn (Adem *et al.*, 1994); (Dore *et al.*, 1996), and this corresponded to an increase in IGF-1 receptor levels (Adem *et al.*, 1994). These data support our model and are perhaps due to a defect in IGF-1 receptor trafficking and signal transduction.

The implications of the IGF-1 signal transduction model to ALS and neurodegeneration are three-fold. First, delivery of IGF-1 ligand alone to areas of degeneration would not be efficacious as a therapeutic for ALS if the signal transducing machinery is non-functional. Therefore, therapy must be developed with the understanding that appropriate trafficking of the IGF-1 signal from the axon to cell body is essential. Second, the development of diagnostics that monitor IGF-1 signaling potential are crucial and should provide insights into

sporadic forms of ALS (see below). While two genes and six other chromosomal loci have been identified for the inheritable forms of ALS, in more that 90% of the cases of ALS there is no known genetic link. It is anticipated that a portion of these patients have defects in the IGF-1 signal transduction cascade. Third, in addition to IGF-1, other growth factors have been shown to promote anti-apoptosis in motor neurons (Seeburger and Springer, 1993); (Bohn, 2004) or animal models of ALS (Wang *et al.*, 2002); (Azzouz *et al.*, 2004). It is plausible that defects in signal transduction by these growth factors may also lead to neurodegeneration.

The IGF-1 signal transduction model correlates very well with previous hypotheses for ALS disease progression. Pathology from patients and animal models have implied that neurodegeneration could be due to protein aggregation, axonal strangulation by abnormal neurofilament regulation, an impairment in retrograde transport, and glutamate-mediated excitotoxicity (reviewed in (Bruijn *et al.*, 2004)). Of these hypotheses, the first three would be expected to negatively impact IGF-1 signal transduction by blocking appropriate trafficking of protein complexes that contain activated receptor and signaling molecules. Furthermore, it was recently shown that IGF-1 can protect motor neurons from glutamate excitotoxicity (Vincent *et al.*, 2004). Thus, a defect in IGF-1 signaling could make the neurons more susceptible to this apoptotic insult. Taken together, our findings with Alsin enable the formulation of the first model that accounts for all

of the previous pathological data, and provide a novel insight into the

neurodegeneration associated with ALS.

Alsin regulation of IGF-1R endocytosis and signal transduction

In addition to its Vps9 domain, Alsin also possesses several other domains

that are expected to impact Alsin function. At its NH_2-terminus, Alsin has an

RCC1-like domain (RLD) which contains five sets of RCC1 repeats and is

predicted to form a seven-bladed beta propeller structure (Topp *et al.*, 2004). This

domain is present in more than 90 proteins and appears to mediate interactions

with other proteins (Topp *et al.*, 2004). Based on overexpression studies, we

previously suggested that this domain negatively regulates the membrane

association of Alsin, perhaps through interaction with a protein that sequesters

Alsin into the cytoplasm (Topp *et al.*, 2004). Alsin also contains Dbl homology

(DH) and Pleckstrin homology (PH) domains (Hadano *et al.*, 2001); (Yang *et al.*,

2001), a characteristic of proteins that have GEF activity for members of the Rho

GTPase family (Zheng, 2001). Indeed, it was found that Alsin interacts

specifically with and is a nucleotide exchange factor for Rac1 (Topp *et al.*, 2004);

(Kanekura *et al.*, 2005). Adjacent to the Rac1 GEF domain lie 8 sets of a motif

known as MORN (Membrane occupation and recognition nexus) (Hadano *et al.*,

2001); (Yang *et al.*, 2001). The MORN repeat, while largely uncharacterized, is

present in a family of proteins known as the junctophilins (Takeshima *et al.*,

2000). Recently, it has been shown that mutations acquired by aberrant splicing in junctophilin-3 lead to the neurodegenerative disorder Huntington disease-like 2 (HDL-2) (Holmes *et al.*, 2001), suggesting the normal function of this protein is crucial to neuron maintenance. In addition, junctophilin-2, a protein with decreased expression in cardiomyopathies, associates in caveolar fractions by means of its interaction with caveolin-3 (Minamisawa *et al.*, 2004).

Based on the presence of these domains, it is likely that Alsin's regulation of the IGF-1 signaling pathway requires more than just the Vps9 domain. To address the importance of these other domains in Alsin function, PC12 cells lines will be generated that contain point mutations in either the Rac1 GEF and Rab5 GEF domains. Because of the recent advance in inducible cell systems and the potential issues that arise from continual overexpression, stable cell lines will be constructed that are inducible. Since previous work was performed with ΔVps9d Alsin, which is a truncation that is missing almost all of the expected Rab5 interaction surface and may expose hydrophobic residues to solvent (Delprato *et al.*, 2004), it is remotely possible that this truncation produces its dominant-negative effect by means other than simple loss of Rab5 nucleotide exchange activity. To address this, experiments will be performed comparing the ΔVps9d Alsin truncation with Alsin containing a single point mutant at residue 1599 (Asp). Mutation of this residue from Asp to Ala has been shown to drastically reduce the Rab5 GEF activity of another member of the Vps9 family, Rabex-5

(Delprato *et al.*, 2004). The requirement of Alsin Rac1 GEF activity for IGF-1-mediated signaling will be determined by conducting experiments with Alsin mutated at a single residue in the DH domain. Mutation of residue 701 (Thr) to Ala inhibited the interaction between Alsin and Rac1, thus blocking Rac1 GEF activity (Kanekura *et al.*, 2005). IGF-1 signal transduction will be monitored at three stages in the pathway: tyrosine phosphorylation of Shc and IRS-1, serine/threonine phosphorylation of Akt and ERK1/2, and transcription of the immediate early gene c-fos.

In addition to determining the role that these domains play in IGF-1-mediated signal transduction, receptor endocytosis experiments will be performed on NWT3b cells (NIH3T3 cell line stably expressing the human IGF-1R). Endocytosis will be studied by both indirect immunofluorescence with antibodies to the alpha subunit of the IGF-1 receptor and with biotinylated IGF-1 ligand. This experimental setting allows the monitoring of both receptor trafficking to endosomes and the visualization of "earlier" endocytic compartments containing IGF-1 ligand.

Identification of protein and lipid components that regulate Alsin function

In addition to domains that catalyze guanine nucleotide exchange on Rac1 and Rab5, Alsin also possesses other domains which could serve to regulate these activities. In particular, two pieces of evidence suggest that the beta propeller domain may provide negative regulation. First, overexpression of individual domains indicates that the Rac1 GEF and Rab5 GEF domains are present on small structures which are likely endosomes (Otomo *et al.*, 2003); (Topp *et al.*, 2004); (data not shown). Expression of the RCC1-like domain (RLD) appears to inhibit this endosomal localization, as its inclusion results in the localization of Alsin to the cytoplasm (Otomo *et al.*, 2003); (Topp *et al.*, 2004). Secondly, it was shown that, upon removal of this domain, Alsin is present on endocytic structures and induces the formation of enlarged endosomes (Otomo *et al.*, 2003), a process known to require the activation of Rab5 (Stenmark *et al.*, 1994); (Roberts *et al.*, 1999); (Barbieri *et al.*, 2003). Indeed, while overexpression of RLD-deleted Alsin or the Vps9 domain alone stimulates this process, expression of WT Alsin does not (Topp *et al.*, 2004). Together, these data strongly suggest that the beta propeller domain regulates both the localization of Alsin and the activity of the Rab5 GEF domain.

How could the RCC1-like domain regulate Alsin function? Perhaps this domain autoinhibits the Rac1 and Rab5 GEF activities directly through inter- or intra-molecular interactions that block the association of these domains with their target GTPases (Topp *et al.*, 2004). Another hypothesis is that the RLD interacts with a protein that sequesters Alsin in the cytoplasm. One would anticipate that removal of this negative regulation would be required to allow the nucleotide exchange domains of Alsin to act on Rac1 and Rab5. Since Alsin has been shown to specifically regulate the IGF-1 signal transduction pathway, it is likely that one or more upstream components of the IGF-1 signaling pathway positively regulates Alsin. Indeed, data supports this hypothesis since Alsin is recruited to endosomes upon stimulation with IGF-1 (data not shown). Additionally, it was observed that upon stimulation with IGF-1, Alsin expression causes endosome-endosome fusion as observed by an enlargement in IGF-1 ligand- and receptor-positive endosomes (Figures 24C, 25B, 25C). This indicates that something upstream in the IGF-1 pathway triggers both Alsin endosomal recruitment and Alsin Rab5 GEF activity.

Taken together, these data strongly point to the RCC1-like domain as a key regulatory module of Alsin function. Therefore, the identification of proteins that interact with this domain is of key interest. Inducible PC12 cell lines will be generated that express Alsin or the beta propeller domain of Alsin alone as TAP (tandem affinity purification) tag fusions (Rigaut *et al.*, 1999). This tag has been shown to greatly improve yield and purity for the isolation of protein complexes

(Puig *et al.*, 2001). Alsin will be purified from cells that are unstimulated or stimulated with IGF-1, and protein interactors will be identified by mass spectrometry. The interaction surface will then be mapped with recombinant domains of Alsin or coexpression in cell culture, with the expectation that the beta propeller domain will be required. The requirement for these interactions in IGF-1 signaling and receptor endocytosis will then be determined. Lefkowitz's group has shown that IGF-1R trafficking and signaling require $G_{\beta\gamma}$ protein subunits (Luttrell *et al.*, 1995) and beta-arrestins (Lin *et al.*, 1998); (Povsic *et al.*, 2003). Perhaps either of these proteins or the phosphorylated IGF-1R itself is responsible for recruiting Alsin upon IGF-1 stimulation.

In addition to its beta propeller domain, Alsin also possesses two other domains (PH domain, MORN repeats) which are expected to serve a role in regulating Alsin function. Proteins containing either of these domains (PH domain, MORN repeats) have been shown to interact with phospholipids. Phospholipids or their metabolites are crucial mediators or cell signaling and membrane trafficking. For instance, $PI(4,5)P_2$, which is predominantly found at the plasma membrane, is hydrolyzed by phospholipase C to generate the key second messengers inositolpolyphosphate 3 (IP3) and diaglycerol (DAG) (De Camilli *et al.*, 1996); (Wenk and De Camilli, 2004). PI(3) kinases phosphorylate $PI(4,5)P_2$ to $PI(3,4,5)P_3$ transiently in response to stimulation by growth factors (Roth, 2004); (Wenk and De Camilli, 2004). Furthermore, PI(3)P is known to

localize to early endosomes where it plays a key role in recruiting endocytic machinery (Roth, 2004); (Wenk and De Camilli, 2004).

MORN repeats are found not only in Alsin, but also in the junctophilin family of proteins (Takeshima *et al.*, 2000). Studies on the junctophilins, proteins that are associated with the plasma membrane, suggest that the MORN repeats of Alsin may facilitate an interaction with phospholipids of the plasma membrane. Since Alsin is not generally localized to the cell surface, it is possible that recruitment of this domain requires the local production of phospholipids, such as $PI(3,4,5)P_3$. However, it is also possible that the MORN repeats of Alsin bind to $PI(4,5)P_2$ upon IGF-1 stimulation. It would be anticipated that this interaction would require a release of the potential autoinhibition mediated by the beta propeller domain (see above). In addition to the MORN repeats, Alsin also contains a central PH domain. PH domains interact with various phospholipids and many guanine nucleotide exchange factors for Rho GTPases interact specifically with $PI(3,4,5)P_3$, via their PH domains (Zheng, 2001); (Roth, 2004). In many instances, $PI(3,4,5)P_3$ stimulates Rho GEF activity (Zheng, 2001), and this serves to modulate the actin cytoskeleton (Hall, 1998); (Kaibuchi *et al.*, 1999); (Sah *et al.*, 2000). Indeed, we have observed previously that Alsin Rac1 guanine nucleotide exchange occurs *in vivo*, but not in a cell-free system lacking membranes (Topp *et al.*, 2004), suggesting that there is a lipid requirement for activity.

Two methods will be utilized to determine the phospholipid(s) with which the MORN repeats and PH domain of Alsin interact. First, the localization of each domain will be determined by expressing each in cells as fluorescent fusion proteins. This method has proven useful with studies on both PH and FYVE (interact specifically with PI(3)P) domains (Balla and Varnai, 2002). Localization will be studied in both the resting state and in cells stimulated with IGF-1. The second method will involve the expression of each phospholipid-binding domain as a recombinant protein. Liposomes will be formed that specifically incorporate each of the phospholipids, and interactions with the MORN repeats and PH domain determined by centrifugation. Based on these results, mutations will be made in each domain that abolish these interactions, allowing the phospholipids requirements for Alsin regulation of IGF-1R trafficking and signaling to be characterized. Since it has been argued that phospholipids binding is likely not the sole determinant of localization in proteins containing these domains (Roth, 2004), it will be worthwhile to study these mutations in concert with those that disrupt interactions between Alsin and its protein interaction partners (described above).

Characterization of Alsin-deficient mice

It was found that cells lacking Alsin (-/-) are impaired in IGF-1-mediated, but not EGF-mediated signal transduction (Figure 28). In addition, as observed

with the dominant-negative studies with ΔVps9d Alsin, IGF-1R endocytosis is drastically reduced in Alsin-deficient (-/-) neurons (Devon et al., in preparation). These data show that Alsin is required for IGF-1 signaling and receptor trafficking. Experiments are currently underway to determine the effects of loss-of-Alsin function on IGF-1 both as a mitogenic and a survival factor.

Studies with SOD1 mutant mice have provided much information on the pathogenesis of ALS (reviewed in (Bruijn *et al.*, 2004)). Since sporadic and familial ALS are similar clinically and pathologically, these mice have enabled the formulation of four hypothesis for ALS disease progression: (1) toxicity due to formation of intracellular aggregates, (2) abnormal trafficking and axonal strangulation due to disruption of neurofilaments, (3) calcium-mediated apoptosis by glutamate excitotoxicity, and (4) disruption in retrograde axonal transport, though the exact mechanism of action is unknown (reviewed in (Bruijn *et al.*, 2004)). In addition, SOD1 mutant mice have provided a model for the development of therapeutics. The mice overexpress SOD1 with point mutations that have been identified in patients with the disease, with the G85R, G37R, and G93A mutations being the most extensively characterized (Bruijn *et al.*, 2004). Although only 1-2% of the cases of ALS are due to mutations in SOD1, the pathology of the SOD1 mouse models appears to closely mimic that observed in patients with the human disease (Bruijn *et al.*, 2004). Both are characterized by the accumulation of hyper-phosphorylated neurofilament proteins and

ubiquitinated protein aggregates, which form inclusion bodies (Bendotti and

Carri, 2004). Similar to patients, the SOD1 mutant mice possess severe muscular

dysfunction (Bendotti and Carri, 2004). This is observed in mouse models as the

following behaviors: impairment in evoked response and extension reflex, an

inability to stay on a rotating bar, and a reduction in stride length on an inclined

ramp (Bendotti and Carri, 2004).

Similar behavioral experiments will be performed on Alsin-deficient (-/-)

mice. It is anticipated that loss-of-Alsin function will result in neurodegeneration;

however, two important caveats must be mentioned. First, unlike SOD1-related

disease, disease due to mutations in Alsin occurs at a much earlier onset and

progresses much more slowly (Devon *et al*., 2005). Second, a unique

characteristic of Alsin, as compared with SOD1, is its remarkably high expression

in the cerebellum (Hadano *et al*., 2001); (Otomo *et al*., 2003); (Yamanaka *et al*.,

2003); (Devon *et al*., 2005). This may implicate a novel site of pathology

previously unobserved in ALS. Accordingly, behavioral tests that are focused on

motor neurons may not be sufficient. Novel behavioral experiments that

incorporate an aspect of cerebellar function are warranted and should be modeled

after those developed for investigation of cerebellar disorders such as the spino-

cerebellar ataxias (SCAs) (Zoghbi and Botas, 2002); (Taroni and DiDonato,

2004).

Potential diagnostics for ALS

IGF-1 and its cognate receptor are expressed in all tissues. However, greater than 80% of circulating IGF-1 is synthesized in the liver and is regulated by growth hormone (directly) and insulin (indirectly) (Kaaks, 2004). Upon secretion into the bloodstream, IGF-1 circulates bound to one of six proteins of the IGF-binding protein (IGFBP) family (Holly, 2004). IGFBP-3 is the main carrier of IGF-1, and 75% of IGF-1 is sequestered in the bloodstream by this molecule (Fang *et al.*, 2004). Interestingly, IGF-1 interacts with IGFBPs with much greater affinity that its receptor (Holly, 2004); (Fang *et al.*, 2004), suggesting that active mechanisms are required to dissociate IGF-1 from IGFBPs. Indeed, entry into the interstitial fluid requires dissociation of IGF-1 from IGFBP-3, as this complex is too large to pass through the vascular endothelium (Fang *et al.*, 2004). Because of its interaction with IGFBPs, IGFBP-3 in particular, the concentration of IGF-1 in circulation is 100 ηM, which is 50-100 times higher than the level required for cellular regulation (Holly, 2004). IGFBPs regulate IGF-1 both positively and negatively. The positive regulation comes from their ability to increase the half-life of IGF-1 in the blood; however, IGF-1 that is bound to IGFBPs appears to be incapable of activating IGF-1 receptors, serving to negatively regulate IGF-1 (Fang *et al.*, 2004).

An additional level of regulation of IGF-1 levels is provided by proteases that specifically cleave IGFBPs, releasing free IGF-1 that is competent to activate

cell signaling cascades (Holly, 2004). Protease activity is blocked by protease inhibitors which are found in the bloodstream, but not in the extracellular fluid (Holly, 2004). Thus, IGF-1 in circulation is present in stable higher molecular weight complexes with IGFBPs. IGF-1 that crosses the vascular endothelium is free, enabling it to interact with its receptor on target cells and initiate signal transduction cascades.

A previous study showed that patients with ALS had decreased and increased serum levels of IGF-1 and IGFBPs, respectively (Torres-Aleman *et al.*, 1998). In combination, this would be expected to decrease the amount of free, or "bioactive" IGF-1. Based on our studies with Alsin, we would propose that this might be a common feature of ALS. This warrants further investigation into the levels of active IGF-1 in patients with ALS. We propose that IGF-1 and IGFBP-3 levels be determined in patients with both familial and sporadic ALS. Methods exist for quantitating the specific amounts of each of these proteins and have been used previously to monitor levels in patients with cancer (Pollak, 2001). Indeed, elevated levels of IGF-1 are known to be a primary risk factor in many cancers (see below; (LeRoith and Roberts, 2003)). If a connection can be made between "bioactive" IGF-1 and ALS, determining the serum levels of IGF-1 and IGFBP-3 could be an important test for clinicians in the diagnosis of ALS. It will be important to monitor IGF-1 in both serum and extracellular fluid, as serum levels of IGF-1 are not necessarily equivalent to those available for target cells, due to

the various modes of regulation described above. As the technology to detect the IGFBP proteases and their inhibitors is developed, the quantitation of these molecules may also prove beneficial.

In addition to determining the level of IGF-1 input, it is equally, if not more important, to determine the ability of target cells to respond to IGF-1 stimulation. Future diagnostics should monitor IGF-1 signal transduction. Although much future work is required in research development, two potential assays do come to mind. First, in fibroblasts isolated from patients signaling could be monitored in response to IGF-1 and other growth factors. Since we have shown that Alsin-deficient (-/-) mice exhibit a reduction in ERK1/2 and Akt activation in response to IGF-1, but not EGF, it is possible that fibroblasts from patients will be affected similarly. Second, IGF-1 activation of cells is known to trigger the secretion of annexins (Zhao *et al.*, 2003). The ability of patient fibroblasts to secrete annexins could be determined in response to IGF-1. These methods, with much future development and optimization, could provide the framework for a diagnostic that monitors the IGF-1 signal transduction pathway.

Potential treatments for ALS

Although much information has been gained in the last decade as to the pathology of ALS, there is still no therapy for patients suffering from this disease. The only drug that has been shown to delay the course of ALS, riluzole, has only

a modest effect on survival (Gordon, 2005). This is perhaps because riluzole is thought to affect glutamate release (Cleveland and Rothstein, 2001), a likely late stage in disease progression since apoptotic neurons are though to release glutamate into the extracellular fluid. In fact, while riluzole increases survival by a few months it does not affect strength or function (Gordon, 2005). Many other therapeutics have been attempted in clinical trials, but all have failed to slow the disease or promote survival. Some of these treatments include: growth factors (CNTF and BDNF), antioxidants (vitamin E), anti-apoptotic drugs (selegeline), and drugs to regulate glutamate levels (lamotrigine, dextromorphan, gabapentin, topiromate) (Gordon, 2005). Novel studies on animal models aimed at blocking apoptosis have provided new hope, however. Inhibition of apoptosis by overexpression of the anti-apoptotic protein Bcl-2 (Kostic *et al.*, 1997), intraventricular delivery of a pan caspase inhibitor (Li *et al.*, 2000), and administration of minocycline (Kriz *et al.*, 2002); (Van Den Bosch *et al.*, 2002); (Zhu *et al.*, 2002), which delays cytochrome c release, (Zhu *et al.*, 2002), all prolong survival. Although these methods have shown promise in mice, their ability to improve survival in patients with ALS is unknown. Furthermore, because these methods inhibit an apoptotic cascade that has already been initiated, these methods, while they may prolong survival, would not be expected to increase muscle strength or improve quality of life.

One recent study has shown, however, that IGF-1 injected subcutaneously had a positive effect as determined by the Appel scale (Gordon, 2005). Based on preliminary results, a phase III trial was initiated and is currently in progress (ALS Association, 2004). In contrast to the Appel scale, this trial is monitoring disease progression by manual muscle testing (MMT), which has been shown to be a better method of detection than those previously used (Gordon, 2005). It is important to note that the ability of IGF-1 to reach the target tissue may be limited by this method (Bruijn *et al.*, 2004). To improve delivery of IGF-1 to motor neurons, Gage and colleagues have used recombinant adeno-associated adenoviral (AAV) expression of IGF-1 (Kaspar *et al.*, 2003). After injection of the virus into muscles, it was taken up by motor neurons and transported in a retrograde manner back to the cell body (Kaspar *et al.*, 2003). This method prolonged survival and delayed disease progression in an animal model, even when introduced at the time of disease onset (Kaspar *et al.*, 2003). Adeno-associated viral expression has been shown to be safe in other instances (Boillee and Cleveland, 2004), and clinical trials with IGF-1 and ALS are anticipated. IGF-1 is an attractive therapeutic because of its mitogenicity and its potency as a survival factor, which suggest that IGF-1 treatment might stimulate growth in addition to inhibiting apoptosis.

As described above (Potential diagnostics for ALS), IGF-1 "bioactivity" is regulated by interaction with IGFBPs. IGF-1:IGFBP complexes are dissociated

by proteolytic cleavage of IGFBPs, which is regulated by protease inhibitors that are present in the bloodstream, but not in the interstitial fluid. Therefore, IGF-1 that has crossed the vascular endothelium (or has been secreted by motor neurons or other cells) is likely to be active because it is not bound to IGFBPs. Since the interaction between IGF-1 and IGFBPs is much stronger that the interaction between IGF-1 and its receptor (Fang *et al*., 2004), increases in IGFBP levels in the interstitial fluid due to a decrease in proteolytic activity (either by a decrease in protease levels or an increase in protease inhibitor levels) would be expected to negatively impact IGF-1 signaling. If the regulation of IGFBPs is observed to be abnormal, it would be prudent to increase the "bioactivity" of IGF-1 by delivering IGFBP proteases (which are specific to individual IGFBPs) or small molecule inhibitors of IGFBPs.

Our studies with Alsin (Chapter 4) imply that increasing the input of IGF-1 to motor neurons may not be sufficient. If the neurons are incapable of transducing the signal to the cell body, the ability of IGF-1 to function as a mitogenic or survival factor is likely very limited. Certainly, this method should be effective for patients with decreased levels of IGF-1 who retain normal capacity of IGF-1 signal transduction. However, for those patients with a deficiency in this pathway, increasing IGF-1 levels will not be enough. In this case, gene therapy in which Alsin or another key regulatory molecule is delivered to the motor neurons with IGF-1 may prove beneficial. The development of small

molecules that potentiate the IGF-1 signal transduction pathway provides another alternative. Further investigation into the regulation of IGF-1R trafficking and signaling in the normal and diseased state is likely to provide much in the way of therapeutic potential.

IGF-1 and cancer

Any discussion on IGF-1 would be lacking if its potential role in cancer was not mentioned. Much work has suggested that high levels of circulating IGF-1 are a major risk factor for the development of several cancers (LeRoith and Roberts, 2003). In addition, IGF-1R levels are a predictor of breast cancer outcome, and carcinomas often overexpress the IGF-1R at higher levels than normal cells (LeRoith and Roberts, 2003). Therefore, direct administration of IGF-1 to the target tissue must be strictly controlled. Clinical trials with IGF-1 have revealed no major acute side effects, and the long-term use of IGF-1 did not increase the incidence of cancers (Dore *et al.*, 1997). These authors argue that the administration of low doses of IGF-1 is safe even for extended periods of time (Dore *et al.*, 1997). Since signal transduction by IGF-1 is limited by the level of receptor in the cell, unless cells have been mutated (are pre-disposed) and overexpress higher levels of IGF-1R, the risk of cancer is likely to be minimal. However, the utilization of IGF-1 as a therapeutic requires a much greater understanding of IGF-1 and its role in cancer. Although our knowledge of IGF-1

is not complete, it is becoming obvious that IGF-1 signal transduction, which can

lead to disease if inhibited or over-activated, must be subject to a very precise

regulation.

Bibliography

Adams, T.E., Epa, V.C., Garrett, T.P., and Ward, C.W. (2000). Structure and
function of the type 1 insulin-like growth factor receptor. Cell Mol Life
Sci *57*, 1050-1093.

Adem, A., Ekblom, J., Gillberg, P.G., Jossan, S.S., Hoog, A., Winblad, B.,
Aquilonius, S.M., Wang, L.H., and Sara, V. (1994). Insulin-like growth
factor-1 receptors in human spinal cord: changes in amyotrophic lateral
sclerosis. J Neural Transm Gen Sect *97*, 73-84.

Allison, D.W., Gelfand, V.I., Spector, I., and Craig, A.M. (1998). Role of actin in
anchoring postsynaptic receptors in cultured hippocampal neurons:
differential attachment of NMDA versus AMPA receptors. J Neurosci *18*,
2423-2436.

ALS Association (2004). A phase III trial of IGF-1 in patients with ALS.
Available at: http://www.alsa.org. Access "Drug Trials" under heading
"On the Inside", then access "Myotrophin®". Accessed March 5, 2005.

Aoki, K., Barker, C., Danthinne, X., Imperiale, M.J., and Nabel, G.J. (1999).
Efficient generation of recombinant adenoviral vectors by Cre-lox
recombination in vitro. Mol Med *5*, 224-231.

Aparicio, S., Chapman, J., Stupka, E., Putnam, N., Chia, J.M., Dehal, P., Christoffels, A., Rash, S., Hoon, S., Smit, A., Gelpke, M.D., Roach, J., Oh, T., Ho, I.Y., Wong, M., Detter, C., Verhoef, F., Predki, P., Tay, A., Lucas, S., Richardson, P., Smith, S.F., Clark, M.S., Edwards, Y.J., Doggett, N., Zharkikh, A., Tavtigian, S.V., Pruss, D., Barnstead, M., Evans, C., Baden, H., Powell, J., Glusman, G., Rowen, L., Hood, L., Tan, Y.H., Elgar, G., Hawkins, T., Venkatesh, B., Rokhsar, D., and Brenner, S. (2002). Whole-genome shotgun assembly and analysis of the genome of Fugu rubripes. Science *297*, 1301-1310.

Arighi, C.N., Hartnell, L.M., Aguilar, R.C., Haft, C.R., and Bonifacino, J.S. (2004). Role of the mammalian retromer in sorting of the cation-independent mannose 6-phosphate receptor. J Cell Biol *165*, 123-133.

Ayala, F.J., Rzhetsky, A., and Ayala, F.J. (1998). Origin of the metazoan phyla: molecular clocks confirm paleontological estimates. Proc Natl Acad Sci USA *95*, 606-611.

Azzouz, M., Ralph, G.S., Storkebaum, E., Walmsley, L.E., Mitrophanous, K.A., Kingsman, S.M., Carmeliet, P., and Mazarakis, N.D. (2004). VEGF delivery with retrogradely transported lentivector prolongs survival in a mouse ALS model. Nature *429*, 413-417.

Baass, P.C., Di Guglielmo, G.M., Authier, F., Posner, B.I., and Bergeron, J.J. (1995). Compartmentalized signal transduction by receptor tyrosine kinases. Trends Cell Biol *5*, 465-470.

Balla, T., and Varnai, P. (2002). Visualizing cellular phosphoinositide pools with GFP-fused protein-modules. Sci STKE *2002*, PL3.

Bankaitis, V.A., Johnson, L.M., and Emr, S.D. (1986). Isolation of yeast mutants defective in protein targeting to the vacuole. Proc Natl Acad Sci U S A *83*, 9075-9079.

Barbieri, M.A., Hoffenberg, S., Roberts, R., Mukhopadhyay, A., Pomrehn, A., Dickey, B.F., and Stahl, P.D. (1998). Evidence for a symmetrical requirement for Rab5-GTP in in vitro endosome-endosome fusion. J Biol Chem *273*, 25850-25855.

Barbieri, M.A., Kong, C., Chen, P.-I., Horazdovsky, B.F., and Stahl, P.D. (2003). The SRC homology 2 domain of Rin1 mediates its binding to the epidermal growth factor receptor and regulates receptor endocytosis. J Biol Chem *278*, 32027-32036.

Barker, P.A., Hussain, N.K., and McPherson, P.S. (2002). Retrograde signaling by the neurotrophins follows a well-worn trk. Trends Neurosci *25*, 379-381.

Bateman, A., Birney, E., Cerruti, L., Durbin, R., Etwiller, L., Eddy, S.R.,
Griffiths-Jones, S., Howe, K.L., Marshall, M., and Sonnhammer, E.L.L.
(2002). The Pfam Protein Families Database. Nucl. Acids. Res. *30*, 276-
280.

Beattie, E.C., Carroll, R.C., Yu, X., Morishita, W., Yasuda, H., von Zastrow, M.,
and Malenka, R.C. (2000). Regulation of AMPA receptor endocytosis by a
signaling mechanism shared with LTD. Nat Neurosci *3*, 1291-1300.

Beattie, E.C., Zhou, J., Grimes, M.L., Bunnett, N.W., Howe, C.L., and Mobley,
W.C. (1996). A signaling endosome hypothesis to explain NGF actions:
potential implications for neurodegeneration. Cold Spring Harb Symp
Quant Biol *61*, 389-406.

Ben Hamida, M., Hentati, F., and Ben Hamida, C. (1990). Hereditary motor
system diseases (chronic juvenile amyotrophic lateral sclerosis).
Conditions combining a bilateral pyramidal syndrome with limb and
bulbar amyotrophy. Brain. *113*, 347-363.

Benard, V., Bohl, B.P., and Bokoch, G.M. (1999). Characterization of rac and
cdc42 activation in chemoattractant-stimulated human neutrophils using a
novel assay for active GTPases. J Biol Chem *274*, 13198-13204.

Bendotti, C., and Carri, M.T. (2004). Lessons from models of SOD1-linked
familial ALS. Trends Mol Med *10*, 393-400.

Bernstein, B.W., DeWit, M., and Bamburg, J.R. (1998). Actin disassembles reversibly during electrically induced recycling of synaptic vesicles in cultured neurons. Brain Res Mol Brain Res *53*, 236-251.

Bevan, A.P., Drake, P.G., Bergeron, J.J., and Posner, B.I. (1996). Intracellular signal transduction: The role of endosomes. Trends in Endocrinology and Metabolism *7*, 13-21.

Bischoff, F.R., and Ponstingl, H. (1991). Catalysis of guanine nucleotide exchange on Ran by the mitotic regulator RCC1. Nature. *354*, 80-82.

Blakesley, V.A., Kato, H., Roberts, C.T., Jr., and LeRoith, D. (1995). Mutation of a conserved amino acid residue (tryptophan 1173) in the tyrosine kinase domain of the IGF-I receptor abolishes autophosphorylation but does not eliminate biologic function. J Biol Chem *270*, 2764-2769.

Bohn, M.C. (2004). Motoneurons crave glial cell line-derived neurotrophic factor. Exp Neurol *190*, 263-275.

Boillee, S., and Cleveland, D.W. (2004). Gene therapy for ALS delivers. Trends Neurosci *27*, 235-238.

Bokoch, G.M., and Diebold, B.A. (2002). Current molecular models for NADPH oxidase regulation by Rac GTPase. Blood *100*, 2692-2696.

Bolis, A., Corbetta, S., Cioce, A., and de Curtis, I. (2003). Differential distribution of Rac1 and Rac3 GTPases in the developing mouse brain: implications for a role of Rac3 in Purkinje cell differentiation. Eur J Neurosci *18*, 2417-2424.

Bonhoeffer, T., and Yuste, R. (2002). Spine motility. Phenomenology, mechanisms, and function. Neuron *35*, 1019-1027.

Brown, L., and Baer, R. (1994). HEN1 encodes a 20-kilodalton phosphoprotein that binds an extended E-box motif as a homodimer. Mol Cell Biol *14*, 1245-1255.

Brown, R.H., Jr. (1995). Amyotrophic lateral sclerosis: recent insights from genetics and transgenic mice. Cell *80*, 687-692.

Brown, R.H., Jr. (2001). Amyotrophic lateral sclerosis and other motor neuron diseases. In: Harrison's Principles of Internal Medicine, eds. E. Braunwald, A.S. Fauci, D.L. Kasper, S.L. Hauser, D.L. Longo, and J.L. Jamerson, New York: McGraw-Hill, 2412-2416.

Brudno, M., Do, C.B., Cooper, G.M., Kim, M.F., Davydov, E., Green, E.D., Sidow, A., and Batzoglou, S. (2003). LAGAN and Multi-LAGAN: efficient tools for large-scale multiple alignment of genomic DNA. Genome Res *13*, 721-731.

Brugnera, E., Haney, L., Grimsley, C., Lu, M., Walk, S.F., Tosello-Trampont, A.C., Macara, I.G., Madhani, H., Fink, G.R., and Ravichandran, K.S. (2002). Unconventional Rac-GEF activity is mediated through the Dock180-ELMO complex. Nat Cell Biol *4*, 574-582.

Bruijn, L.I., Miller, T.M., and Cleveland, D.W. (2004). Unraveling the mechanisms involved in motor neuron degeneration in ALS. Annu Rev Neurosci *27*, 723-749.

Bucci, C., Parton, R.G., Mather, I.H., Stunnenberg, H., Simons, K., Hoflack, B., and Zerial, M. (1992). The small GTPase rab5 functions as a regulatory factor in the early endocytic pathway. Cell *70*, 715-728.

Burd, C.G., Peterson, M., Cowles, C.R., and Emr, S.D. (1997). A novel Sec18p/NSF-dependent complex required for Golgi-to-endosome transport in yeast. Mol Biol Cell *8*, 1089-1104.

Butler, A.A., Yakar, S., Gewolb, I.H., Karas, M., Okubo, Y., and LeRoith, D. (1998). Insulin-like growth factor-I receptor signal transduction: at the interface between physiology and cell biology. Comp Biochem Physiol B Biochem Mol Biol *121*, 19-26.

Carroll, R.C., Beattie, E.C., Xia, H., Luscher, C., Altschuler, Y., Nicoll, R.A., Malenka, R.C., and von Zastrow, M. (1999a). Dynamin-dependent endocytosis of ionotropic glutamate receptors. Proc Natl Acad Sci U S A *96*, 14112-14117.

Carroll, R.C., Lissin, D.V., von Zastrow, M., Nicoll, R.A., and Malenka, R.C. (1999b). Rapid redistribution of glutamate receptors contributes to long-term depression in hippocampal cultures. Nat Neurosci *2*, 454-460.

Cavalli, V., Corti, M., and Gruenberg, J. (2001). Endocytosis and signaling cascades: a close encounter. FEBS Lett *498*, 190-196.

Ceresa, B.P., and Schmid, S.L. (2000). Regulation of signal transduction by endocytosis. Curr Opin Cell Biol *12*, 204-210.

Chance, P.F., Rabin, B.A., Ryan, S.G., Ding, Y., Scavina, M., Crain, B., Griffin, J.W., and Cornblath, D.R. (1998). Linkage of the gene for an autosomal dominant form of juvenile amyotrophic lateral sclerosis to chromosome 9q34. Am J Hum Genet *62*, 633-640.

Chao, M.V. (2003). Neurotrophins and their receptors: a convergence point for may signaling pathways. Nat Rev Neurosci *4*, 299-309.

Chow, J.C., Condorelli, G., and Smith, R.J. (1998). Insulin-like growth factor-I receptor internalization regulates signaling via the Shc/mitogen-activated protein kinase pathway, but not the insulin receptor substrate-1 pathway. J Biol Chem *273*, 4672-4680.

Christoforidis, S., McBride, H.M., Burgoyne, R.D., and Zerial, M. (1999a). The Rab5 effector EEA1 is a core component of endosome docking. Nature *397*, 621-625.

Christoforidis, S., Miaczynska, M., Ashman, K., Wilm, M., Zhao, L., Yip, S.C., Waterfield, M.D., Backer, J.M., and Zerial, M. (1999b). Phosphatidylinositol-3-OH kinases are Rab5 effectors. Nat Cell Biol *1*, 249-252.

Clague, M.J., and Urbe, S. (2001). The interface of receptor trafficking and signalling. J Cell Sci *114*, 3075-3081.

Cleveland, D.W., and Rothstein, J.D. (2001). From Charcot to Lou Gehrig: deciphering selective motor neuron death in ALS. Nat Rev Neurosci *2*, 806-819.

Cluskey, S., and Ramsden, D.B. (2001). Mechanisms of neurodegeneration in amyotrophic lateral sclerosis. Mol Pathol *54*, 386-392.

Cole, N., and Siddique, T. (1999). Genetic disorders of motor neurons. Semin Neurol *19*, 407-418.

Colicos, M.A., Collins, B.E., Sailor, M.J., and Goda, Y. (2001). Remodeling of synaptic actin induced by photoconductive stimulation. Cell *107*, 605-616.

Collard, J.F., Cote, F., and Julien, J.P. (1995). Defective axonal transport in a transgenic mouse model of amyotrophic lateral sclerosis. Nature *375*, 61-64.

Condorelli, G., Bueno, R., and Smith, R.J. (1994). Two alternatively spliced forms of the human insulin-like growth factor I receptor have distinct biological activities and internalization kinetics. J Biol Chem *269*, 8510-8516.

Conibear, E., and Stevens, T.H. (1998). Multiple sorting pathways between the late Golgi and the vacuole in yeast. Biochim Biophys Acta *1404*, 211-230.

Cote, F., Collard, J.F., and Julien, J.P. (1993). Progressive neuronopathy in transgenic mice expressing the human neurofilament heavy gene: a mouse model of amyotrophic lateral sclerosis. Cell *73*, 35-46.

Couillard-Despres, S., Zhu, Q., Wong, P.C., Price, D.L., Cleveland, D.W., and Julien, J.P. (1998). Protective effect of neurofilament heavy gene overexpression in motor neuron disease induced by mutant superoxide dismutase. Proc Natl Acad Sci U S A *95*, 9626-9630.

Cuff, J.A., Clamp, M.E., Siddiqui, A.S., Finlay, M., and Barton, G.J. (1998). JPred: a consensus secondary structure prediction server. Bioinformatics *14*, 892-893.

D'Mello, S.R., Borodezt, K., and Soltoff, S.P. (1997). Insulin-like growth factor and potassium depolarization maintain neuronal survival by distinct pathways: possible involvement of PI 3-kinase in IGF-1 signaling. J Neurosci *17*, 1548-1560.

Dailey, M.E., and Smith, S.J. (1996). The dynamics of dendritic structure in developing hippocampal slices. J Neurosci *16*, 2983-2994.

Dale, L.B., Bhattacharya, M., Seachrist, J.L., Anborgh, P.H., and Ferguson, S.S. (2001). Agonist-stimulated and tonic internalization of metabotropic glutamate receptor 1a in human embryonic kidney 293 cells: agonist-stimulated endocytosis is beta-arrestin1 isoform-specific. Mol Pharmacol *60*, 1243-1253.

Davies, B.A., Topp, J.D., Sfeir, A.J., Katzmann, D.J., Carney, D.S., Tall, G.G., Friedberg, A.S., Deng, L., Chen, Z., and Horazdovsky, B.F. (2003). Vps9p CUE domain ubiquitin binding is required for efficient endocytic protein traffic. J Biol Chem *278*, 19826-19833.

De Camilli, P., Emr, S.D., McPherson, P.S., and Novick, P. (1996). Phosphoinositides as regulators in membrane traffic. Science *271*, 1533-1539.

Deloche, O., Yeung, B.G., Payne, G.S., and Schekman, R. (2001). Vps10p transport from the trans-Golgi network to the endosome is mediated by clathrin-coated vesicles. Mol Biol Cell *12*, 475-485.

Delprato, A., Merithew, E., and Lambright, D.G. (2004). Structure, exchange determinants, and family-wide rab specificity of the tandem helical bundle and Vps9 domains of Rabex-5. Cell *118*, 607-617.

Denny, P., Swift, S., Connor, F., and Ashworth, A. (1992). An SRY-related gene expressed during spermatogenesis in the mouse encodes a sequence-specific DNA-binding protein. Embo J *11*, 3705-3712.

Devon, R.S., Helm, J.R., Rouleau, G.A., Leitner, Y., Lerman-Sagie, T., Lev, D., and Hayden, M.R. (2003). The first nonsense mutation in alsin results in a homogeneous phenotype of infantile-onset ascending spastic paralysis with bulbar involvement in two siblings. Clin Genet *64*, 210-215.

Devon, R.S., Schwab, C., Topp, J.D., Orban, P.C., Yang, Y.Z., Pape, T.D., Helm, J.R., Davidson, T.L., Rogers, D.A., Gros-Louis, F., Rouleau, G., Horazdovsky, B.F., Leavitt, B.R., and Hayden, M.R. (2005). Cross-species characterization of the ALS2 gene and analysis of its pattern of expression in development and adulthood. Neurobiol Dis *18*, 243-257.

Di Fiore, P.P., and De Camilli, P. (2001). Endocytosis and signaling. an inseparable partnership. Cell *106*, 1-4.

Dobrossy, L., Pavelic, Z.P., Vaughan, M., Porter, N., and Bernacki, R.J. (1980). Elevation of lysosomal enzymes in primary Lewis lung tumor correlated with the initiation of metastasis. Cancer Res *40*, 3281-3285.

Doray, B., Ghosh, P., Griffith, J., Geuze, H.J., and Kornfeld, S. (2002). Cooperation of GGAs and AP-1 in packaging MPRs at the trans-Golgi network. Science *297*, 1700-1703.

Dore, S., Kar, S., and Quirion, R. (1997). Rediscovering an old friend, IGF-I: potential use in the treatment of neurodegenerative diseases. Trends Neurosci *20*, 326-331.

Dore, S., Krieger, C., Kar, S., and Quirion, R. (1996). Distribution and levels of insulin-like growth factor (IGF-I and IGF-II) and insulin receptor binding sites in the spinal cords of amyotrophic lateral sclerosis (ALS) patients. Brain Res Mol Brain Res *41*, 128-133.

Dudek, H., Datta, S.R., Franke, T.F., Birnbaum, M.J., Yao, R., Cooper, G.M., Segal, R.A., Kaplan, D.R., and Greenberg, M.E. (1997). Regulation of neuronal survival by the serine-threonine protein kinase Akt. Science *275*, 661-665.

Ehlers, M.D. (2000). Reinsertion or degradation of AMPA receptors determined by activity-dependent endocytic sorting. Neuron *28*, 511-525.

Esters, H., Alexandrov, K., Constantinescu, A.T., Goody, R.S., and Scheidig, A.J. (2000). High-resolution crystal structure of S. cerevisiae Ypt51(DeltaC15)-GppNHp, a small GTP-binding protein involved in regulation of endocytosis. J Mol Biol *298*, 111-121.

Eymard-Pierre, E., Lesca, G., Dollet, S., Santorelli, F.M., di Capua, M., Bertini, E., and Boespflug-Tanguy, O. (2002). Infantile-onset ascending hereditary spastic paralysis is associated with mutations in the alsin gene. Am J Hum Genet *71*, 518-527.

Fang, P., Hwa, V., and Rosenfeld, R. (2004). IGFBPs and cancer. Novartis Found Symp *262*, 215-230; discussion 230-214, 265-218.

Fiala, J.C., Feinberg, M., Popov, V., and Harris, K.M. (1998). Synaptogenesis via dendritic filopodia in developing hippocampal area CA1. J Neurosci *18*, 8900-8911.

Forbes, B.E., Hartfield, P.J., McNeil, K.A., Surinya, K.H., Milner, S.J., Cosgrove, L.J., and Wallace, J.C. (2002). Characteristics of binding of insulin-like growth factor (IGF)-I and IGF-II analogues to the type 1 IGF receptor determined by BIAcore analysis. Eur J Biochem *269*, 961-968.

Foti, M., Moukil, M.A., Dudognon, P., and Carpentier, J.L. (2004). Insulin and IGF-1 receptor trafficking and signalling. Novartis Found Symp *262*, 125-141; discussion 141-127, 265-128.

Fourgeaud, L., Bessis, A.S., Rossignol, F., Pin, J.P., Olivo-Marin, J.C., and Hemar, A. (2003). The metabotropic glutamate receptor mGluR5 is endocytosed by a clathrin-independent pathway. J Biol Chem *278*, 12222-12230.

Gabel, C.A., Goldberg, D.E., and Kornfeld, S. (1983). Identification and characterization of cells deficient in the mannose 6-phosphate receptor: evidence for an alternate pathway for lysosomal enzyme targeting. Proc Natl Acad Sci U S A *80*, 775-779.

Gallo, G., and Letourneau, P.C. (2000). Neurotrophins and the dynamic regulation of the neuronal cytoskeleton. J Neurobiol *44*, 159-173.

Gascon, G.G., Chavis, P., Yaghmour, A., Stigsby, B., Shums, A., Ozand, P., and Siddique, T. (1995). Familial childhood primary lateral sclerosis with associated gaze paresis. Neuropediatrics *26*, 313-319.

Gerard, R.D. and Meidell, R.S. (1995). Adenoviral vectors. In: DNA cloning: a practical approach, ed. B.D. Hames and D.M. Glover, Oxford: Oxford University Press.

Gerrard, S.R., Bryant, N.J., and Stevens, T.H. (2000). VPS21 controls entry of endocytosed and biosynthetic proteins into the yeast prevacuolar compartment. Mol Biol Cell *11*, 613-626.

Ghosh, P., Dahms, N.M., and Kornfeld, S. (2003). Mannose 6-phosphate receptors: new twists in the tale. Nat Rev Mol Cell Biol *4*, 202-212.

Gillooly, D.J., Morrow, I.C., Lindsay, M., Gould, R., Bryant, N.J., Gaullier, J.M., Parton, R.G., and Stenmark, H. (2000). Localization of phosphatidylinositol 3-phosphate in yeast and mammalian cells. Embo J *19*, 4577-4588.

Ginty, D.D., and Segal, R.A. (2002). Retrograde neurotrophin signaling: Trk-ing along the axon. Curr Opin Neurobiol *12*, 268-274.

Glauman, H., and Ballard, F. (1987). Lysosomes: their role in protein breakdown. Academic Press: New York.

Goldowitz, D., and Hamre, K. (1998). The cells and molecules that make a cerebellum. Trends Neurosci *21*, 375-382.

Gomez-Foix, A.M., Coats, W.S., Baque, S., Alam, T., Gerard, R.D., and Newgard, C.B. (1992). Adenovirus-mediated transfer of the muscle glycogen phosphorylase gene into hepatocytes confers altered regulation of glycogen metabolism. J Biol Chem *267*, 25129-25134.

Gordon, P.H. (2005). Advances in clinical trials for amyotrophic lateral sclerosis. Curr Neurol Neurosci Rep *5*, 48-54.

Gorvel, J.P., Chavrier, P., Zerial, M., and Gruenberg, J. (1991). rab5 controls early endosome fusion in vitro. Cell *64*, 915-925.

Gournier, H., Stenmark, H., Rybin, V., Lippe, R., and Zerial, M. (1998). Two distinct effectors of the small GTPase Rab5 cooperate in endocytic membrane fusion. Embo J *17*, 1930-1940.

Gray, N.W., Fourgeaud, L., Huang, B., Chen, J., Cao, H., Oswald, B.J., Hemar, A., and McNiven, M.A. (2003). Dynamin 3 Is a Component of the Postsynapse, Where it Interacts with mGluR5 and Homer. Curr Biol *13*, 510-515.

Grimes, M.L., and Miettinen, H.M. (2003). Receptor tyrosine kinase and G-protein coupled receptor signaling and sorting within endosomes. J Neurochem *84*, 905-918.

Gros-Louis, F., Meijer, I.A., Hand, C.K., Dube, M.P., MacGregor, D.L., Seni, M.H., Devon, R.S., Hayden, M.R., Andermann, F., Andermann, E., and Rouleau, G.A. (2003). An ALS2 gene mutation causes hereditary spastic paraplegia in a Pakistani kindred. Ann Neurol *53*, 144-145.

Guegan, C., Vila, M., Rosoklija, G., Hays, A.P., and Przedborski, S. (2001). Recruitment of the mitochondrial-dependent apoptotic pathway in amyotrophic lateral sclerosis. J Neurosci *21*, 6569-6576.

Haataja, L., Kaartinen, V., Groffen, J., and Heisterkamp, N. (2002). The small GTPase Rac3 interacts with the integrin-binding protein CIB and promotes integrin alpha(IIb)beta(3)-mediated adhesion and spreading. J Biol Chem *277*, 8321-8328.

Hadano, S., Hand, C.K., Osuga, H., Yanagisawa, Y., Otomo, A., Devon, R.S., Miyamoto, N., Showguchi-Miyata, J., Okada, Y., Singaraja, R., Figlewicz, D.A., Kwiatkowski, T., Hosler, B.A., Sagie, T., Skaug, J., Nasir, J., Brown, R.H., Jr., Scherer, S.W., Rouleau, G.A., Hayden, M.R., and Ikeda, J.E. (2001). A gene encoding a putative GTPase regulator is mutated in familial amyotrophic lateral sclerosis 2. Nat Genet *29*, 166-173.

Hafezparast, M., Klocke, R., Ruhrberg, C., Marquardt, A., Ahmad-Annuar, A., Bowen, S., Lalli, G., Witherden, A.S., Hummerich, H., Nicholson, S., Morgan, P.J., Oozageer, R., Priestley, J.V., Averill, S., King, V.R., Ball, S., Peters, J., Toda, T., Yamamoto, A., Hiraoka, Y., Augustin, M., Korthaus, D., Wattler, S., Wabnitz, P., Dickneite, C., Lampel, S., Boehme, F., Peraus, G., Popp, A., Rudelius, M., Schlegel, J., Fuchs, H., Hrabe de Angelis, M., Schiavo, G., Shima, D.T., Russ, A.P., Stumm, G., Martin, J.E., and Fisher, E.M. (2003). Mutations in dynein link motor neuron degeneration to defects in retrograde transport. Science *300*, 808-812.

Hall, A. (1998). Rho GTPases and the actin cytoskeleton. Science *279*, 509-514.

Hama, H., Tall, G.G., and Horazdovsky, B.F. (1999). Vps9p Is a Guanine Nucleotide Exchange Factor Involved in Vesicle-Mediated Vacuolar Protein Transport. J. Biol. Chem. *274*, 15284-15291.

Hand, C.K., and Rouleau, G.A. (2002). Familial amyotrophic lateral sclerosis. Muscle Nerve *25*, 135-159.

Hannon, G.J., Demetrick, D., and Beach, D. (1993). Isolation of the Rb-related p130 through its interaction with CDK2 and cyclins. Genes Dev *7*, 2378-2391.

Hart, M.J., Eva, A., Zangrilli, D., Aaronson, S.A., Evans, T., Cerione, R.A., and Zheng, Y. (1994). Cellular transformation and guanine nucleotide exchange activity are catalyzed by a common domain on the dbl oncogene product. J Biol Chem *269*, 62-65.

Heath, P.R., and Shaw, P.J. (2002). Update on the glutamatergic neurotransmitter system and the role of excitotoxicity in amyotrophic lateral sclerosis. Muscle Nerve *26*, 438-458.

Henley, J.R., Krueger, E.W., Oswald, B.J., and McNiven, M.A. (1998). Dynamin-mediated internalization of caveolae. J Cell Biol *141*, 85-99.

Hentati, A., Bejaoui, K., Pericak Vance, M.A., Hentati, F., Speer, M.C., Hung, W.Y., Figlewicz, D.A., Haines, J., Rimmler, J., and Ben Hamida, C. (1994). Linkage of recessive familial amyotrophic lateral sclerosis to chromosome 2q33-q35. Nat Genet *7*, 425-428.

Hentati, A., Ouahchi, K., Pericak Vance, M.A., Nijhawan, D., Ahmad, A., Yang, Y., Rimmler, J., Hung, W., Schlotter, B., Ahmed, A., Ben Hamida, M., Hentati, F., and Siddique, T. (1998). Linkage of a commoner form of recessive amyotrophic lateral sclerosis to chromosome 15q15-q22 markers. Neurogenetics *2*, 55-60.

Hirai, H., and Launey, T. (2000). The regulatory connection between the activity of granule cell NMDA receptors and dendritic differentiation of cerebellar Purkinje cells. J Neurosci *20*, 5217-5224.

Hirst, J., Lui, W.W., Bright, N.A., Totty, N., Seaman, M.N., and Robinson, M.S. (2000). A family of proteins with gamma-adaptin and VHS domains that facilitate trafficking between the trans-Golgi network and the vacuole/lysosome. J Cell Biol *149*, 67-80.

Hitzler, J.K., Soares, H.D., Drolet, D.W., Inaba, T., O'Connel, S., Rosenfeld, M.G., Morgan, J.I., and Look, A.T. (1999). Expression patterns of the hepatic leukemia factor gene in the nervous system of developing and adult mice. Brain Res *820*, 1-11.

Hollenberg, S.M., Sternglanz, R., Cheng, P.F., and Weintraub, H. (1995). Identification of a new family of tissue-specific basic helix-loop-helix proteins with a two-hybrid system. Mol Cell Biol *15*, 3813-3822.

Holly, J. (2004). Physiology of the IGF system. Novartis Found Symp *262*, 19-26; discussion 26-35, 265-268.

Holmes, S.E., O'Hearn, E., Rosenblatt, A., Callahan, C., Hwang, H.S., Ingersoll-Ashworth, R.G., Fleisher, A., Stevanin, G., Brice, A., Potter, N.T., Ross, C.A., and Margolis, R.L. (2001). A repeat expansion in the gene encoding junctophilin-3 is associated with Huntington disease-like 2. Nat Genet *29*, 377-378.

Hong, S., Brooks, B., and Hung, W. (1998). X-linked dominant locus for late-onset familial amyotrophic lateral sclerosis. Soc Neurosci Abst *24*, 478.

Honing, S., Sosa, M., Hille-Rehfeld, A., and von Figura, K. (1997). The 46-kDa mannose 6-phosphate receptor contains multiple binding sites for clathrin adaptors. J Biol Chem *272*, 19884-19890.

Horazdovsky, B.F., Busch, G.R., and Emr, S.D. (1994). VPS21 encodes a rab5-like GTP binding protein that is required for the sorting of yeast vacuolar proteins. Embo J *13*, 1297-1309.

Horiuchi, H., Lippe, R., McBride, H.M., Rubino, M., Woodman, P., Stenmark, H., Rybin, V., Wilm, M., Ashman, K., Mann, M., and Zerial, M. (1997). A novel Rab5 GDP/GTP exchange factor complexed to Rabaptin-5 links nucleotide exchange to effector recruitment and function. Cell *90*, 1149-1159.

Hosler, B.A., Siddique, T., Sapp, P.C., Sailor, W., Huang, M.C., Hossain, A., Daube, J.R., Nance, M., Fan, C., Kaplan, J., Hung, W.Y., McKenna Yasek, D., Haines, J.L., Pericak Vance, M.A., Horvitz, H.R., and Brown, R.H. (2000). Linkage of familial amyotrophic lateral sclerosis with frontotemporal dementia to chromosome 9q21-q22. JAMA *284*, 1664-1669.

Howe, C.L., and Mobley, W.C. (2005). Long-distance retrograde neurotrophic signaling. Curr Opin Neurobiol *15*, 40-48.

Howe, C.L., Valletta, J.S., Rusnak, A.S., and Mobley, W.C. (2001). NGF signaling from clathrin-coated vesicles: evidence that signaling endosomes serve as a platform for the Ras-MAPK pathway. Neuron *32*, 801-814.

Huang, E.J., and Reichardt, L.F. (2003). Trk receptors: roles in neuronal signal transduction. Annu Rev Biochem *72*, 609-642.

Hunyady, L., Baukal, A.J., Gaborik, Z., Olivares-Reyes, J.A., Bor, M., Szaszak, M., Lodge, R., Catt, K.J., and Balla, T. (2002). Differential PI 3-kinase dependence of early and late phases of recycling of the internalized AT1 angiotensin receptor. J Cell Biol *157*, 1211-1222.

Huttner, W.B., Schiebler, W., Greengard, P., and De Camilli, P. (1983). Synapsin I (protein I), a nerve terminal-specific phosphoprotein. III. Its association with synaptic vesicles studied in a highly purified synaptic vesicle preparation. J Cell Biol *96*, 1374-1388.

Johnson, K.F., and Kornfeld, S. (1992). The cytoplasmic tail of the mannose 6-phosphate/insulin-like growth factor-II receptor has two signals for lysosomal enzyme sorting in the Golgi. J Cell Biol *119*, 249-257.

Jones, E.W. (1977). Proteinase mutants of Saccharomyces cerevisiae. Genetics *85*, 23-33.

Julien, J.P. (2001). Amyotrophic lateral sclerosis. unfolding the toxicity of the misfolded. Cell *104*, 581-591.

Kaaks, R. (2004). Nutrition, insulin, IGF-1 metabolism and cancer risk: a summary of epidemiological evidence. Novartis Found Symp *262*, 247-260; discussion 260-268.

Kaibuchi, K., Kuroda, S., and Amano, M. (1999). Regulation of the cytoskeleton and cell adhesion by the Rho family GTPases in mammalian cells. Annu Rev Biochem *68*, 459-486.

Kanekura, K., Hashimoto, Y., Kita, Y., Sasabe, J., Aiso, S., Nishimoto, I., and Matsuoka, M. (2005). A Rac1/Phosphatidylinositol 3-Kinase/Akt3 Anti-apoptotic Pathway, Triggered by AlsinLF, the Product of the ALS2 Gene, Antagonizes Cu/Zn-superoxide Dismutase (SOD1) Mutant-induced Motoneuronal Cell Death. J Biol Chem *280*, 4532-4543.

Kaspar, B.K., Llado, J., Sherkat, N., Rothstein, J.D., and Gage, F.H. (2003). Retrograde viral delivery of IGF-1 prolongs survival in a mouse ALS model. Science *301*, 839-842.

Kato, H., Faria, T.N., Stannard, B., Roberts, C.T., Jr., and LeRoith, D. (1993). Role of tyrosine kinase activity in signal transduction by the insulin-like growth factor-I (IGF-I) receptor. Characterization of kinase-deficient IGF-I receptors and the action of an IGF-I-mimetic antibody (alpha IR-3). J Biol Chem *268*, 2655-2661.

Klionsky, D.J., Banta, L.M., and Emr, S.D. (1988). Intracellular sorting and
processing of a yeast vacuolar hydrolase: proteinase A propeptide contains
vacuolar targeting information. Mol Cell Biol *8*, 2105-2116.

Kornfeld, S. (1986). Trafficking of lysosomal enzymes in normal and disease
states. J Clin Invest *77*, 1-6.

Kornfeld, S. (1992). Structure and function of the mannose 6-
phosphate/insulin-like growth factor II receptors. Annu Rev Biochem *61*,
307-330.

Kornfeld, S., and Mellman, I. (1989). The biogenesis of lysosomes. Annu Rev
Cell Biol *5*, 483-525.

Koster, A., Saftig, P., Matzner, U., von Figura, K., Peters, C., and Pohlmann, R.
(1993). Targeted disruption of the M(r) 46,000 mannose 6-phosphate
receptor gene in mice results in misrouting of lysosomal proteins. Embo J
12, 5219-5223.

Kostic, V., Jackson-Lewis, V., de Bilbao, F., Dubois-Dauphin, M., and
Przedborski, S. (1997). Bcl-2: prolonging life in a transgenic mouse model
of familial amyotrophic lateral sclerosis. Science *277*, 559-562.

Kriz, J., Nguyen, M.D., and Julien, J.P. (2002). Minocycline slows disease
progression in a mouse model of amyotrophic lateral sclerosis. Neurobiol
Dis *10*, 268-278.

Lambright, D.G., Sondek, J., Bohm, A., Skiba, N.P., Hamm, H.E., and Sigler, P.B. (1996). The 2.0 A crystal structure of a heterotrimeric G protein. Nature *379*, 311-319.

LaMonte, B.H., Wallace, K.E., Holloway, B.A., Shelly, S.S., Ascano, J., Tokito, M., Van Winkle, T., Howland, D.S., and Holzbaur, E.L. (2002). Disruption of dynein/dynactin inhibits axonal transport in motor neurons causing late-onset progressive degeneration. Neuron *34*, 715-727.

Lanzetti, L., Palamidessi, A., Areces, L., Scita, G., and Di Fiore, P.P. (2004). Rab5 is a signalling GTPase involved in actin remodelling by receptor tyrosine kinases. Nature *429*, 309-314.

Lanzetti, L., Rybin, V., Malabarba, M.G., Christoforidis, S., Scita, G., Zerial, M., and Di Fiore, P.P. (2000). The Eps8 protein coordinates EGF receptor signalling through Rac and trafficking through Rab5. Nature *408*, 374-377.

Leahy, M., Lyons, A., Krause, D., and O'Connor, R. (2004). Impaired Shc, Ras, and MAPK activation but normal Akt activation in FL5.12 cells expressing an insulin-like growth factor I receptor mutated at tyrosines 1250 and 1251. J Biol Chem *279*, 18306-18313.

Leavitt, B.R. (2002). Hereditary motor neuron disease caused by mutations in the ALS2 gene: the long and the short of it. Clin Genet *62*, 265-269.

Lee, S.H., Liu, L., Wang, Y.T., and Sheng, M. (2002). Clathrin adaptor AP2 and NSF interact with overlapping sites of GluR2 and play distinct roles in AMPA receptor trafficking and hippocampal LTD. Neuron *36*, 661-674.

Lee, S.H., Valtschanoff, J.G., Kharazia, V.N., Weinberg, R., and Sheng, M. (2001). Biochemical and morphological characterization of an intracellular membrane compartment containing AMPA receptors. Neuropharmacology *41*, 680-692.

Leof, E.B. (2000). Growth factor receptor signalling: location, location, location. Trends Cell Biol *10*, 343-348.

Lerman-Sagie, T., Filiano, J., Smith, D.W., and Korson, M. (1996). Infantile onset of hereditary ascending spastic paralysis with bulbar involvement. J Child Neurol *11*, 54-57.

LeRoith, D., and Roberts, C.T., Jr. (2003). The insulin-like growth factor system and cancer. Cancer Lett *195*, 127-137.

Levy, S., and Hannenhalli, S. (2002). Identification of transcription factor binding sites in the human genome sequence. Mamm Genome *13*, 510-514.

Li, M., Ona, V.O., Guegan, C., Chen, M., Jackson-Lewis, V., Andrews, L.J., Olszewski, A.J., Stieg, P.E., Lee, J.P., Przedborski, S., and Friedlander, R.M. (2000). Functional role of caspase-1 and caspase-3 in an ALS transgenic mouse model. Science *288*, 335-339.

Li, Z., Aizenman, C.D., and Cline, H.T. (2002). Regulation of rho GTPases by crosstalk and neuronal activity in vivo. Neuron *33*, 741-750.

Lin, F.T., Daaka, Y., and Lefkowitz, R.J. (1998). beta-arrestins regulate mitogenic signaling and clathrin-mediated endocytosis of the insulin-like growth factor I receptor. J Biol Chem *273*, 31640-31643.

Lin, J.W., Ju, W., Foster, K., Lee, S.H., Ahmadian, G., Wyszynski, M., Wang, Y.T., and Sheng, M. (2000). Distinct molecular mechanisms and divergent endocytic pathways of AMPA receptor internalization. Nat Neurosci *3*, 1282-1290.

Lippe, R., Miaczynska, M., Rybin, V., Runge, A., and Zerial, M. (2001). Functional synergy between Rab5 effector Rabaptin-5 and exchange factor Rabex-5 when physically associated in a complex. Mol Biol Cell *12*, 2219-2228.

Ludolph, A.C., Meyer, T., and Riepe, M.W. (2000). The role of excitotoxicity in ALS--what is the evidence? J Neurol *247 Suppl 1*, I7-16.

Luis Albasanz, J., Fernandez, M., and Martin, M. (2002). Internalization of metabotropic glutamate receptor in C6 cells through clathrin-coated vesicles. Brain Res Mol Brain Res *99*, 54-66.

Luscher, C., Xia, H., Beattie, E.C., Carroll, R.C., von Zastrow, M., Malenka, R.C., and Nicoll, R.A. (1999). Role of AMPA receptor cycling in synaptic transmission and plasticity. Neuron *24*, 649-658.

Luttrell, L.M., van Biesen, T., Hawes, B.E., Koch, W.J., Touhara, K., and
Lefkowitz, R.J. (1995). G beta gamma subunits mediate mitogen-activated
protein kinase activation by the tyrosine kinase insulin-like growth factor
1 receptor. J Biol Chem *270*, 16495-16498.

Makalowski, W., and Boguski, M.S. (1998). Evolutionary parameters of the
transcribed mammalian genome: an analysis of 2,820 orthologous rodent
and human sequences. Proc Natl Acad Sci U S A *95*, 9407-9412.

Man, H.Y., Lin, J.W., Ju, W.H., Ahmadian, G., Liu, L., Becker, L.E., Sheng, M.,
and Wang, Y.T. (2000). Regulation of AMPA receptor-mediated synaptic
transmission by clathrin-dependent receptor internalization. Neuron *25*,
649-662.

Marchler-Bauer, A., Anderson, J.B., DeWeese-Scott, C., Fedorova, N.D., Geer,
L.Y., He, S., Hurwitz, D.I., Jackson, J.D., Jacobs, A.R., Lanczycki, C.J.,
Liebert, C.A., Liu, C., Madej, T., Marchler, G.H., Mazumder, R.,
Nikolskaya, A.N., Panchenko, A.R., Rao, B.S., Shoemaker, B.A.,
Simonyan, V., Song, J.S., Thiessen, P.A., Vasudevan, S., Wang, Y.,
Yamashita, R.A., Yin, J.J., and Bryant, S.H. (2003). CDD: a curated
Entrez database of conserved domain alignments. Nucleic Acids Res *31*,
383-387.

Marcusson, E.G., Horazdovsky, B.F., Cereghino, J.L., Gharakhanian, E., and Emr, S.D. (1994). The sorting receptor for yeast vacuolar carboxypeptidase Y is encoded by the VPS10 gene. Cell *77*, 579-586.

Mattera, R., Arighi, C.N., Lodge, R., Zerial, M., and Bonifacino, J.S. (2003). Divalent interaction of the GGAs with the Rabaptin-5-Rabex-5 complex. Embo J *22*, 78-88.

Mayor, C., Brudno, M., Schwartz, J.R., Poliakov, A., Rubin, E.M., Frazer, K.A., Pachter, L.S., and Dubchak, I. (2000). VISTA: visualizing global DNA sequence alignments of arbitrary length. Bioinformatics *16*, 1046-1047.

McBride, H.M., Rybin, V., Murphy, C., Giner, A., Teasdale, R., and Zerial, M. (1999). Oligomeric complexes link Rab5 effectors with NSF and drive membrane fusion via interactions between EEA1 and syntaxin 13. Cell *98*, 377-386.

McLauchlan, H., Newell, J., Morrice, N., Osborne, A., West, M., and Smythe, E. (1998). A novel role for Rab5-GDI in ligand sequestration into clathrin-coated pits. Curr Biol *8*, 34-45.

McLysaght, A., Enright, A.J., Skrabanek, L., and Wolfe, K.H. (2000). Estimation of synteny conservation and genome compaction between pufferfish (Fugu) and human. Yeast *17*, 22-36.

McPherson, P.S., Kay, B.K., and Hussain, N.K. (2001). Signaling on the endocytic pathway. Traffic *2*, 375-384.

Melikian, H.E., and Buckley, K.M. (1999). Membrane trafficking regulates the activity of the human dopamine transporter. J Neurosci *19*, 7699-7710.

Merithew, E., Hatherly, S., Dumas, J.J., Lawe, D.C., Heller-Harrison, R., and Lambright, D.G. (2001). Structural plasticity of an invariant hydrophobic triad in the switch regions of Rab GTPases is a determinant of effector recognition. J Biol Chem *276*, 13982-13988.

Miaczynska, M., Christoforidis, S., Giner, A., Shevchenko, A., Uttenweiler-Joseph, S., Habermann, B., Wilm, M., Parton, R.G., and Zerial, M. (2004a). APPL proteins link Rab5 to nuclear signal transduction via an endosomal compartment. Cell *116*, 445-456.

Miaczynska, M., Pelkmans, L., and Zerial, M. (2004b). Not just a sink: endosomes in control of signal transduction. Curr Opin Cell Biol *16*, 400-406.

Miles, C., Elgar, G., Coles, E., Kleinjan, D.J., van Heyningen, V., and Hastie, N. (1998). Complete sequencing of the Fugu WAGR region from WT1 to PAX6: dramatic compaction and conservation of synteny with human chromosome 11p13. Proc Natl Acad Sci U S A *95*, 13068-13072.

Miller, J. (1972). Experiments in Molecular Genetics. Cold Spring Harbor Laboratory: Cold Spring Harbor.

Minamisawa, S., Oshikawa, J., Takeshima, H., Hoshijima, M., Wang, Y., Chien, K.R., Ishikawa, Y., and Matsuoka, R. (2004). Junctophilin type 2 is associated with caveolin-3 and is down-regulated in the hypertrophic and dilated cardiomyopathies. Biochem Biophys Res Commun *325*, 852-856.

Mitchem, K.L., Hibbard, E., Beyer, L.A., Bosom, K., Dootz, G.A., Dolan, D.F., Johnson, K.R., Raphael, Y., and Kohrman, D.C. (2002). Mutation of the novel gene Tmie results in sensory cell defects in the inner ear of spinner, a mouse model of human hearing loss DFNB6. Hum Mol Genet *11*, 1887-1898.

Morales, M., Colicos, M.A., and Goda, Y. (2000). Actin-dependent regulation of neurotransmitter release at central synapses. Neuron *27*, 539-550.

Mulder, D.W., Kurland, L.T., Offord, K.P., and Beard, C.M. (1986). Familial adult motor neuron disease: amyotrophic lateral sclerosis. Neurology *36*, 511-517.

Munch, C., Sedlmeier, R., Meyer, T., Homberg, V., Sperfeld, A.D., Kurt, A., Prudlo, J., Peraus, G., Hanemann, C.O., Stumm, G., and Ludolph, A.C. (2004). Point mutations of the p150 subunit of dynactin (DCTN1) gene in ALS. Neurology *63*, 724-726.

Mundell, S.J., Matharu, A.L., Pula, G., Roberts, P.J., and Kelly, E. (2001). Agonist-induced internalization of the metabotropic glutamate receptor 1a is arrestin- and dynamin-dependent. J Neurochem *78*, 546-551.

Murase, S., Mosser, E., and Schuman, E.M. (2002). Depolarization drives beta-Catenin into neuronal spines promoting changes in synaptic structure and function. Neuron *35*, 91-105.

Murzin, A.G. (1992). Structural principles for the propeller assembly of beta-sheets: the preference for seven-fold symmetry. Proteins. *14*, 191-201.

Myers, M.G., Jr., Sun, X.J., and White, M.F. (1994). The IRS-1 signaling system. Trends Biochem Sci *19*, 289-293.

Nicholas, K.B. (1997). GeneDoc: analysis and visualization of genetic variation. EMBNEW.NEWS *4*, 14.

Nielsen, E., Christoforidis, S., Uttenweiler-Joseph, S., Miaczynska, M., Dewitte, F., Wilm, M., Hoflack, B., and Zerial, M. (2000). Rabenosyn-5, a novel Rab5 effector, is complexed with hVPS45 and recruited to endosomes through a FYVE finger domain. J Cell Biol *151*, 601-612.

Nielsen, E., Severin, F., Backer, J.M., Hyman, A.A., and Zerial, M. (1999). Rab5 regulates motility of early endosomes on microtubules. Nat Cell Biol *1*, 376-382.

Nikolic, M., Chou, M.M., Lu, W., Mayer, B.J., and Tsai, L.H. (1998). The p35/Cdk5 kinase is a neuron-specific Rac effector that inhibits Pak1 activity. Nature *395*, 194-198.

Nikolic, M., Dudek, H., Kwon, Y.T., Ramos, Y.F., and Tsai, L.H. (1996). The cdk5/p35 kinase is essential for neurite outgrowth during neuronal differentiation. Genes Dev *10*, 816-825.

Nishiki, T., Nihonmatsu, I., Tsuhara, Y., Kawasaki, M., Sekiguchi, M., Sato, K., Mizoguchi, A., and Takahashi, M. (2001). Distribution of soluble N-ethylmaleimide fusion protein attachment proteins (SNAPs) in the rat nervous system. Neuroscience *107*, 363-371.

Nong, Y., Huang, Y.Q., Ju, W., Kalia, L.V., Ahmadian, G., Wang, Y.T., and Salter, M.W. (2003). Glycine binding primes NMDA receptor internalization. Nature *422*, 302-307.

Otomo, A., Hadano, S., Okada, T., Mizumura, H., Kunita, R., Nishijima, H., Showguchi-Miyata, J., Yanagisawa, Y., Kohiki, E., Suga, E., Yasuda, M., Osuga, H., Nishimoto, T., Narumiya, S., and Ikeda, J.E. (2003). ALS2, a novel guanine nucleotide exchange factor for the small GTPase Rab5, is implicated in endosomal dynamics. Hum Mol Genet *12*, 1671-1687.

Overdier, D.G., Ye, H., Peterson, R.S., Clevidence, D.E., and Costa, R.H. (1997). The winged helix transcriptional activator HFH-3 is expressed in the distal tubules of embryonic and adult mouse kidney. J Biol Chem *272*, 13725-13730.

Palade, G. (1975). Intracellular aspects of the process of protein synthesis. Science *189*, 347-358.

Parrizas, M., Saltiel, A.R., and LeRoith, D. (1997). Insulin-like growth factor 1 inhibits apoptosis using the phosphatidylinositol 3'-kinase and mitogen-activated protein kinase pathways. J Biol Chem *272*, 154-161.

Pasinelli, P., Houseweart, M.K., Brown, R.H., Jr., and Cleveland, D.W. (2000). Caspase-1 and -3 are sequentially activated in motor neuron death in Cu,Zn superoxide dismutase-mediated familial amyotrophic lateral sclerosis. Proc Natl Acad Sci U S A *97*, 13901-13906.

Pesole, G., and Liuni, S. (1999). Internet resources for the functional analysis of 5' and 3' untranslated regions of eukaryotic mRNAs. Trends Genet *15*, 378.

Peterson, M.R., Burd, C.G., and Emr, S.D. (1999). Vac1p coordinates Rab and phosphatidylinositol 3-kinase signaling in Vps45p-dependent vesicle docking/fusion at the endosome. Curr Biol *9*, 159-162.

Pfeffer, S.R. (1994). Rab GTPases: master regulators of membrane trafficking. Curr Opin Cell Biol *6*, 522-526.

Pfeffer, S.R. (2001). Rab GTPases: specifying and deciphering organelle identity and function. Trends Cell Biol *11*, 487-491.

Pierrou, S., Hellqvist, M., Samuelsson, L., Enerbèack, S., and Carlsson, P. (1994). Cloning and characterization of seven human forkhead proteins: binding site specificity and DNA bending. Embo J *13*, 5002-5012.

Pollak, M. (2001). Insulin-like growth factors and prostate cancer. Epidemiol Rev *23*, 59-66.

Poole, A.R., Tiltman, K.J., Recklies, A.D., and Stoker, T.A. (1978). Differences in secretion of the proteinase cathepsin B at the edges of human breast carcinomas and fibroadenomas. Nature *273*, 545-547.

Povsic, T.J., Kohout, T.A., and Lefkowitz, R.J. (2003). Beta-arrestin1 mediates insulin-like growth factor 1 (IGF-1) activation of phosphatidylinositol 3-kinase (PI3K) and anti-apoptosis. J Biol Chem *278*, 51334-51339.

Pramatarova, A., Figlewicz, D.A., Krizus, A., Han, F.Y., Ceballos-Picot, I., Nicole, A., Dib, M., Meininger, V., Brown, R.H., and Rouleau, G.A. (1995). Identification of new mutations in the Cu/Zn superoxide dismutase gene of patients with familial amyotrophic lateral sclerosis. Am J Hum Genet *56*, 592-596.

Pryer, N.K., Wuestehube, L.J., and Schekman, R. (1992). Vesicle-mediated protein sorting. Annu Rev Biochem *61*, 471-516.

Puertollano, R., Aguilar, R.C., Gorshkova, I., Crouch, R.J., and Bonifacino, J.S. (2001). Sorting of mannose 6-phosphate receptors mediated by the GGAs. Science *292*, 1712-1716.

Puig, O., Caspary, F., Rigaut, G., Rutz, B., Bouveret, E., Bragado-Nilsson, E., Wilm, M., and Seraphin, B. (2001). The tandem affinity purification (TAP) method: a general procedure of protein complex purification. Methods *24*, 218-229.

Qualmann, B., Kessels, M.M., and Kelly, R.B. (2000). Molecular links between endocytosis and the actin cytoskeleton. J Cell Biol *150*, F111-116.

Raymond, C.K., Howald-Stevenson, I., Vater, C.A., and Stevens, T.H. (1992). Morphological classification of the yeast vacuolar protein sorting mutants: evidence for a prevacuolar compartment in class E vps mutants. Mol Biol Cell *3*, 1389-1402.

Renault, L., Nassar, N., Vetter, I., Becker, J., Klebe, C., Roth, M., and Wittinghofer, A. (1998). The 1.7 A crystal structure of the regulator of chromosome condensation (RCC1) reveals a seven-bladed propeller. Nature *392*, 97-101.

Riccio, A., Pierchala, B.A., Ciarallo, C.L., and Ginty, D.D. (1997). An NGF-TrkA-mediated retrograde signal to transcription factor CREB in sympathetic neurons. Science *277*, 1097-1100.

Rigaut, G., Shevchenko, A., Rutz, B., Wilm, M., Mann, M., and Seraphin, B. (1999). A generic protein purification method for protein complex characterization and proteome exploration. Nat Biotechnol *17*, 1030-1032.

Roberts, R.L., Barbieri, M.A., Pryse, K.M., Chua, M., Morisaki, J.H., and Stahl, P.D. (1999). Endosome fusion in living cells overexpressing GFP-rab5. J Cell Sci *112 (Pt 21)*, 3667-3675.

Robinson, J.S., Klionsky, D.J., Banta, L.M., and Emr, S.D. (1988). Protein sorting in Saccharomyces cerevisiae: isolation of mutants defective in the delivery and processing of multiple vacuolar hydrolases. Mol Cell Biol *8*, 4936-4948.

Roche, K.W., Standley, S., McCallum, J., Dune Ly, C., Ehlers, M.D., and Wenthold, R.J. (2001). Molecular determinants of NMDA receptor internalization. Nat Neurosci *4*, 794-802.

Rosen, D.R. (1993). Mutations in Cu/Zn superoxide dismutase gene are associated with familial amyotrophic lateral sclerosis. Nature *364*, 362.

Rosen, D.R., Siddique, T., Patterson, D., Figlewicz, D.A., Sapp, P., Hentati, A., Donaldson, D., Goto, J., O'Regan, J.P., Deng, H.X., and et al. (1993). Mutations in Cu/Zn superoxide dismutase gene are associated with familial amyotrophic lateral sclerosis. Nature *362*, 59-62.

Ross, C.A., and Poirier, M.A. (2004). Protein aggregation and neurodegenerative disease. Nat Med *10 Suppl*, S10-17.

Roth, M.G. (2004). Phosphoinositides in constitutive membrane traffic. Physiol Rev *84*, 699-730.

Rothman, J.E., and Orci, L. (1992). Molecular dissection of the secretory pathway. Nature *355*, 409-415.

Rothman, J.H., Howald, I., and Stevens, T.H. (1989). Characterization of genes required for protein sorting and vacuolar function in the yeast Saccharomyces cerevisiae. Embo J *8*, 2057-2065.

Rothman, J.H., and Stevens, T.H. (1986). Protein sorting in yeast: mutants defective in vacuole biogenesis mislocalize vacuolar proteins into the late secretory pathway. Cell *47*, 1041-1051.

Rothstein, J.D., Dykes-Hoberg, M., Pardo, C.A., Bristol, L.A., Jin, L., Kuncl, R.W., Kanai, Y., Hediger, M.A., Wang, Y., Schielke, J.P., and Welty, D.F. (1996). Knockout of glutamate transporters reveals a major role for astroglial transport in excitotoxicity and clearance of glutamate. Neuron *16*, 675-686.

Rothstein, J.D., Van Kammen, M., Levey, A.I., Martin, L.J., and Kuncl, R.W. (1995). Selective loss of glial glutamate transporter GLT-1 in amyotrophic lateral sclerosis. Ann Neurol *38*, 73-84.

Rowland, L.P., and Shneider, N.A. (2001). Amyotrophic lateral sclerosis. N Engl J Med *344*, 1688-1700.

Rubin, G.M., Yandell, M.D., Wortman, J.R., Gabor Miklos, G.L., Nelson, C.R., Hariharan, I.K., Fortini, M.E., Li, P.W., Apweiler, R., Fleischmann, W., Cherry, J.M., Henikoff, S., Skupski, M.P., Misra, S., Ashburner, M., Birney, E., Boguski, M.S., Brody, T., Brokstein, P., Celniker, S.E., Chervitz, S.A., Coates, D., Cravchik, A., Gabrielian, A., Galle, R.F., Gelbart, W.M., George, R.A., Goldstein, L.S., Gong, F., Guan, P., Harris, N.L., Hay, B.A., Hoskins, R.A., Li, J., Li, Z., Hynes, R.O., Jones, S.J., Kuehl, P.M., Lemaitre, B., Littleton, J.T., Morrison, D.K., Mungall, C., O'Farrell, P.H., Pickeral, O.K., Shue, C., Vosshall, L.B., Zhang, J., Zhao, Q., Zheng, X.H., and Lewis, S. (2000). Comparative genomics of the eukaryotes. Science *287*, 2204-2215.

Rubino, M., Miaczynska, M., Lippe, R., and Zerial, M. (2000). Selective membrane recruitment of EEA1 suggests a role in directional transport of clathrin-coated vesicles to early endosomes. J Biol Chem *275*, 3745-3748.

Rukenstein, A., Rydel, R.E., and Greene, L.A. (1991). Multiple agents rescue PC12 cells from serum-free cell death by translation- and transcription-independent mechanisms. J Neurosci *11*, 2552-2563.

Rybin, V., Ullrich, O., Rubino, M., Alexandrov, K., Simon, I., Seabra, M.C., Goody, R., and Zerial, M. (1996). GTPase activity of Rab5 acts as a timer for endocytic membrane fusion. Nature *383*, 266-269.

Sah, V.P., Seasholtz, T.M., Sagi, S.A., and Brown, J.H. (2000). The role of Rho in G protein-coupled receptor signal transduction. Annu Rev Pharmacol Toxicol *40*, 459-489.

Saito, K., Murai, J., Kajiho, H., Kontani, K., Kurosu, H., and Katada, T. (2002). A novel binding protein composed of homophilic tetramer exhibits unique properties for the small GTPase Rab5. J Biol Chem *277*, 3412-3418.

Sander, E.E., van Delft, S., ten Klooster, J.P., Reid, T., van der Kammen, R.A., Michiels, F., and Collard, J.G. (1998). Matrix-dependent Tiam1/Rac signaling in epithelial cells promotes either cell-cell adhesion or cell migration and is regulated by phosphatidylinositol 3-kinase. J Cell Biol *143*, 1385-1398.

Schwaiger, H., Hasilik, A., von Figura, K., Wiemken, A., and Tanner, W. (1982). Carbohydrate-free carboxypeptidase Y is transferred into the lysosome-like yeast vacuole. Biochem Biophys Res Commun *104*, 950-956.

Scita, G., Nordstrom, J., Carbone, R., Tenca, P., Giardina, G., Gutkind, S., Bjarnegard, M., Betsholtz, C., and Di Fiore, P.P. (1999). EPS8 and E3B1 transduce signals from Ras to Rac. Nature *401*, 290-293.

Seabra, M.C., and Wasmeier, C. (2004). Controlling the location and activation of Rab GTPases. Curr Opin Cell Biol *16*, 451-457.

Seachrist, J.L., and Ferguson, S.S. (2003). Regulation of G protein-coupled receptor endocytosis and trafficking by Rab GTPases. Life Sci *74*, 225-235.

Seachrist, J.L., Laporte, S.A., Dale, L.B., Babwah, A.V., Caron, M.G., Anborgh, P.H., and Ferguson, S.S. (2002). Rab5 association with the angiotensin II type 1A receptor promotes Rab5 GTP binding and vesicular fusion. J Biol Chem *277*, 679-685.

Seeburger, J.L., and Springer, J.E. (1993). Experimental rationale for the therapeutic use of neurotrophins in amyotrophic lateral sclerosis. Exp Neurol *124*, 64-72.

Shaw, P.J. (2001). Genetic inroads in familial ALS. Nat Genet *29*, 103-104.

Shaw, P.J., and Eggett, C.J. (2000). Molecular factors underlying selective vulnerability of motor neurons to neurodegeneration in amyotrophic lateral sclerosis. J Neurol *247 Suppl 1*, I17-27.

Sheffield, P., Garrard, S., and Derewenda, Z. (1999). Overcoming expression and purification problems of RhoGDI using a family of "parallel" expression vectors. Protein Expr Purif *15*, 34-39.

Sheng, M., and Pak, D.T. (2000). Ligand-gated ion channel interactions with cytoskeletal and signaling proteins. Annu Rev Physiol *62*, 755-778.

Shinohara, M., Terada, Y., Iwamatsu, A., Shinohara, A., Mochizuki, N., Higuchi, M., Gotoh, Y., Ihara, S., Nagata, S., Itoh, H., Fukui, Y., and Jessberger, R. (2002). SWAP-70 is a guanine-nucleotide-exchange factor that mediates signalling of membrane ruffling. Nature *416*, 759-763.

Shupliakov, O., Bloom, O., Gustafsson, J.S., Kjaerulff, O., Low, P., Tomilin, N., Pieribone, V.A., Greengard, P., and Brodin, L. (2002). Impaired recycling of synaptic vesicles after acute perturbation of the presynaptic actin cytoskeleton. Proc Natl Acad Sci U S A *99*, 14476-14481.

Siddique, T., Figlewicz, D.A., Pericak-Vance, M., Haines, J.L., Rouleau, G., Jeffers, A.J., Sapp, P., Hung, W.-Y., Bebout, J., McKenna-Yasek, D., Deng, G., Horvitz, H.R., Gusella, J.F., Brown, R.H., Jr., and A.D., R. (1991). Linkage of a gene causing familial amyotrophic lateral sclerosis to chromosome 21 and evidence of genetic locus heterogeneity. N Engl J Med *324*, 1381-1384.

Simonsen, A., Lippe, R., Christoforidis, S., Gaullier, J.M., Brech, A., Callaghan, J., Toh, B.H., Murphy, C., Zerial, M., and Stenmark, H. (1998). EEA1 links PI(3)K function to Rab5 regulation of endosome fusion. Nature *394*, 494-498.

Sin, W.C., Haas, K., Ruthazer, E.S., and Cline, H.T. (2002). Dendrite growth increased by visual activity requires NMDA receptor and Rho GTPases. Nature *419*, 475-480.

Sivars, U., Aivazian, D., and Pfeffer, S.R. (2003). Yip3 catalyses the dissociation of endosomal Rab-GDI complexes. Nature *425*, 856-859.

Snyder, E.M., Philpot, B.D., Huber, K.M., Dong, X., Fallon, J.R., and Bear, M.F. (2001). Internalization of ionotropic glutamate receptors in response to mGluR activation. Nat Neurosci *4*, 1079-1085.

Sofroniew, M.V., Howe, C.L., and Mobley, W.C. (2001). Nerve growth factor signaling, neuroprotection, and neural repair. Annu Rev Neurosci *24*, 1217-1281.

Somsel Rodman, J., and Wandinger-Ness, A. (2000). Rab GTPases coordinate endocytosis. J Cell Sci *113 Pt 2*, 183-192.

Sorkin, A., and Von Zastrow, M. (2002). Signal transduction and endocytosis: close encounters of many kinds. Nat Rev Mol Cell Biol *3*, 600-614.

Spaargaren, M., and Bos, J.L. (1999). Rab5 induces Rac-independent lamellipodia formation and cell migration. Mol Biol Cell *10*, 3239-3250.

Sprang, S.R. (1997). G protein mechanisms: insights from structural analysis. Annu Rev Biochem *66*, 639-678.

Stack, J.H., Horazdovsky, B., and Emr, S.D. (1995). Receptor-mediated protein sorting to the vacuole in yeast: roles for a protein kinase, a lipid kinase and GTP-binding proteins. Annu Rev Cell Dev Biol *11*, 1-33.

Stenmark, H., Parton, R.G., Steele-Mortimer, O., Lutcke, A., Gruenberg, J., and Zerial, M. (1994). Inhibition of rab5 GTPase activity stimulates membrane fusion in endocytosis. EMBO J. *13*, 1287-1296.

Stevens, T., Esmon, B., and Schekman, R. (1982). Early stages in the yeast secretory pathway are required for transport of carboxypeptidase Y to the vacuole. Cell *30*, 439-448.

Takeshima, H., Komazaki, S., Nishi, M., Iino, M., and Kangawa, K. (2000). Junctophilins: a novel family of junctional membrane complex proteins. Mol Cell *6*, 11-22.

Tall, G.G., Barbieri, M.A., Stahl, P.D., and Horazdovsky, B.F. (2001). Ras-activated endocytosis is mediated by the Rab5 guanine nucleotide exchange activity of RIN1. Dev Cell *1*, 73-82.

Tall, G.G., Hama, H., DeWald, D.B., and Horazdovsky, B.F. (1999). The phosphatidylinositol 3-phosphate binding protein Vac1p interacts with a Rab GTPase and a Sec1p homologue to facilitate vesicle-mediated vacuolar protein sorting. Mol Biol Cell *10*, 1873-1889.

Tan, T.C., Valova, V.A., Malladi, C.S., Graham, M.E., Berven, L.A., Jupp, O.J., Hansra, G., McClure, S.J., Sarcevic, B., Boadle, R.A., Larsen, M.R., Cousin, M.A., and Robinson, P.J. (2003). Cdk5 is essential for synaptic vesicle endocytosis. Nat Cell Biol *5*, 701-710.

Taroni, F., and DiDonato, S. (2004). Pathways to motor incoordination: the inherited ataxias. Nat Rev Neurosci *5*, 641-655.

Tatsumoto, T., Xie, X., Blumenthal, R., Okamoto, I., and Miki, T. (1999). Human ECT2 is an exchange factor for Rho GTPases, phosphorylated in G2/M phases, and involved in cytokinesis. J Cell Biol *147*, 921-928.

Tatusova, T.A., and Madden, T.L. (1999). BLAST 2 Sequences, a new tool for comparing protein and nucleotide sequences. FEMS Microbiol Lett *174*, 247-250.

Teis, D., and Huber, L.A. (2003). The odd couple: signal transduction and endocytosis. Cell Mol Life Sci *60*, 2020-2033.

Togashi, H., Abe, K., Mizoguchi, A., Takaoka, K., Chisaka, O., and Takeichi, M. (2002). Cadherin regulates dendritic spine morphogenesis. Neuron *35*, 77-89.

Topp, J.D., Gray, N.W., Gerard, R.D., and Horazdovsky, B.F. (2004). Alsin is a Rab5 and Rac1 guanine nucleotide exchange factor. J Biol Chem *279*, 24612-24623.

Torres-Aleman, I., Barrios, V., and Berciano, J. (1998). The peripheral insulin-like growth factor system in amyotrophic lateral sclerosis and in multiple sclerosis. Neurology *50*, 772-776.

Trejo, J.L., Carro, E., Garcia-Galloway, E., and Torres-Aleman, I. (2004). Role of insulin-like growth factor I signaling in neurodegenerative diseases. J Mol Med *82*, 156-162.

Trotti, D., Aoki, M., Pasinelli, P., Berger, U.V., Danbolt, N.C., Brown, R.H., Jr., and Hediger, M.A. (2001). Amyotrophic lateral sclerosis-linked glutamate transporter mutant has impaired glutamate clearance capacity. J Biol Chem *276*, 576-582.

Van Den Bosch, L., Tilkin, P., Lemmens, G., and Robberecht, W. (2002). Minocycline delays disease onset and mortality in a transgenic model of ALS. Neuroreport *13*, 1067-1070.

Vieira, A.V., Lamaze, C., and Schmid, S.L. (1996). Control of EGF receptor signaling by clathrin-mediated endocytosis. Science *274*, 2086-2089.

Vincent, A.M., and Feldman, E.L. (2002). Control of cell survival by IGF signaling pathways. Growth Horm IGF Res *12*, 193-197.

Vincent, A.M., Mobley, B.C., Hiller, A., and Feldman, E.L. (2004). IGF-I prevents glutamate-induced motor neuron programmed cell death. Neurobiol Dis *16*, 407-416.

Voogd, J., and Glickstein, M. (1998). The anatomy of the cerebellum. Trends Neurosci *21*, 370-375.

Vukosavic, S., Stefanis, L., Jackson-Lewis, V., Guegan, C., Romero, N., Chen, C., Dubois-Dauphin, M., and Przedborski, S. (2000). Delaying caspase activation by Bcl-2: A clue to disease retardation in a transgenic mouse model of amyotrophic lateral sclerosis. J Neurosci *20*, 9119-9125.

Wada, Y., Ohsumi, Y., and Anraku, Y. (1992). Genes for directing vacuolar morphogenesis in Saccharomyces cerevisiae. I. Isolation and characterization of two classes of vam mutants. J Biol Chem *267*, 18665-18670.

Wall, M.A., Coleman, D.E., Lee, E., Iñiguez-Lluhi, J.A., Posner, B.A., Gilman, A.G., and Sprang, S.R. (1995). The structure of the G protein Heterotrimer $G_{i\alpha1}\beta_{1\gamma s}$. Cell *83*, 1047-1058.

Wang, L.J., Lu, Y.Y., Muramatsu, S., Ikeguchi, K., Fujimoto, K., Okada, T., Mizukami, H., Matsushita, T., Hanazono, Y., Kume, A., Nagatsu, T., Ozawa, K., and Nakano, I. (2002). Neuroprotective effects of glial cell line-derived neurotrophic factor mediated by an adeno-associated virus vector in a transgenic animal model of amyotrophic lateral sclerosis. J Neurosci *22*, 6920-6928.

Wang, Y.T., and Linden, D.J. (2000). Expression of cerebellar long-term depression requires postsynaptic clathrin-mediated endocytosis. Neuron *25*, 635-647.

Watson, F.L., Heerssen, H.M., Bhattacharyya, A., Klesse, L., Lin, M.Z., and Segal, R.A. (2001). Neurotrophins use the Erk5 pathway to mediate a retrograde survival response. Nat Neurosci *4*, 981-988.

Watson, F.L., Heerssen, H.M., Moheban, D.B., Lin, M.Z., Sauvageot, C.M., Bhattacharyya, A., Pomeroy, S.L., and Segal, R.A. (1999). Rapid nuclear responses to target-derived neurotrophins require retrograde transport of ligand-receptor complex. J Neurosci *19*, 7889-7900.

Welch, H.C., Coadwell, W.J., Ellson, C.D., Ferguson, G.J., Andrews, S.R., Erdjument-Bromage, H., Tempst, P., Hawkins, P.T., and Stephens, L.R. (2002). P-Rex1, a PtdIns(3,4,5)P3- and Gbetagamma-regulated guanine-nucleotide exchange factor for Rac. Cell *108*, 809-821.

Welch, H.C., Coadwell, W.J., Stephens, L.R., and Hawkins, P.T. (2003). Phosphoinositide 3-kinase-dependent activation of Rac. FEBS Lett *546*, 93-97.

Wenk, M.R., and De Camilli, P. (2004). Protein-lipid interactions and phosphoinositide metabolism in membrane traffic: insights from vesicle recycling in nerve terminals. Proc Natl Acad Sci U S A *101*, 8262-8269.

Wiley, H.S., and Burke, P.M. (2001). Regulation of receptor tyrosine kinase signaling by endocytic trafficking. Traffic *2*, 12-18.

Williamson, T.L., and Cleveland, D.W. (1999). Slowing of axonal transport is a very early event in the toxicity of ALS-linked SOD1 mutants to motor neurons. Nat Neurosci *2*, 50-56.

Winther, J.R., Stevens, T.H., and Kielland-Brandt, M.C. (1991). Yeast carboxypeptidase Y requires glycosylation for efficient intracellular transport, but not for vacuolar sorting, in vivo stability, or activity. Eur J Biochem *197*, 681-689.

Wray, G.A., Levinton, J.S., and Shapiro, L.H. (1996). Molecular evidence for deep Precambrian divergences among metazoan phyla. Science *274*, 568-573.

Xiao, G.H., Shoarinejad, F., Jin, F., Golemis, E.A., and Yeung, R.S. (1997). The tuberous sclerosis 2 gene product, tuberin, functions as a Rab5 GTPase activating protein (GAP) in modulating endocytosis. J Biol Chem *272*, 6097-6100.

Xiao, M.Y., Zhou, Q., and Nicoll, R.A. (2001). Metabotropic glutamate receptor activation causes a rapid redistribution of AMPA receptors. Neuropharmacology *41*, 664-671.

Yamanaka, K., Vande Velde, C., Eymard-Pierre, E., Bertini, E., Boespflug-Tanguy, O., and Cleveland, D.W. (2003). Unstable mutants in the peripheral endosomal membrane component ALS2 cause early-onset motor neuron disease. Proc Natl Acad Sci U S A *100*, 16041-16046.

Yang, Y., Hentati, A., Deng, H.X., Dabbagh, O., Sasaki, T., Hirano, M., Hung, W.Y., Ouahchi, K., Yan, J., Azim, A.C., Cole, N., Gascon, G., Yagmour, A., Ben Hamida, M., Pericak Vance, M., Hentati, F., and Siddique, T. (2001). The gene encoding alsin, a protein with three guanine-nucleotide exchange factor domains, is mutated in a form of recessive amyotrophic lateral sclerosis. Nat Genet *29*, 160-165.

Yarden, Y., and Sliwkowski, M.X. (2001). Untangling the ErbB signalling network. Nat Rev Mol Cell Biol *2*, 127-137.

Ye, H., Kuruvilla, R., Zweifel, L.S., and Ginty, D.D. (2003). Evidence in support of signaling endosome-based retrograde survival of sympathetic neurons. Neuron *39*, 57-68.

Yeh, R.F., Lim, L.P., and Burge, C.B. (2001). Computational inference of homologous gene structures in the human genome. Genome Res *11*, 803-816.

Zapf, A., Hsu, D., and Olefsky, J.M. (1994). Comparison of the intracellular itineraries of insulin-like growth factor-I and insulin and their receptors in Rat-1 fibroblasts. Endocrinology *134*, 2445-2452.

Zerial, M., and McBride, H. (2001). Rab proteins as membrane organizers. Nat Rev Mol Cell Biol *2*, 107-117.

Zhao, W.Q., Chen, G.H., Chen, H., Pascale, A., Ravindranath, L., Quon, M.J., and Alkon, D.L. (2003). Secretion of Annexin II via activation of insulin receptor and insulin-like growth factor receptor. J Biol Chem *278*, 4205-4215.

Zheng, Y. (2001). Dbl family guanine nucleotide exchange factors. Trends Biochem Sci *26*, 724-732.

Zhou, Q., Xiao, M., and Nicoll, R.A. (2001). Contribution of cytoskeleton to the internalization of AMPA receptors. Proc Natl Acad Sci U S A *98*, 1261-1266.

Zhu, G., Liu, J., Terzyan, S., Zhai, P., Li, G., and Zhang, X.C. (2003). High resolution crystal structures of human Rab5a and five mutants with substitutions in the catalytically important phosphate-binding loop. J Biol Chem *278*, 2452-2460.

Zhu, S., Stavrovskaya, I.G., Drozda, M., Kim, B.Y., Ona, V., Li, M., Sarang, S., Liu, A.S., Hartley, D.M., Wu du, C., Gullans, S., Ferrante, R.J., Przedborski, S., Kristal, B.S., and Friedlander, R.M. (2002). Minocycline inhibits cytochrome c release and delays progression of amyotrophic lateral sclerosis in mice. Nature *417*, 74-78.

Zhu, Y., Doray, B., Poussu, A., Lehto, V.P., and Kornfeld, S. (2001). Binding of GGA2 to the lysosomal enzyme sorting motif of the mannose 6-phosphate receptor. Science *292*, 1716-1718.

Ziv, N.E., and Smith, S.J. (1996). Evidence for a role of dendritic filopodia in

synaptogenesis and spine formation. Neuron *17*, 91-102.

Zoghbi, H.Y., and Botas, J. (2002). Mouse and fly models of neurodegeneration.

Trends Genet *18*, 463-471.

Vitae

Justin David Topp, the son of Brenda Smith and Joel Topp, was born on December 7, 1977 in Waterloo, IA. After completing his high school education in May 1996 from Guilford High in Rockford, IL, he enrolled in the College of Engineering at the University of Iowa (August 1996). From September 1998 until August 2000, Justin performed research in the lab of Dr. Mark Stamnes at the University of Iowa. Justin was the recipient of numerous scholarships and awards during his undergraduate studies. In June 1999, he was awarded a Summer Undergraduate Research Fellowship from the Department of Physiology and Biophysics at the University of Iowa College of Medicine, and continued his work with Dr. Stamnes. In May 2000, Justin graduated from the University of Iowa, College of Engineering, with a Bachelors Degree in Science and Engineering in Biomedical Engineering (with Honors and Distinction). In August 2000, Justin began doctoral work in the Graduate School of the Biomedical Sciences at the University of Texas Southwestern Medical Center at Dallas (under the mentorship of Dr. Bruce F. Horazdovsky), and received his Doctorate of Philosophy in Biochemistry in April 2005. During his graduate studies, Justin was a recipient of both the Jonsson Scholarship (August 2000) and a National Science Foundation Pre-doctoral fellowship (September 2001). In November 2002, Dr. Horazdovsky and his lab moved from the University of Texas Southwestern Medical Center at Dallas to the Mayo Clinic in Rochester, MN. In March 2003, Justin met his future wife, Meta Catherine Sandberg; Justin and Meta were married on May 30, 2004. In April 2005, Justin will begin post-doctoral research in the lab of Drs. Brown and Goldstein at the University of Texas Southwestern Medical Center at Dallas.

Permanent Address:

6401 Maple Avenue
Apt. # 6307
Dallas, TX 75325